THÈSE

présentée à

L'UNIVERSITE SCIENTIFIQUE ET MEDICALE ET L'INSTITUT NATIONAL POLYTECHNIQUE DE GRENOBLE

pour obtenir le grade

DOCTEUR ES·SCIENCES PHYSIQUES

par

Jean-Jacques PRÉJEAN

SUJET

L'AIMANTATION DES VERRES DE SPINS : CONSTRUCTION ET RELAXATION DES AIMANTATIONS RÉMANENTES, RÉPONSE MACROSCOPIQUE EN FAIBLE CHAMP INVERSE OU TRANSVERSE.

Soutenue le 1er Février 1980 devant la commission d'Examen

A. BLANDIN	Président
A. MAYNARD	
P. MONOD	Examinateurs
W.A. PHILLIPS	
J. SOULETIE	
R. TOURNIER	

A mes parents

A mes amis

A tous ceux qui m'ont aidé, consciemment ou non, à vivre au sens le plus profond.

R E M E R C I E M E N T S

J'exprime mes remerciements à Monsieur le Professeur A. BLANDIN pour l'honneur qu'il me fait en présidant le jury, ainsi qu'à Messieurs A. MAYNARD, P. MONOD, A. PHILLIPS, J. SOULETIE, R. TOURNIER qui ont bien voulu faire partie de la Commission d'Examen.

Monsieur le Professeur DREYFUS m'a accueilli au CRTBT. Lui-même ainsi que Messieurs A. LACAZE et R. TOURNIER qui lui ont depuis succédé à la direction du laboratoire ont toujours manifesté un grand intérêt pour mon travail. Qu'ils en soient ici remerciés.

L'aide, la patience, l'amitié de J. SOULETIE ont été pour moi bien plus qu'une simple direction de mes travaux.

La lecture de ce mémoire témoigne de l'apport qu'a constitué le passage de P. MONOD dans ce laboratoire et de l'aide bienveillante qu'il m'a constamment prodiguée depuis.

Tous ceux qui me connaissent savent à quel point la collaboration, la compétence, la disponibilité, les conseils et l'amitié de mes camarades de travail, chercheurs et I.T.A., ont plus que contribué à la bonne marche de mes recherches et à me soutenir le moral dans les moments difficiles. Je ne peux toutes et tous les citer ici, mais chacun se reconnaîtra dans ces remerciements.

J'ai abusé de la bonne volonté de D. DEVILLERS et A. MAZET qui ont non seulement dactylographié ce mémoire en corrigeant d'elles-mêmes les nombreuses fautes contenues dans le manuscrit, mais ont dû aussi procéder aux modifications sans fin que j'ai apportées jusqu'à ce jour.

Nous regrettons tous en cet instant l'absence de Bruno TISSIER qui m'a formé sur les techniques expérimentales, qui m'a supporté dans son bureau et avec lequel j'avais des projets expérimentaux dans le domaine qui nous était devenu commun.

S O M M A I R E

I N T R O D U C T I O N

Le comportement des impuretés magnétiques, diluées dans un métal est un sujet d'études expérimentales et théoriques déjà anciennes.

On peut distinguer trois limites différentes :

i) Régime à une impureté : c'est la limite des très faibles concentrations d'impuretés, connu sous le nom de l'effet Kondo. L'interaction dominante est celle de l'impureté avec les électrons de conduction.

ii) Régime des fortes concentrations : Par exemple Au_4Mn, où un ordre magnétique spatial s'installe. L'ordre est dû aux interactions d'échange (ferro ou antiferromagnétiques) entre les impuretés premières voisines.

iii) Régime intermédiaire : Les mesures de susceptibilité magnétique à haute température montrent une température de Curie-Weiss importante (Néel, Weil). L'observation d'un maximum de susceptibilité (Kittel), de l'hystérésis et du traînage magnétique (Kouvel, Tournier), des lois d'échelle en concentration (Blandin, Souletie) est antérieure à l'usage du terme "verre de spins".

L'expression "verre de spins" est apparue il y a une dizaine d'années pour caractériser "l'ordre" magnétique qui s'établit à basse température, entre les impuretés. L'interaction entre ces impuretés est du type RKKY : $J_{ij} \approx \cos(2k_F r_{ij})/r_{ij}^3$.

La découverte d'un pic aigu de susceptibilité $\chi(T)$ à $T = T_g$ (par Cannella et Mydosh) dans ces alliages (AuFe, CuMn, AuMn, AgMn) explique le regain d'intérêt expérimental et théorique de ces systèmes.

Le pic aigu sur $\chi(T)$ suggère une transition de phase à T_g : la nouvelle phase basse température fut baptisée verre de spins.

Mise à part l'anomalie observée sur $\chi(T)$, aucune "singularité" caractéristique d'une transition de phase n'a pu être observée. En effet, les mesures de chaleur spécifique, de résistivité, de résonance magnétique (T_1, T_2 en RMN par exemple) montrent un comportement continu des hautes températures vers les basses températures.

Très vite, on s'est posé la question de distinguer les deux régimes $T < T_g$ et $T > T_g$. L'absence d'une nette différence sur les mesures thermostatiques a laissé la place à l'étude de la dynamique de ces systèmes : le comportement en temps du même système. Les études magnétiques montrent qu'à $T > T_g$, l'aimantation répond instantanément à une perturbation extérieure (variation du champ magnétique par exemple). Par contre, à $T < T_g$, on a observé un phénomène d'hystérésis assez notable, ainsi qu'un type de relaxation, non exponentielle, comme réponse à une variation de champ.

Pour fixer les idées ainsi que la terminologie, il est très utile de décrire certains exemples typiques :

* Si l'on refroidit le système depuis une température supérieure à T_g, sous champ magnétique H, jusqu'à $T < T_g$, on observe une aimantation $M_a(H,T)$, stable au cours du temps et ne présentant pas d'anomalie à T_g. On peut définir ainsi une susceptibilité notée $\chi_a(H,T)$ définie par :

$$\chi_a(H,T) = M_a(H,T)/H \ .$$

* Si on coupe le champ appliqué H, à $T < T_g$, on observe d'abord une décroissance brutale de l'aimantation, mais il reste une aimantation résiduelle (l'aimantation rémanente) qui décroît très lentement au cours du temps : $\sigma_r(H,T,t)$.

On appellera, <u>aimantation réversible</u>, la réponse du système dans le temps de mesure, à une variation de champ :

$$M_{rév.} = M_a(H,T) - \sigma_r(H,T,t).$$

On définira ainsi la susceptibilité réversible par $\chi_{rév.} = \frac{M_a(H,T) - \sigma_r(H,T,t)}{H}$. La susceptibilité réversible $\chi_{rév.}$ dépend donc du temps de mesure t et tend vers $\chi_a(H)$ à temps infini :

$$\chi_a(H,T) = \lim_{t \to \infty} \chi_{rév.}(H,T,t).$$

Cette démonstration expérimentale (Tholence) indique clairement la dépendance en t de la susceptibilité réversible et appelle des précautions en ce qui concerne la définition de la "singularité" à T_g : En effet, à temps infini, $\chi_{rév.}$ coïncide avec χ_a et ne présente pas le pic caractéristique à T_g. La dépendance en temps de la susceptibilité réversible entraîne une dépendance temporelle de T_g. Ceci justifie a posteriori le terme "verre de spins", par analogie avec la transition vitreuse dans les verres ordinaires. En plus des mesures de susceptibilité, les études par neutrons, effet Mössbauer, par Muons (échelle de temps de la mesure : 10^{-8} sec. typiquement) ont été interprétées comme déterminant une valeur de T_g supérieure à la valeur trouvée par les mesures de susceptibilité alternative où l'échelle de temps est $\sim 10^{-2}$ sec.

Etant donné cet ensemble de résultats, il nous semble primordial d'associer les mesures de susceptibilité et le comportement hors d'équilibre à T_g. La dépendance de $\chi(T)$ et σ_r ne peut pas être oubliée dans la définition de T_g et par la suite de la nouvelle phase à $T < T_g$. Avec cette vision de T_g et de la "phase" verre de spins, nous nous sommes intéressés à l'étude des propriétés hors d'équilibre de l'alliage CuMn, connu pour être un verre de spins. Par exemple, nous avons pu montrer que σ_r est une fonction de la variable réduite : T Log t/τ_o, τ_o étant un temps caractéristique. Notre travail est avant tout expérimental ; néanmoins, nous nous sommes fixés comme objectif de tirer les conclusions fondamentales dont il faut tenir compte dans une théorie microscopique des verres de spins.

Dans la première partie, nous avons montré que, à $T < T_g$:

* La relaxation de l'aimantation révèle la présence d'une large distribution des temps de relaxation. On a associé ces temps de relaxation à des barrières de potentiel largement distribuées.

* La relaxation d'énergie, associée à celle de l'aimantation, indique que ces barrières séparent des états d'énergiesdifférentes.

* Le mode de relaxation (franchissement d'une barrière de potentiel) est du type activation thermique. Ceci résulte de la dépendance en temps t et en température T.

* A chaque champ magnétique et à chaque température est associé un état d'équilibre (stable ou métastable) caractérisé par une aimantation $M_a(H,T)$ et correspond à un état de basse énergie, vers lequel le système relaxe (aimantation, énergie) lorsqu'il est préparé hors d'équilibre.

* L'aimantation thermo-rémanente est fonction de $\frac{T}{T_o}$ Lnt/τ_o où τ_o est de l'ordre de 10^{-11} sec dans CuMn, et où T_o a la même dépendance en concentration que la température du maximum de susceptibilité alternative mesurée à fréquence constante.

La conséquence naturelle de ces propriétés générales à tous les verres de spins doit être une nette dépendance de la température T_g du maximum de susceptibilité alternative en fonction de la fréquence ω (typiquement correspondant à des temps de mesure de 10^{-2} s ou moins).

Dans certains cas ($LaAl_2Gd$), on observe effectivement une variation significative de T_g en $(\text{Log } \omega)^{-1}$.

Il est, par contre, surprenant de ne trouver qu'une très faible dépendance en fréquence de T_g dans l'alliage CuMn, et de n'en trouver aucune dans AgMn.

Dans ces systèmes, la discordance entre, d'une part les résultats de susceptibilité alternative au voisinage de T_g et, d'autre part le comportement en $T \text{ Log } \frac{t}{\tau_o}$ de l'aimantation rémanente, suggère que T_g, dépendant du temps, ne peut dépasser une valeur maximale T_c, fixe dans le temps, au-delà de laquelle le système est simplement paramagnétique. Nous avançons l'hypothèse qu'au-dessus de T_c, les corrélations ayant permis de construire les entités magnétiques entrant en jeu dans la construction de l'aimantation rémanente, sont détruites. C'est à cette température T_c

que peut se poser le problème d'une transition de phase s'il doit se poser.

L'aimantation rémanente étant construite en champ positif à basse température, il est possible d'imaginer ainsi la réponse du système en champs négatifs croissants : l'aimantation rémanente positive sera progressivement détruite et une aimantation négative construite selon les propriétés générales décrites plus haut. Le cycle d'hystérésis obtenu ne montre aucune singularité. C'est ce qui est observé expérimentalement dans AuFe. Cette image se révèle fausse dans CuMn où nous mettons en évidence qu'un champ négatif faible va basculer globalement l'aimantation rémanente construite en champ positif : le système se présente comme un grain monodomaine possédant un champ d'anisotropie H_a très faible devant l'ordre de grandeur des champs nécessaires à la construction de l'aimantation rémanente saturée σ_r. L'énergie d'anisotropie macroscopique $\sigma_r.H_a$ est peu sensible à la température, varie comme le carré de la concentration de manganèse et dépend de l'état métallurgique de l'alliage. Cette étude, exposée dans la seconde partie, montre une nette différence de réponse en champ inverse d'un système à l'autre, alors que les mécanismes de construction et de relaxation des aimantations à $T < T_g$ sont identiques pour tous les verres de spins. Peut-on pour autant introduire une nouvelle classification parmi les verres de spins ?

Pour comprendre cette différence, nous avons introduit dans CuMn des impuretés ne changeant pas la valeur de l'aimantation rémanente mais qui sont connues pour leur fort couplage spin-orbite : nous montrons que l'énergie d'anisotropie macroscopique croît linéairement avec la concentration de ces impuretés à un taux proportionnel à la section efficace du mécanisme de diffusion spin-flip dû au couplage spin-orbite. L'introduction d'atomes d'or ou de platine à une concentration aussi faible que 1 % atomique suffit à modifier le cycle d'hystérésis du système CuMn pour le rendre équivalent à celui d'AuFe.

Ces résultats, présentés à la fin de la seconde partie, lèvent dans les propriétés générales des verres de spins une ambiguité qui pouvait

subsister par l'examen des cycles d'hystérésis : Si les électrons de conduction n'ont aucune interaction d'ordre magnétique avec la matrice, l'ensemble constitué par les spins des impuretés magnétiques et les électrons libres fournira, lorsqu'une aimantation est construite dans une symétrie, une réponse collective et instantanée à toute sollicitation d'un champ extérieur de symétrie différente. Cette propriété, confirmée par des expériences de RPE et RMN en présence d'aimantation rémanente, prouve que seule une interaction isotrope par rotation est responsable des barrières et différents niveaux d'énergie caractérisant les verres de spins métalliques : nous pouvons conclure que cette interaction est de type RKKY et exclure des mécanismes tels que l'interaction dipolaire à laquelle certains auteurs ont prêté un rôle important dans ces systèmes.

Une interaction d'ordre magnétique des électrons de conduction avec la matrice (via le couplage spin-orbite) introduit un couplage indirect des impuretés magnétiques (interagissantes par le processus RKKY) avec le réseau. Il en résulte un couple macroscopique s'opposant à la rotation ou au basculement.

Dans la troisième partie, nous présentons un travail plus ancien portant sur des systèmes supraconducteurs :

L'observation d'un effet réentrant dans la dépendance en température T du champ critique H_c dans le composé $La_{3-c}InGd_c$ (Crow, Guertin, Parks) avait été interprétée (Bennemann) à l'aide de modèles mettant en jeu l'aimantation des impuretés magnétiques. Nous avons testé expérimentalement la validité de ces modèles en mesurant directement l'aimantation M de ces impuretés dans l'état normal. Celle-ci obéit aux lois d'échelles en concentration ($M/c = f(H/c, T/c)$) caractéristiques des verres de spins. Nous montrons que la décroissance de champ critique due à la présence du gadolinium peut également s'exprimer selon une loi réduite :

$$\frac{H_c(T,c=0) - H_c(T,c)}{c} = \alpha + f\left(\frac{M(H_c(T),T,c)}{c}\right).$$

C H A P I T R E I

RELAXATION DE L'AIMANTATION REMANENTE SATUREE ET DE L'ENERGIE ASSOCIEE A $T < T_g$

La relaxation très lente et de nature logarithmique des aimantations de verres de spins à des températures inférieures à T_g avait suggéré les hypothèses suivantes :

1 - L'existence de barrières de potentiel, importantes et distribuées sur de larges domaines d'énergie, est responsable du retard à la relaxation.

2 - Des processus d'activation thermique gouvernent le franchissement de ces barrières (loi d'Arrhénius).

C'est le second point que nous avons démontré expérimentalement en étudiant la relaxation de l'aimantation rémanente saturée sur une gamme de temps t supérieure à 2 décades (de 1 mn à quelques centaines de minutes après coupure du champ) et sur toute la gamme de température T où cette aimantation peut être observée ($T < T_g$).

Dans la première publication ("Time and temperature evolution of the saturated thermoremanent magnetization of a spin glass"), nous présentons nos résultats expérimentaux réalisés sur 3 échantillons de CuMn (.5, 1, 8 at% Mn) et montrons sans ambiguité qu'il est possible d'exprimer les dépendances en temps et température de l'aimantation rémanente saturée en fonction d'une variable unique $T \text{ Ln } t/\tau_o$ (τ de l'ordre de 10^{-11} s).

Louis Néel a utilisé les deux mêmes hypothèses que celles énoncées plus haut pour développer sa théorie des grains fins, ce qui a conduit de nombreux auteurs à développer, dans le cas des verres de spins,

des modèles issus de cette théorie.

Il est alors supposé que le système est divisé en "domaines" ("nuages", "objets magnétiques") et que les barrières de potentiel de hauteur W séparent des orientations faciles d'aimantation M_g de ces parties du système.

L'expression de l'aimantation rémanente σ_r est alors obtenue en intégrant, sur l'ensemble des temps de relaxation τ, la relaxation de l'aimantation des objets magnétiques de moment M_g :

$$\sigma_r = \int_{\tau} M_g \exp(-t/\tau) \quad \text{avec } \tau = \tau_o \exp(W/k_B T).$$

Si $t >> \tau_o$, on peut considérer avec une très bonne approximation que :

$$\exp(-t/\tau) = 0 \quad \text{si } W < kT \text{ Ln } t/\tau_o$$

$$= 1 \quad \text{si } W > kT \text{ Ln } t/\tau_o ,$$

ce qui implique $\sigma_r = \int_{W \geq kT \text{Ln} t/\tau_o} M_g$.

Ce modèle simple peut rendre compte de situations microscopiques plus complexes comme nous le verrons plus loin. Le résultat final montre que, si la distribution des barrières de potentiel est peu dépendante de la température, l'aimantation rémanente est fonction d'une variable unique T Ln t/τ_o.

Nous observons expérimentalement par exemple que toute déviation à un comportement linéaire en température à temps constant implique une déviation correspondante par rapport à un comportement linéaire en Ln t à température constante.

Dans ce problème, il existe une inconnue supplémentaire dont l'existence ne peut pas être déduite a priori de l'étude de la relaxation

de l'aimantation rémanente : les états d'énergie séparés par les barrières de potentiel sont-ils différents ? La réponse a été donnée par J. Odin qui a pu mesurer directement une relaxation d'énergie en présence d'aimantation rémanente dans le système Au-Fe (et, très récemment, dans CuMn et $(EuS)_{50\%}$-$(GdS)_{50\%}$). La corrélation très simple de ces mesures avec celles de relaxation d'aimantation, que nous avons effectuées sur un même échantillon (dans les mêmes conditions d'histoire magnétique et thermique), est présentée dans une seconde publication ("Magnetization and energy relaxation in spin glass $AuFe_{4\%}$ below T_g").

JOURNAL DE PHYSIQUE *Colloque C6, supplément au n° 8, Tome 39, août 1978, page C6-907*

TIME AND TEMPERATURE EVOLUTION OF THE SATURATED THERMOREMANENT MAGNETIZATION OF A SPIN GLASS

J.J. Prejean,

Centre de Recherches sur les Très Basses Températures, C.N.R.S., BP 166 X, 38042 Grenoble Cédex, France.

Résumé.- Nous avons étudié la variation avec la température T et le temps τ de l'aimantation thermorémanente saturée σ_{rs} d'un verre de spin pour 3 concentrations de Mn dans Cu. La relation entre les dépendances en température et en temps est semblable à celle résultant d'une distribution de systèmes à deux niveaux thermiquement activés (loi d'Arrhénius).

Abstract.- We have studied the dependence of the saturated thermoremanent magnetization σ_{rs} of a spin glass on the temperature T and the time τ, for 3 concentrations of Mn in Cu. The temperature and time dependences are linked by the type of relation which the assumption of a distribution of thermally activated two level systems implies (Arrhenius law).

We have studied the saturated thermoremanent magnetization, for 3 concentrations (C = 0.5 %, 2 % 8 %) for the spin glass system Cu Mn.

The thermoremanent magnetization σ_r is obtained by cooling the sample from $T > T_g$ (T_g is the temperature of the cusp in the reversible a.c. susceptibility /1/) down to a final temperature $T < T_g$ with a magnetic field H_a applied. Then the magnetic field is withdrawn and the remanent magnetization $\sigma_r(T, H_a)$ is measured as a function of time τ : the origin of time is taken at the moment when H_a becomes null.

For a given measuring time τ_m, and a given temperature T, $\sigma_r(T, \tau_m)$ depends on H_a as shown on the insert of figure 1 : it increases, goes through a maximum and reaches a saturation value $\sigma_{rs}(T, \tau_m)$

The figure 1 shows the dependence of σ_{rs}, at τ_m = 60 s, with the external temperature T. On this diagram, one observes that for more than 90 % of its variation, σ_{rs} follows closely an exponential behaviour :

$$\sigma_{rs} = \sigma_o \exp(- aT) \qquad (1)$$

On figure 2, the dependence on time at T = 6.15 K of σ_{rs} of a Cu Mn 2 % is observed to show sizable deviations to an initially logarithmic behaviour.

DISCUSSION.- The remanent properties of spin glasses have been interpreted with models /2/ derived from the Neel's theory of fine magnetic particles /3/. This theory relies on two main assumptions :

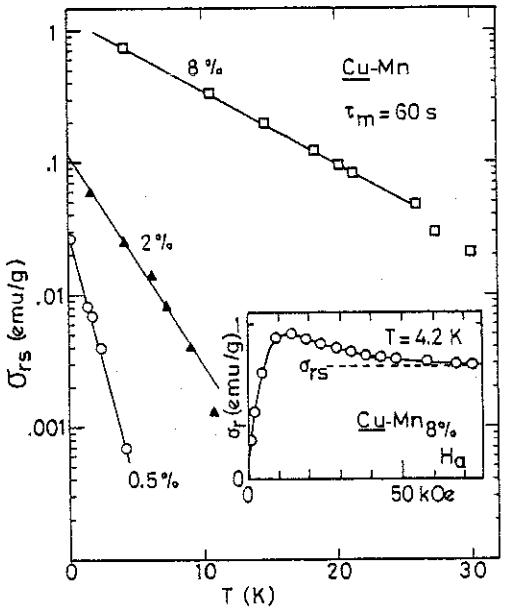

Fig. 1 : Temperature dependence of σ_{rs} at time τ = 60 s for the 3 studied concentrations of Mn. Insert : dependence of σ_{rs} (at T = 4.2 K, τ = 60 s) on the cooling field H_a for the Cu Mn 8 % sample.

a) Potential barriers of energy W separate two easy orientations for the magnetization of some small domains or regions of the system. The average time necessary for the magnetization to jump over the barrier, due to thermal fluctuations, is thus given by the Arrehenius law :

$$\tau = \tau_o \exp(W/kT) \qquad (2)$$

b) To first order, it is assumed that the distribution P(W) of the energy W is a constant over a wide range of temperature.

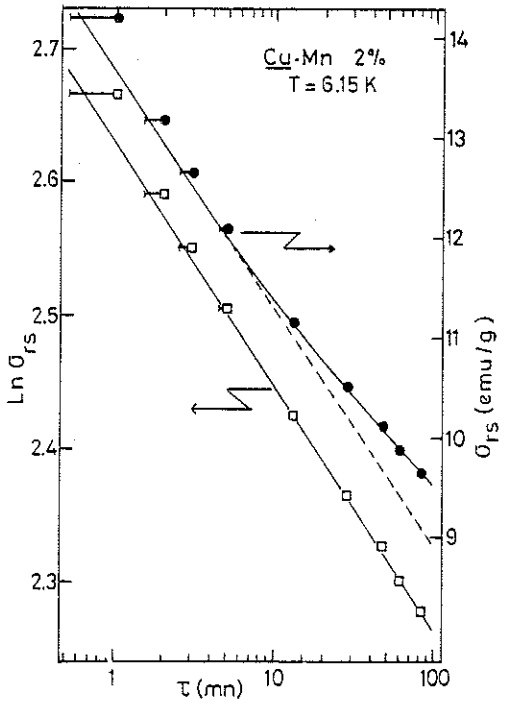

Fig. 2 : Dependence on time at 6.15 K of σ_{rs} of the Cu Mn 2 % sample. 2 diagrams are presented : σ_{rs} vs Log τ, Log σ_{rs} vs Log τ.

This model is able to account, for example, for the logarithmic dependence of the magnetization with time which is very generally observed on a limited extension of time.

For large variations of the remanent magnetization (as shown on figure 1 when σ_{rs} varies over two orders of magnitude), assumption (b) is not sufficient as pointed out by Tholence and Tournier /2/ who accounted for the exponential dependence of σ_{rs} on the temperature in the frame of a slightly more sophistical model : independent "antiferromagnetic clouds", each containing n spins, having an anisotropy energy $W \sim n$, and contributing with its uncompensated moment $M_g \simeq \mu \sqrt{n}$ to σ_{rs} below its blocking temperature $T_B = W/k \ln \frac{\tau}{\tau_o}$. A gaussian distribution of the moments M_g is needed : $P(M_g) \sim \exp(- M_g^2/2M_{g_o}^2)$.

It is the purpose of the present paper to show that, although assumption (b) thus fails to be valid when the temperature is varied over a very wide range, assumption (a), namely the relevance of the Arrhenius law, seems to remain established all the same.

The main feature associated with eq. (2) is that it associates the time and the temperature in the same unique variable which is actualy : kT Ln $\frac{\tau}{\tau_o}$.

Thus expression (1) should be generalized as

$$\sigma_{rs} = \sigma_o \exp\left(- \frac{T}{T_o} \operatorname{Ln} \frac{\tau}{\tau_o}\right) \qquad (3)$$

which implies :

$\operatorname{Ln} \sigma_{rs} = A - \frac{T}{T_o} \operatorname{Ln} \tau$ for a fixed temperature.

It is observed (figure 2) that Ln σ_{rs} remains a linear function of Ln τ over 3 decades in time. The values of the parameters T_o and τ_o by checking, at each temperature T, the validity of eq. (3) in describing the evolution of σ_{rs} with time, have been found to be nearly constant for each concentration, and the typical values are reported on table I. It is thus seen that the temperature and the time dependences of the thermoremanent magnetization are indeed closely correlated in agreement with the predictions of eq. (2). The theoretical justification of the experimentally determined values of τ_o remains, so far, a weak and difficult point in these types of approach, even when they are applied to systems of fine particles which are more accurately defined.

Besides eq. (2) is a simplification even in Neel's approach where it is shown that τ_o should depend on the external field as well as on temperature.

Mn Concentration	σ_o(emu/g)	T_o(K)	Ln $\frac{1}{\tau_o}$
0.5 %	0.028	32	39
2 %	0.105	84	30
8 %	1.25	273	30

Table I

CONCLUSION.- It is confirmed that the memory effects observed in spin glasses below T_g are connected with an activated process.

The exponential behaviour noticed previously in the σ_{rs} versus T dependence is confirmed through the time dependence of the saturated thermoremanent magnetization. Notice that this feature was also present in the data of computation experiments /4/, with a Monte-Carlo method and samples elaborated according to the requirement of the Edwards and Anderson model.

ACKNOWLEDGMENTS.- We thank Drs Souletie, Tournier, Tholence, Monod for many helpful discussions and assistance in preparing this paper.

References

/1/ Cannela, V., Mydosh, J.A., Phys. Rev. B6 (1972) 4220.

/2/ Tholence, J.L., Tournier, R., Physica 86-88B (1977) 873-874, and Holtzberg, F., Tholence, J.L. and Tournier, R., Amorphous Magnetism II, (Plenum Press, New-York and London) 1977, 155.

/3/ Neel, L., Annales de Géophysique 5 (1949) 99, and J. Phys. Soc. Japan 17, Sup. B1 (1962) 676.

/4/ Binder, J., Advances in Solid State Physics, Festkörperprobleme XVII (1977) 55.

MAGNETIZATION AND ENERGY RELAXATIONS IN SPIN GLASS AuFe 4 at% BELOW T_g

A. BERTON, J. CHAUSSY, J. ODIN*, J. J. PREJEAN, R. RAMMAL, J. SOULETIE and R. TOURNIER

CRTBT-CNRS (associated USMG), B.P. 166 X, 38042 Grenoble Cédex, France

We present data on AuFe 4% showing: a relaxation of the saturated remanent magnetization significative of a wide distribution of barriers; an associated energy relaxation implying that the barriers separate levels of different energies; a time-temperature correlation of these relaxations which implies thermally activated processes.

We present the results of measurements of the isothermal relaxation of the saturated remanent magnetization M_{RS} and of the associated energy flow $\dot{Q}$ in spin glass AuFe 4 at% at $T < T_g \approx 20$ K. The sample is cooled from $T > T_g$ down to $T_i = 1.4$ K in a field (25 kOe) sufficient to saturate the thermoremanent magnetization. The field is then removed at $T = T_i$. Next the temperature is raised up to $T_1 > T_i$ at a time which establishes the origin in the measurement of the relaxation of M_{RS} and of $\dot{Q}$ vs. time t. After about one hour of observation the energy flow $\dot{Q}$ becomes of the order of the sensitivity (0.01 μW) of our detection. The temperature is then raised to $T_2 \approx 1.2T_1$ and the relaxations of M_{RS} and $\dot{Q}$ are studied at T_2. Figs. 1 and 2 show that M_{RS} varies like $\log t$ [1, 2] and $\dot{Q}$ like t^{-1} [3, 4] at different temperatures T_1, T_2, etc. No relaxation is observed on a pure Au sample whatever its history. In contrast the relaxation of M_{RS} and $\dot{Q}$ is always associated with a variation of the applied field with respect to the value in which the sample has been cooled. These observations lead to the following remarks: there are objects (clusters, clouds, etc.) carrying a magnetic moment which have a slow evolution towards "equilibrium" indicative of the existence of very high potential barriers W. These barriers W separate configurations of different energies as shown by the existence of a $\dot{Q}$. These remarks lead us to adopt the picture of asymmetric double well potentials characterized by a barrier height W (which fixes the time scale) and an energy splitting ε. The nonexponential relaxation of M_{RS} and of $\dot{Q}$ shows that there is a wide distribution of the barriers W and of the splittings ε. This is not unexpected in a disordered system where no special value of the energy is anticipated. The evolution of the saturated remanent magnetization can be described

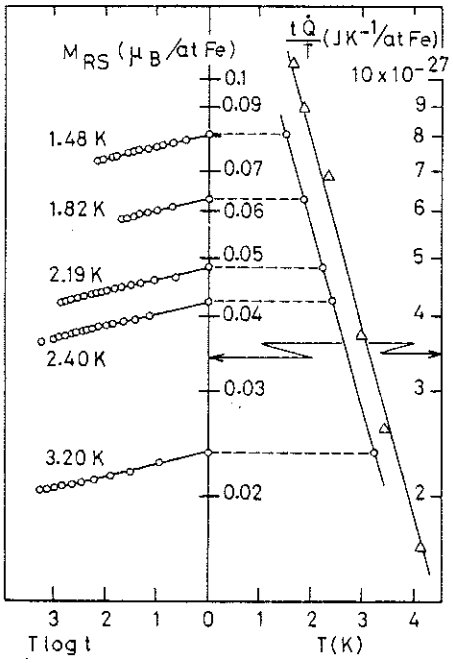

Fig. 1. Left: remanent magnetization versus $T \log t$ (t in minutes) at various temperatures for AuFe 4% at. Right: temperature dependence of M_{RS} (○) and of $t\dot{Q}/T$ (△) at $t = 60$ s for AuFe 4 at%.

in terms of the reduced variable $T \ln(t/\tau_0)$ (fig. 1) with $\tau_0 \approx 10^{-13}$ s. This particular time–temperature dependence occurs because of a cut off at $W_c = kT \ln(t/\tau_0)$ which limits (in an activated process) the barriers which can be observed at a temperature T on the scale of the measuring time t.

An object will therefore have to cross a barrier $W - \varepsilon$ to reach "equilibrium". Let $\overline{Mg}$ be an average value of the moment of an object. If $\mathcal{P}(\varepsilon)$ and $P(W)$ are the distributions of the energies ε and of the barrier heights W, we can write the saturated remanent magnetization M_{RS} and the

*Also with Laboratoire d'Electrotechnique ERA 534 of CNRS.

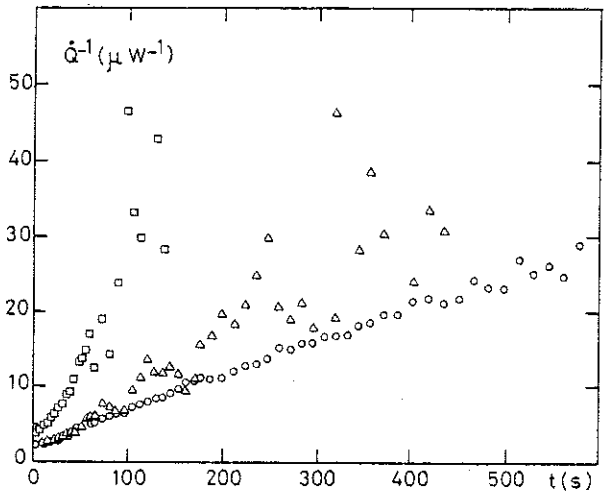

Fig. 2. Time dependence of reciprocal power delivered by a 10 g AuFe 4 at% sample at various temperatures: (○) 1.65 K; (△) 2.98 K; (□) 4.1 K.

stored energy Q as:

$$M_{RS} \approx \int_0^\infty P(W)\,dW \int_0^\infty \mathcal{P}(\varepsilon)\,d\varepsilon \overline{M}_g \times \exp(-t/\tau), \quad (1)$$

$$Q = \int_0^\infty P(W)\,dW \int_0^\infty \mathcal{P}(\varepsilon)\varepsilon\left[\exp(-t/\tau)\right]\,d\varepsilon, \quad (2)$$

where for an activated process $\tau = \tau_0 \exp(W - \varepsilon)/kT$. The same cut-off argument as above implies:

$$M_{RS} = \overline{M}_g \int_{W_c}^\infty P(W)\,dW \int_0^{W-W_c} \mathcal{P}(\varepsilon)\,d\varepsilon, \quad (3)$$

$$Q = \int_{W_c}^\infty P(W)\,dW \int_0^{W-W_c} \varepsilon \mathcal{P}(\varepsilon)\,d\varepsilon. \quad (4)$$

Derivating under the integrand the expression for the energy one obtains:

$$\dot{Q} = \frac{kT}{t} \int_{W_c}^\infty P(W)(W - W_c)\mathcal{P}(W - W_c)\,dW. \quad (5)$$

Inasmuch as $\mathcal{P}(\varepsilon)$ does not vary too much on the scale of the variations of $W - W_c$ it is easy to see that $\dot{Q}$ and M_{RS} are related by:

$$\dot{Q} = (kT/t) M_{RS}\left[T \ln(t/\tau_0)\right]/\overline{M}_g, \quad (6)$$

which justifies the leading term in t^{-1} of the energy flow relaxation seen in fig. 2. The validity of this equation is better seen in fig. 1 where the variations of $t\dot{Q}/kT$ are compared to those of M_{RS}. We obtain for the average moment of an object $\overline{M}_g \approx 95\mu_B$ which compares with previous independent estimations.

The results of fig. 1 are well approximated by a law [2]:

$$M_{RS}(T, t)/M_{RS}(0) \approx \exp(-T/T_0)\ln(t/\tau_0) = (t/\tau_0)^{-T/T_0}, \quad (7)$$

with $T_0 = 49$ K $\approx 2.5 T_g$. It is remarkable that the saturated remanent magnetization (and therefore the energy) seems to follow a power law $M_{RS}(t) \sim Q(t) \sim t^{-a}$ where the exponent $a = T/T_0 \sim 0.4 T/T_g$ is linear in temperature. Except for a difference in the numerical factor, this is in agreement with results of numerical simulation [5] on simplified models of spin glasses yielding in the vicinity of T_g, $a \approx (d/4)T/T_g$ in dimension d. This unusual behavior is indicative of the importance of the fluctuations over all the domain $T < T_g$. Exponents linear in temperature have been derived in the ferromagnetic xy model [6] through a correct treatment of the transverse spin fluctuations. It is to be feared that, like for this case, the search for a solution of the spin glass problem will have to go through a description of the defects and of the textures (the objects?) which would characterize an eventual new phase.

References

[1] F. Holtzberg, J. L. Tholence and R. Tournier, in: Amorphous Magnetism II, eds. R. A. Levy and R. Hasegawa (Plenum Press, New York and London, 1977) p. 155.
[2] J. J. Prejean, J. de Phys. Colloq. 39 (1978) C6-907.
[3] G. J. Nieuwenhuys and J. A. Mydosh, Physica 86–88B (1977) 880.
[4] A. Berton, J. Chaussy, J. Odin, R. Rammal, J. Souletie and R. Tournier, Compt. Rend. Acad. Sci. and J. Phys. Lett., to be published.
[5] K. Binder and R. Stauffer, Phys. Lett. 57 A (1976) 177.
[6] S. Miyashita, H. Nishimori, A. Kuroda and M. Susuki, Progr. Theor. Phys. 60 (1978) 1669.

C H A P I T R E I I

MODELE DE SYSTEMES A 2 NIVEAUX DANS LES VERRES DE SPINS CONSEQUENCES SUR LA CONSTRUCTION ET LA RELAXATION DES AIMANTATIONS A T < T_g, COMPARAISON AVEC L'EXPERIENCE SUR LE SYSTEME CuMn

L'étude expérimentale du comportement de l'aimantation thermorémanente saturée et de l'énergie associée nous a permis de tirer trois conclusions essentielles dans la caractérisation de l'état verre de spins :

1 - La relaxation de cette aimantation est significative de la présence d'une large distribution de barrières de potentiel.

2 - La relaxation d'énergie, associée à la relaxation de cette aimantation, implique que ces barrières séparent des niveaux différents largement distribués en énergie.

3 - La corrélation temps-température de ces relaxations montre sans ambiguité que le franchissement des barrières est gouverné par des processus d'activation thermique.

Ces conclusions font immédiatement penser à l'utilisation d'un modèle classique de doubles puits de potentiel asymétriques pour rendre compte phénoménologiquement de l'expérience.

Les questions qui se posent à ce stade de l'étude sont :

1 - Le développement d'un tel modèle pour décrire l'état d'équilibre du système en présence de champ, la construction et la relaxation des aimantations, la susceptibilité réversible, est-il

compatible avec les observations expérimentales ?

2 - Quelle réalité physique et microscopique se cache derrière l'abstraction des systèmes à 2 niveaux ?

Avant de tenter de résoudre ces questions dans la publication présentée plus loin ("Two-Levels-Systems ..."), nous devons préciser le modèle que nous allons développer et son domaine de validité.

Dans un premier temps, nous supposons quelques hypothèses simples :

1 - Il existe des objets magnétiques, de moments M_g, possédant une énergie d'anisotropie uniaxiale W (d'origine non définie), en présence d'un champ interne h (constant dans le temps) et d'un champ externe H, parallèles à l'axe d'anisotropie. L'axe positif des champs et aimantations sera pris dans le sens de H.

2 - Dans un système désordonné comme le sont les verres de spins, il n'existe aucune valeur privilégiée de l'énergie d'anisotropie (W) ou dessplittings ($\varepsilon_o = M_g|h|$) : nous supposons que W et h sont largement distribués, ce que confirme l'expérience.

3 - Les distributions de W (P(W)) et de h(P(h)) ne sont pas affectées par la température T et le champ externe H.

Considérons la collection de N moments M_g ayant la même énergie d'anisotropie W et soumis au même champ h. Si $P_{\uparrow\downarrow}$ désigne la probabilité de retournement d'un moment M_g d'une position parallèle à une position antiparallèle à l'axe positif et $P_{\downarrow\uparrow}$ la probabilité de retournement inverse, les équations classiques de relaxation des N moments M_g conduisent à l'expression :

$$\frac{dM}{dt} = - \frac{M - M_{éq}}{\tau_{eff}} \qquad (1)$$

où M est l'aimantation résultante des N moments, $M_{éq}$ cette aimantation à l'équilibre et :

$$\frac{1}{\tau_{eff}} = P_{\uparrow\downarrow} + P_{\downarrow\uparrow} \qquad M_{éq} = N\, M_g \frac{P_{\downarrow\uparrow} - P_{\uparrow\downarrow}}{P_{\uparrow\downarrow} + P_{\downarrow\uparrow}} \qquad (2)$$

Dans le cas où h et H sont nuls, les probabilités $P_{\uparrow\downarrow}$ et $P_{\downarrow\uparrow}$ sont équivalentes et nous supposerons qu'elles sont gouvernées par des processus d'activation thermique permettant de surmonter l'énergie d'anisotropie W :

$$P_{\downarrow\uparrow}\ (H=h=0) = P_{\uparrow\downarrow}\ (H=h=0) = \frac{1}{\tau} = \frac{1}{\tau_o} \exp(-\frac{W}{k_B T}) \qquad (3)$$

Les expressions (1) et (2) montrent alors que l'aimantation M relaxe vers une valeur nulle, le temps de relaxation associé étant donné par $\tau_{eff} = \frac{\tau_o}{2} \exp(W/k_B T)$ et l'énergie totale du système étant conservée (image d'un double puits de potentiel symétrique).

La présence d'un champ h + H introduit une différence d'énergie égale à 2 M_g (H+h) entre les 2 niveaux correspondant respectivement à des états d'aimantation M_g de même sens et de sens contraire au champ H+h. Les probabilités correspondantes $P_{\downarrow\uparrow}$ et $P_{\uparrow\downarrow}$ deviennent :

$$P_{\uparrow\downarrow} = \frac{1}{\tau} \exp(-\, M_g \frac{H+h}{kT}) \qquad P_{\downarrow\uparrow} = \frac{1}{\tau} \exp(+\, M_g \frac{H+h}{kT})$$

où les exponentielles sont le facteur de Boltzmann et où τ est donné par l'équation (3).

Un calcul rapide utilisant les expressions (1) et (2) conduit à :

$$\frac{1}{\tau_{eff}} = \frac{2}{\tau} \operatorname{ch}(M_g \frac{H+h}{kT}), \quad M_{éq} = N\, M_g \operatorname{th}(M_g \frac{H+h}{k_B T}) \qquad (4)$$

Le temps de relaxation τ_{eff} de l'aimantation peut être assimilé au temps moyen nécessaire pour franchir une barrière effective W_{eff} au moyen de processus d'activation thermique :

$$W_{eff} = k_B T \text{ Ln } \frac{\tau_{eff}}{\tau_o} = k_B T \text{ Ln } \frac{\tau}{\tau_o} - k_B T \text{ Ln } \left[2ch(M_g \frac{H+h}{kT})\right]$$

et, comme $2\ ch(M_g \frac{H+h}{k_B T}) = \exp(M_g \frac{|H+h|}{k_B T}) \left[1 + \exp(-2\ M_g \frac{|H+h|}{k_B T})\right]$,

on obtient finalement :

$$W_{eff} = W - M_g|H+h| - k_B T \text{ Ln } \left[1 + \exp(-2\ M_g \frac{|H+h|}{k_B T})\right].$$

Le troisième terme, compris entre $k_B T \text{ Ln } 1 = 0$ (pour $\frac{H+h}{T} \to \infty$) et $k_B T \text{ Ln } 2 = 0{,}7\ k_B T$ (pour $\frac{H+h}{T} \to 0$), est borné par $0{,}7\ k_B T$.

En conclusion, notre modèle peut être décrit par une distribution de systèmes à 2 niveaux :

* Un niveau correspond à l'aimantation initiale M_i d'une collection de moments M_g ayant la même énergie d'anisotropie W et soumis au même champ interne h.

* Le second niveau (état fondamental) correspond à l'aimantation à l'équilibre $M_{éq}$ de ces moments dans le champ H. $M_{éq}$ est indépendant de W.

* La barrière à franchir pour passer de l'état initial à l'état final est : $W_{eff} = W - M_g|H+h|$ à $0{,}7\ k_B T$ près.

* W_{eff} et $M_{éq}$ ne dépendent pas des conditions initiales de champ et d'aimantation.

Nous allons maintenant étudier 2 cas particuliers : le champ extérieur est amené à une valeur nulle ou bien le champ extérieur, d'abord nul, est amené à une valeur H.

a) L'état du système présente sous champ une aimantation, le champ extérieur est ramené à 0 (H = 0).

P(h) étant une fonction paire, pour un même module de h, l'aimantation à l'équilibre $N\ M_g\ th(\frac{M_g h}{kT})\ P(h) + N\ M_g\ th(-\frac{M_g h}{kT})\ P(-h)$ est nulle.

La barrière effective est $W_{eff} = W - M_g|h|$.

Soit $\varepsilon_o = M_g|h|$: le système se réduit à un modèle à 2 niveaux d'énergie différent de 2 ε_o, l'état fondamental étant celui correspondant à une aimantation nulle, la barrière effective à franchir pour relaxer de l'état excité (aimantation non nulle) au niveau fondamental étant $W - \varepsilon_o$ à 0,7 $k_B T$ près.

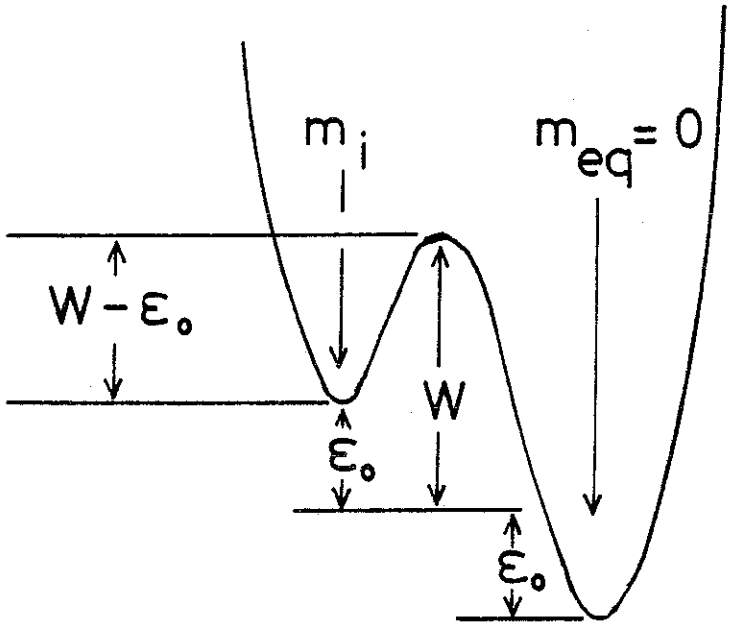

b) Le système est à l'équilibre en champ nul (aimantation nulle). Un champ positif H est appliqué à t = 0.

Nous allons successivement traiter le cas où h est dans le sens ou en sens inverse de H.

1°) $h > 0$ $\qquad M_i \sim \text{th}(\frac{M_g h}{kT}) \qquad\qquad M_{éq} \sim \text{th}(M_g \frac{H+h}{kT})$.

Si $M_g h = \varepsilon_o > kT$, $M_i = M_{éq} = 1$. L'état initial est conservé. Il n'est pas nécessaire de considérer ce cas où il n'y a pas de relaxation.
Si $M_g h = \varepsilon_o < kT$, la relaxation de l'état initial à l'état fondamental

sera gouverné par :

$$W_{eff} \simeq W - M_g H - \varepsilon_o \text{ à } 0{,}7\ k_B T \text{ près}$$

$$\simeq W - M_g H \qquad \text{à } 1{,}7\ k_B T \text{ près}$$

$$\simeq W - M_g H + \varepsilon_o \text{ à } 2{,}7\ k_B T \text{ près.}$$

2°) $h < 0$.

Si $H > |h|$, la barrière effective sera :

$$W_{eff} \simeq W - M_g H + M_g |h| = W + \varepsilon_o - M_g H$$

Si $H < |h|$, $\qquad W_{eff} \simeq W + M_g H - M_g |h| = W - \varepsilon_o + M_g H$

et $M_i = - \text{th} \dfrac{\varepsilon_o}{kT} \qquad M_{éq} = - \text{th}\left(\dfrac{\varepsilon_o - M_g H}{kT}\right)$.

Sitôt que $\varepsilon_o > kT + M_g H$, $M_i = M_\infty = -1$. Il n'y a pas de relaxation. Si $M_g H < \varepsilon_o < kT + M_g H$, il y aura relaxation et $\varepsilon_o \sim M_g H$ à $k_B T$ près.

La barrière effective est alors :

$$W_{eff} \simeq W \text{ à } 1{,}7\ k_B T \text{ près}$$

$$\simeq W + \varepsilon_o - M_g H \text{ à } 2{,}7\ k_B T \text{ près.}$$

Finalement la relaxation de l'état initial à l'état final

- est gouvernée par $\boxed{W_{eff} = W + \varepsilon_o - M_g H}$

avec une approximation à 0,7 ou 2,7 $k_B T$ près selon les cas ;

- peut être représentée par l'image suivante d'un double puits asymétrique :

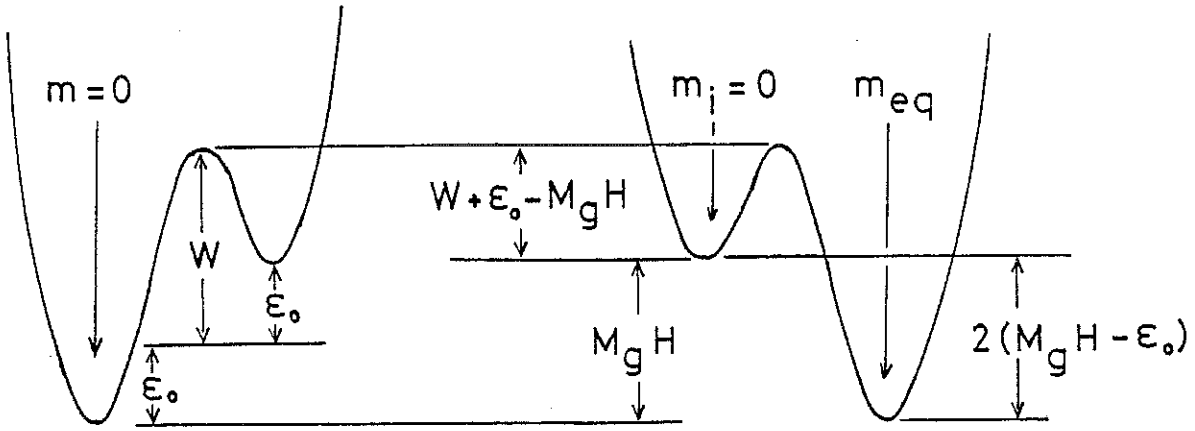

Domaine de validité de ce modèle

1 - Dans la pratique, les valeurs de τ_o ($\sim 10^{-11}$ s) trouvées expérimentalement dans un système tel que CuMn sont telles que, avec les temps de mesure employés ($\sim$ minute), les valeurs de $W_c = kT \text{ Ln } t/\tau_o$ sont de l'ordre de 25 à 30 $k_B T$. Comme nous l'avons vu, les barrières effectives accessibles à l'expérience sont celles de hauteurs égales ou supérieures à W_c. Il est donc possible de faire des approximations de l'ordre de $k_B T$ dans les résultats de notre calcul précédent.

2 - Ce calcul peut se généraliser à des situations microscopiques plus complexes. Pour conserver la possibilité de traiter un tel modèle construit avec les hypothèses simples énoncées au départ, il suffit de supposer que P(W) et P(h) = P(ε_o) sont étendus sur de très larges domaines en énergie et que la distribution d'objets magnétiques (qui ne sont pas forcément des entités fixes dans le temps) soit identifiable statistiquement à une distribution de moments M_g fixes.

Les hypothèses et le domaine de validité de notre modèle étant spécifiés, nous allons en tirer les conséquences sur les propriétés magnétiques d'un système dans l'état verre de spin et les tester expérimentalement sur l'alliage CuMn dans la publication ci-dessous présentée au Journal de Physique.

J. Physique 41 (1980) 1335-1352 NOVEMBRE 1980, PAGE 1335

Classification
Physics Abstracts
75.30 — 75.60

Two-level-systems in spin glasses : a dynamical study of the magnetizations below T_G, application to CuMn systems

J. J. Prejean and J. Souletie

Centre de Recherches sur les Très Basses Températures (*), C.N.R.S., B.P. 166X, 38042 Grenoble Cedex, France

(*Reçu le 11 février 1980, révisé le 19 juin, accepté le 23 juillet 1980*)

Résumé. — Un modèle de distributions d'états à deux niveaux thermiquement activés qui s'impose sur la base des relaxations de l'aimantation et de l'énergie qu'on observe expérimentalement, permet sans autre hypothèse de prédire ou de justifier l'essentiel des phénomènes d'hystérésis dans les verres de spin. On distingue les processus où la température est variée à champ fixe qui conduisent à un état d'équilibre pratique du système et les processus isothermes qui conduisent à une situation hors équilibre et dont la description met en jeu des lois classiques (lois de Rayleigh) en fonction d'une variable réduite T/T_G où T_G comme toute température caractéristique du problème est une fonction du temps t de mesure $\left(T_G \sim \left(\mathrm{Ln}\,\frac{t}{\tau_0}\right)^{-1}\right)$. Des considérations énergétiques fixent une limite supérieure T_c au domaine où ce *scaling* caractéristique d'une transition vitreuse est valable, ce qui permet de concilier les résultats apparemment contradictoires qui font état d'un maximum de la susceptibilité dépendant de la fréquence dans certains systèmes, indépendant de la fréquence dans d'autres. C'est l'existence de distributions bien caractérisées des états à deux niveaux qui est importante plutôt que la description microscopique des objets eux-mêmes cachés derrière le concept d'états à deux niveaux. C'est le désordre qui impose leur caractère aux distributions d'où la généralité du modèle.

Abstract. — A model of distributions of thermally activated two-level-systems (T.L.S.) which imposes itself on the basis of the observed relaxations of the magnetization and of the energy, allows, without further assumptions, to predict or to justify the main features of the hysteresis of spin glasses. We discern the processes where the temperature is varied at constant field which lead to a *quasi equilibrium* from the isothermal processes which lead to a non-equilibrium situation whose description involves classical laws (Rayleigh's laws) in terms of a reduced temperature T/T_G. T_G as any characteristic temperature in the problem is a function of the time t of the measurement : $T_G \sim \left(\mathrm{Ln}\,\frac{t}{\tau_0}\right)^{-1}$. Energetic considerations fix a higher limit T_c to the domain where this *scaling*, characteristic of a glass transition, is valid, which permits to reconcile the apparently contradictory data which report a frequency dependent susceptibility maximum in some systems, a frequency independent one in others. It is the existence of well characterized distributions of T.L.S. which is important rather than the microscopical description of the objects themselves which are hidden behind the T.L.S. concept. This is the disorder which is responsible for the character of the distributions hence for the generality of the model.

1. **Introduction.** — The study of systems of magnetic impurities diluted in noble metal matrices has been a traditional subject of interest in magnetism. The *spin glass* problem deals with the study of the magnetic ordering occurring at low temperatures between randomly distributed magnetic moments interacting through the Rudermann-Kittel-Kasuya-Yoshida interaction. The discovery [1] of a sharp anomaly (the cusp) in the low field susceptibility at a temperature T_G has raised the question of the possibility of a new type of phase transition [2] and has motivated theoretical interest [3]. At temperatures lower than T_G, the existence of time dependent effects in the magnetic properties has been known for a long time [4] but, although phenomenological descriptions exist [5], difficulties remain at several levels. In particular the very presence of unusually long time scales makes problematic the experimental determination of a fundamental state. Further, it appears difficult, at the present time, to reconcile the phenomenological concepts with the pathological variations of the susceptibility at T_G which are suggestive of a phase transition. From a mere experimental point of view contradictions appear :

(*) Laboratoire propre du C.N.R.S., associé avec l'U.S.M.G.

thus one finds [6, 7] or does not find [8] a time dependence of T_G depending on the system which is studied or even on the thermal treatment which the system has experienced [9].

In this paper we will try to clarify some notions and suppress some contradictions by recalling and developing phenomenological arguments of general interest to disordered system with time dependent properties. We will first justify the use of a model involving a distribution of thermally activated asymmetrical double well potentials, then derive the consequencies and illustrate these consequencies with the results of experiments performed mainly on the CuMn system. We will show that it is possible to reach, *in practice*, the fundamental state by field cooling the sample, although any modification of the field at low temperature brings the system out of equilibrium. Non linearities in field and time dependences of the magnetization as well as their consequencies on the reversible susceptibility will also be discussed. We will afterwards speculate about the origin and the nature of the objects hidden behind the abstraction of the double well potential picture and show that it is possible to reconcile the proposed phenomenological description with pathological behaviour occurring at a fixed temperature.

2. **Justification of a model of double well potentials.** — Remanent magnetization measurements [4, 5] were the first which showed the time dependent effects characteristic of the spin glass state. The observation of relaxation of the magnetization after several hours (or several days) implies the existence of unusually large potential barriers which delay the response of some kind of magnetic objects of moment M_s. The non exponential character of these relaxations (apparent for example on figure 4) implies, moreover, a broad distribution $P(W)$ of the values W of the energy of these barriers. This feature is not unexpected in a disordered system where no particular value of W is anticipated. We will therefore assume a distribution $P(W)$ with little or no dependence on W over a considerable range of energies limited to some value W_{max}.

Recent measurements [10, 11] have established that an energy relaxation is always associated with the magnetization relaxations. This fact, among others, implies that the barriers W separate levels of different energies. Let ε_0 be the energy splitting. It is logical to postulate, in a disordered system, the existence of a distribution $P(\varepsilon_0)$ of the zero field splittings for the same reasons which justify the existence of a distribution $P(W)$ i.e. the absence of any priviledged value of the energy. One is then logically led to the concept of a distribution of asymmetrical double well potentials (Fig. 1) for similar reasons to those that led to the models which have been proposed to explain the properties of glasses at very low temperatures [12].

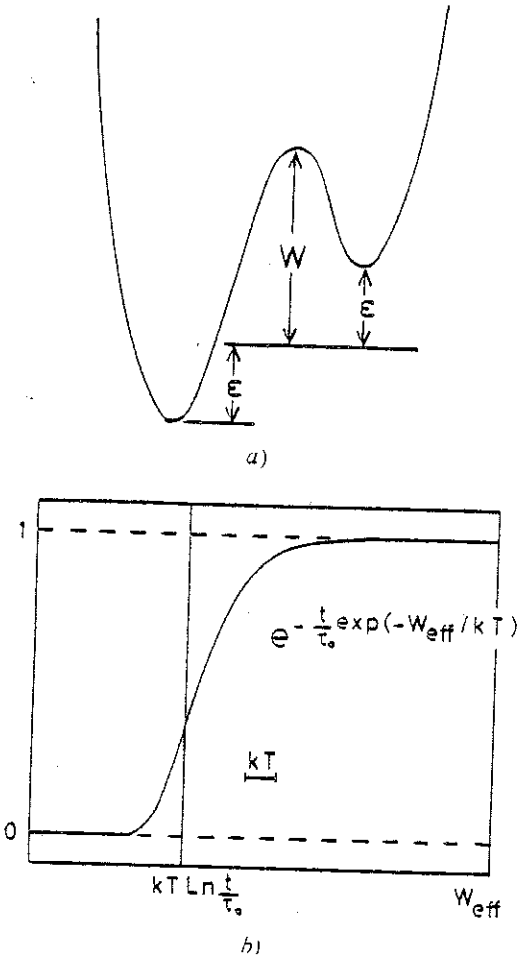

Fig. 1. — An asymmetrical double well potential is represented on figure 1*a* : W is the height of the barrier, ε represents the splitting. The effective barriers for the system are $W_{eff} = W \pm \varepsilon$. Figure 1*b* shows the variations of the relaxation

$$\exp\left(-\frac{t}{\tau}\right) = \exp\left(-\frac{t}{\tau_0}\exp-\frac{W_{eff}}{kT}\right)$$

vs. W_{eff} in an activated process. $W_c = kT \operatorname{Ln}\frac{t}{\tau_0}$ is, with a good approximation, a cut-off in our problem (i.e.

$$\exp\left(-\frac{t}{\tau_0}\right) = \begin{cases} 0 & \text{for } W_{eff} < W_c \\ 1 & \text{for } W_{eff} > W_c \end{cases}$$

if $W_c \gg 2$ or $3\,kT$ (the width of the transition). In CuMn, the order of magnitude of W_c is $25\,kT$ in the usual time scale measurement.

A physical barrier can be crossed either by tunnelling or by thermal activation. While the first process is important in the models considered for the low temperature properties of glasses, it is easy to show experimentally that thermal activation is the phenomenon which governs the relaxations of a spin glass. The relaxation time in this case is given by the Arrhenius law $\tau = \tau_0 \exp\frac{W - \varepsilon_0}{kT}$. The remanent magnetization of objects of moment M_s involves an integration over the values of W and ε_0. Formally we will have to integrate relaxations of the form $M_s \exp -\frac{t}{\tau}$ over the distributions of W and ε_0.

The consideration of the variations of

$$\exp - \frac{t}{\tau_0 \exp \frac{W - \varepsilon_0}{kT}}$$

in terms of W shows that in practice and to a very good approximation (see Fig. 1*b*) :

$$\exp - \frac{t}{\tau_0 \exp \frac{W - \varepsilon_0}{kT}} \begin{cases} = 0 \text{ for } W - \varepsilon_0 < W_c \\ = 1 \text{ for } W - \varepsilon_0 > W_c \end{cases} \quad (1)$$

$\left(\text{where } W_c = kT \operatorname{Ln} \frac{t}{\tau_0}\right)$ and it is therefore possible to put $\exp - \frac{t}{\tau} = 1$ in the integration provided it is restricted to the values $W > W_c + \varepsilon_0$. Inasmuch as $P(\varepsilon_0)$ and $P(W)$ do not depend strongly on the temperature the remanent magnetization (as any other thermodynamic quantity) will be obtained after integration over W and ε_0, as a function of the cut-off $W_c = kT \operatorname{Ln} \frac{t}{\tau_0}$. The measurement time t therefore is always associated with the temperature in such a way that it is possible to observe the same effects in terms of the temperature at fixed time or in terms of log t at fixed temperature. This time temperature correspondance is characteristic of the Arrhenius law and of an activated process. One can check (Figs. 18 and 19) that it was possible to superimpose the temperature and the time dependences of the remanent magnetization of a CuMn 8 at. % in a unique diagram of the variable $kT \operatorname{Ln} \frac{t}{\tau_0}$ (despite the fact that the observed variations which cover several decades in magnitude depart strongly from a simple linearity in T or $\operatorname{Ln} \frac{t}{\tau_0}$). This correspondance allows the characteristic time τ_0 to be determined. We have found τ_0 to be of the order of 10^{-11} s in CuMn for concentrations between 1 and 8 at. % (see chapter 12).

We are now in possession of a model which allows us to make non trivial predictions (such as the above mentioned time-temperature correspondance). This model is by no means new. In the abstract shape in which it is presented, it covers descriptions which have been widely used to describe for example the plasticity of glasses, rubbers and polymers [13] near their glass transition or the magnetism of fine particles (Néel). This generality implies analogies, which can be checked by experiments between properties *a priori* as different as the magnetization of a spin glass and the extension of a rubber [14]. We will make use in what follows of the ideas and vocabulary which were developed by Néel [15], in his description of the properties of small particles (where $\varepsilon_0 = 0$: the double well potentials are symmetrical) or in his theory of magnetism in the Rayleigh domain (in this case the model makes use of two independent random variables and can consequently be identified with the one we use here).

3. **Isothermal processes and field cooling processes. The (quasi) equilibrium state of the systems.** — With the time entering as a third variable the specification of the field and the temperature is not sufficient to determine the magnetization. The hysteresis cycle exemplifies this indeterminacy. The evolution of the magnetization within the hysteresis cycle will depend not only on the time t which is spent on the measurement but also on the thermal path $\mathcal{C}(H(t), T(t))$ through which the chosen initial state has been built up.

In other words the future behaviour of the sample is determined by its history. It is in principle always possible to express a thermal path as the sum of elementary paths where the magnetic field is modified at a constant temperature and where the temperature is modified at constant field ; such paths, because of their simplicity, are chosen by the experimentalist. It is therefore logical to study the isothermal response to a varying field and the response to a constant field when the temperature is varied.

In an isothermal process, the argument leading to equation (1) tells us (see Fig. 1) that a field h such that $M_g h + \varepsilon_0 > W - W_c$ is needed to overcome a barrier W $\left(\text{with } W_c = kT \operatorname{Ln} \frac{t}{\tau_0}\right)$. This means that at low temperature all the energy of the potential barrier must be supplied by the field.

In contrast, in a field cooling process, the magnetization is *blocked* at a temperature T_B such that

$$W + \varepsilon_0 - M_g h = kT_B \operatorname{Ln} \frac{t}{\tau_0} .$$

The magnetic state of the object (the state in which it remains when the temperature is further decreased) is then determined by $th\left(\frac{M_g h - \varepsilon_0}{kT_B}\right)$. The ratio

$$\frac{M_g h - \varepsilon_0}{kT_B} = \frac{(M_g h - \varepsilon_0) \times \operatorname{Ln} \frac{t}{\tau_0}}{W - M_g h + \varepsilon_0}$$

is larger than 1 $\left(\text{and } th \frac{M_g h - \varepsilon_0}{kT_B} \text{ is saturated}\right)$ as soon as $\varepsilon = M_g h - \varepsilon_0$ is of the order of or larger than W/Q $\left(\text{where } Q = \operatorname{Ln} \frac{t}{\tau_0}, \ Q \text{ is of the order}\right.$ of 25 for usual values of t and τ_0) : the system has already chosen its equilibrium state (the lower side of the two-level-systems) at the blocking temperature. In other words we only need to provide an energy $M_g h - \varepsilon_0 = W/25$ to overcome a barrier W in a field cooling process (instead of W at low T). With

our assumptions on the distributions $P(\varepsilon_0)$ and $P(W)$ therefore, the field cooled magnetization $M_a(H, T)$ cannot differ from the thermodynamic equilibrium curve by more than 4 % $(1/Q)$ of the maximum deviation which can be obtained in the same field at temperature T (that is 4 % of the actual width of the hysteresis cycle at temperature T in field H). Neglecting this difference we can define $M_a(H, T)$ as a *practical* determination of the fundamental state.

4. **The field cooled magnetization as the equilibrium magnetization. Experimental evidence.** — Figure 2 shows the magnetization curves obtained for decreasing fields (starting from 75 kOe) at different temperatures in CuMn 8 at.%. At temperatures below $T_G = 40$ K we observe hysteresis. At very

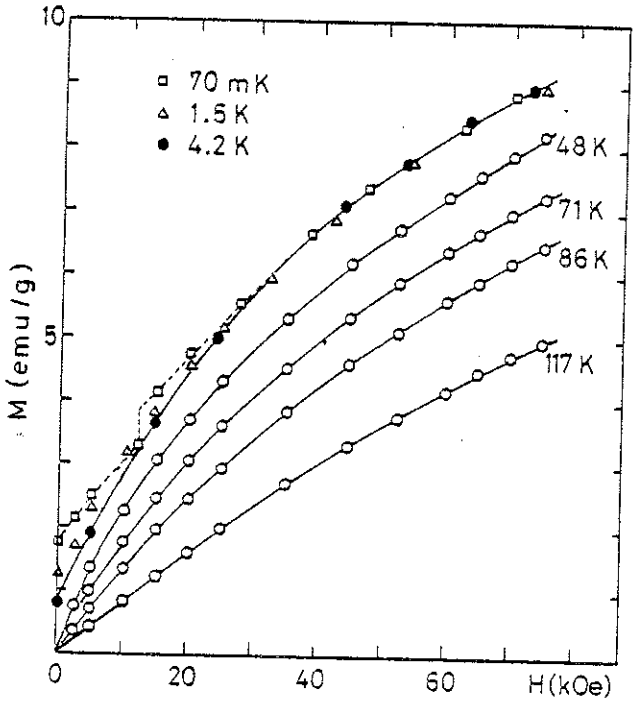

Fig. 2. — The magnetization of a CuMn 8 at. % *vs.* the field H is shown at different temperatures. For $T \geqslant T_G$(40 K), the magnetization does not present any hysteresis. The magnetization curves represented for $T < T_G$ were obtained after cooling the sample in 75 kOe from $T > T_G$ down to $T = 4.2$ K (●), 1.5 K (△) and 70 mK (□) and decreasing the field.

low temperatures we also observe in positive fields the existence of *magnetization jumps* as reported by Tournier in AuFe [4]. These processes reminiscent of Barkhausen jumps in ferromagnetics, by which part of the remanent magnetization is globally reversed in the magnetic field, call for an interpretation different from the one which we propose here. Far from the jump, the general behaviour tends to recover the slower variations that our model attempts to describe, and obeys rules of general validity for all spin glasses.

Once a remanent magnetization has been built up the response of this magnetization to a small transverse field or to an inverse field is very system dependent. In CuMn a very small inverse field H_r is sufficient to reverse completely the remanent magnetization as a whole. Very small quantities (a fraction of one at. %) of non magnetic impurities known to have strong spin orbit coupling are sufficient to increase very strongly the value of H_r to the point of making the magnetization reversal vanish completely, although the values of the magnetization are not greatly modified. This macroscopic response of the remanent magnetization is studied in detail in another work [16]. Here we are concerned only with the initial development and the evolution of the magnetization along the axis of the field (which has been used to build it up).

The field cooled magnetization (Fig. 3) exhibits the behaviour expected for an equilibrium magnetization : it is single valued and stable. When the system is pushed out of balance it tends to relax

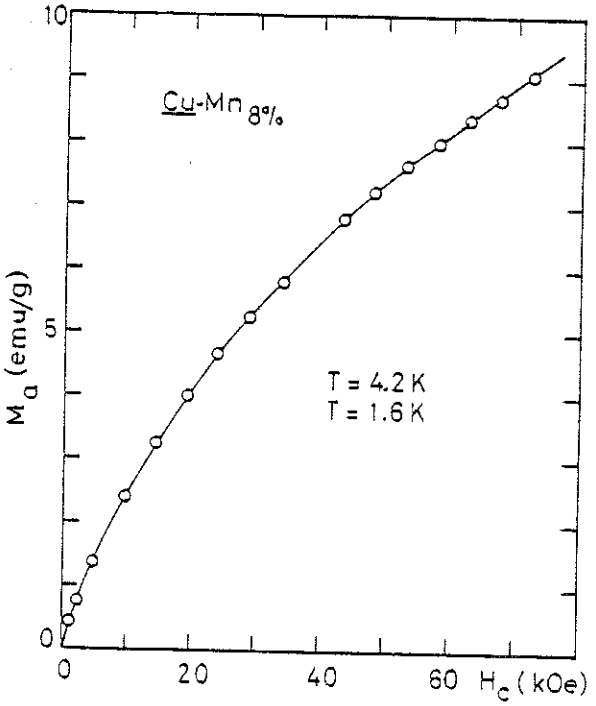

Fig. 3. — The field cooled magnetization $M_a(H_c)$ is shown *vs.* H_c at 1.6 K and 4.2 K. In a field cooling process, the field H_c is applied at $T > T_G$ and the temperature is subsequently decreased. $M_a(H)$ is time independent as long as H_c stays applied. In CuMn, $M_a(H)$ is not very sensitive to the temperature.

towards the equilibrium curve with liberation of energy [10, 11]. These properties are illustrated on figure 4 which shows $M_a(h, T = 20\ \text{K})$ for a CuMn 8 at. %. Each point has been obtained by field cooling the sample from $T \gg 40$ K (T_G). $M_a(H, T)$ has a normal behaviour. It goes to zero in zero field : it can be developed in terms of odd powers of the field and remains time independent as long as the field stays applied. The application, at low temperatures, of a field variation ΔH (however small it may be) has the effect of creating a non equilibrium magnetization which always evolves as a function

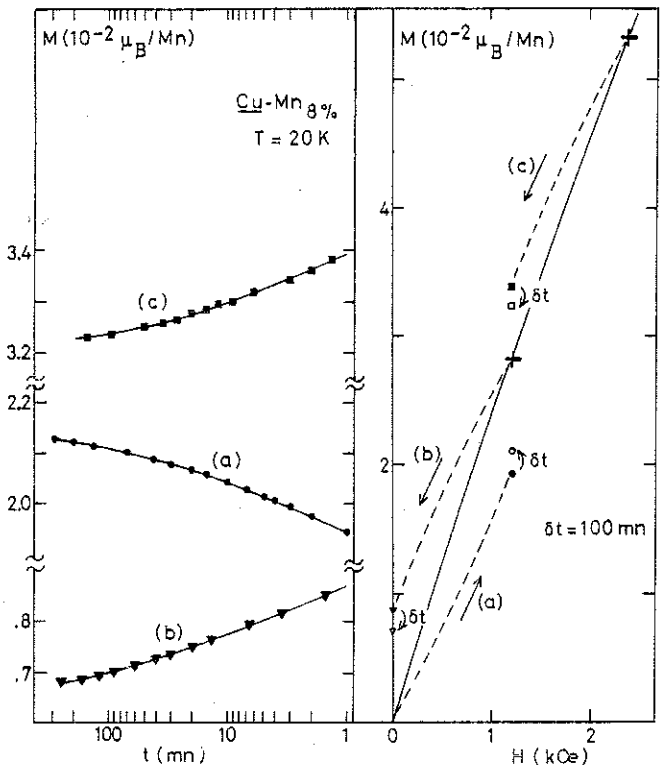

Fig. 4. — Starting from $M_a(H_c)$ (solid line), small isothermal variations ΔH of the field induce magnetization relaxations in the direction of $M_a(H_c + \Delta H)$: (*a*) $H_c = 0, \Delta H = 1.2$ kOe, (*b*) $H_c = 1.2$ kOe, $\Delta H = -1.2$ kOe, (*c*) $H_c = 2.4$ kOe, $\Delta H = -1.2$ kOe. The corresponding pseudologarithmic relaxations are shown *vs.* time on the left side of the figure (the origin of time is taken when the field reaches final value $H_c + \Delta H$).

of time towards the magnetization $M_a(H + \Delta H)$ which represents in principle the equilibrium in the new field. Notice in figure 3 the pseudologarithmic dependences which cannot be explained with a unique relaxation time. We have checked elsewhere [11] that these magnetization relaxations are always associated with an *energy relaxation* from the sample to the bath, irrespective of the fact that the magnetization may increase or decrease.

It seems therefore that there exists for each field an equilibrium corresponding to a fundamental state of minimum energy towards which the system tends to relax at long times. This equilibrium corresponds with a good accuracy to the situation which is reached by field cooling the sample. This, incidentally, is consistent with the fact that no time dependent anomaly has been so far observed in specific heat measurements [17], since in this purely thermal procedure the system is always at equilibrium. It implies conversely that such time effects should be present if a field is applied or removed at low temperatures. Let us make it clear however that effects associated with a purely thermal treatment should become apparent either at a higher order of sensitivity or if the coefficient $Q = \mathrm{Ln}\,\frac{t}{\tau_0}$ could be made much smaller than the usual value of 25. The practical interest of the curve $M_a(H)$ is evident since the knowledge of the response at infinite times amounts to the knowledge of the distribution $P(\varepsilon_0)$. From now on, we will prefer to deal with the actual experimental curve $M_a(h)$ using only the additional hypothesis of a distribution $P(W)$ of barrier heights which determines the evolution of the system in time.

It can be seen in figure 3 that $M_a(H, T < T_G)$ in CuMn 8 at. % depends very little on the temperature. This behaviour which is shared with most of the archetypical spin glasses (AuFe, AuCr, AuMn, AgMn, ...) at low enough concentrations is, however, not general. A rather strong (but always monotonic) temperature dependence is found below T_G in systems such as PtCo [18], where a strong exchange enhancement of the lattice is known to exist ; precipitations associated with a tendency to ferromagnetism may also be responsible for a similar behaviour.

Starting now from a point on the equilibrium curve $M_a(H_0, T)$ we will consider the isothermal response to the first application of a field variation ΔH_F, followed by a decrease of ΔH_R opposite and smaller than any previous variation, using the data of $M_a(H)$ at equilibrium and assuming a distribution $P(W)$ of barriers to fix the time dependences. The definitions which we introduce here are important since the model implies different responses to the first application and to a subsequent decrease [15]. (The first application is performed on a system at equilibrium.)

5. **Isothermal application ΔH_F and decrease ΔH_R of a field.** — Starting from $M_a(H_0)$ the response to the first application of a field variation ΔH_F followed by a decrease ΔH_R would be at infinite times :

$$M(H_0 + \Delta H_F - \Delta H_R) = M_a(H_0) + \int_{H_0}^{H_0 + \Delta H_F - \Delta H_R} M_a'(H)\,\mathrm{d}H = M_a(H_0 + \Delta H_F - \Delta H_R)\,. \qquad (2)$$

At finite times we would have :

$$M(H_0 + \Delta H_F - \Delta H_R) - M_a(H_0) = \int_0^{W_c} P(W)\,\mathrm{d}W \int_{H_0}^{H_0 + \Delta H_F - \Delta H_R} M_a'(H)\,\mathrm{d}H + \int_{W_c}^{W_c + \overline{M}_s \Delta H_F} P(W)\,\mathrm{d}W \times$$

$$\times \int_{H_0}^{H_0 + \Delta H_F - \frac{W - W_c}{\overline{M}_s}} M_a'(H)\,\mathrm{d}H + \int_{W_c}^{W_c + \overline{M}_s \frac{\Delta H_R}{2}} P(W)\,\mathrm{d}W \int_{H_0 + \Delta H_F - \frac{W - W_c}{\overline{M}_s}}^{H_0 + \Delta H_F - \left(\Delta H_R - \frac{W - W_c}{\overline{M}_s}\right)} M_a'(H)\,\mathrm{d}H \qquad (3)$$

(where we have assumed that we can use some average value $\overline{M}_g$ for the moments of the objects). The first term is the response of those objects which are at thermodynamic equilibrium, W being smaller than W_c. The second and the third terms account for the responses to the increase ΔH_F and to the decrease ΔH_R respectively, of those objects for which the effective barrier $W - W_c$ is overcome by the field variation. If the contribution $\overline{M}_g$ was obtained at dH with $W - W_c = 0$, we would have to provide an extra field $\frac{W - W_c}{\overline{M}_g}$ in the direction of the field variation in order to overcome the energy of the barrier (Fig. 5). Thus we have to add the contributions of all W such that $\overline{M}_g\, dH + (W - W_c) < \overline{M}_g \Delta H_F$ for ΔH_F and subtract for $\Delta H_R (| \Delta H_R | < \Delta H_F)$ that of all objects $\overline{M}_g\, dH - (W - W_c) > \overline{M}_g(\Delta H_F - \Delta H_R)$. Those two relations fix the integration limits on dH and W in equation (3).

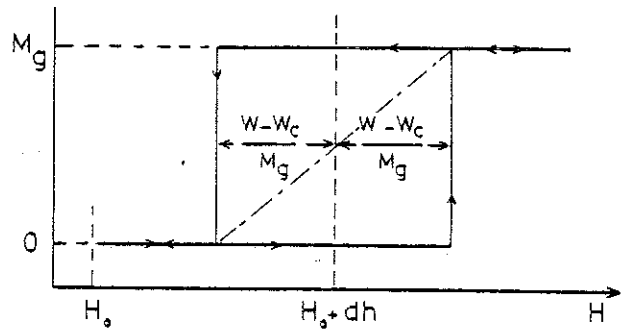

Fig. 5. — Schematic response of a double well potential to an external field. $(W - W_c)$ is the value of the effective barrier (at temperature T) which must be overcomed by the applied field. The dashed dotted line shows the response to a field transverse to the anisotropy axis.

In the so-called *Rayleigh domain* i.e. for excursions $M_g \Delta H_F \ll W_{max} - W_c$, we obtain, assuming we can linearize the variation of $M_a(H)$ in the vicinity of $M_a(H_0)$,

$$M(H_0 + \Delta H_F - \Delta H_R) - M_a(H_0) \simeq$$

$$\simeq A(\Delta H_F - \Delta H_R) + B(\Delta H_F)^2 - \frac{B}{2}(\Delta H_R)^2 . \quad (4)$$

The reversible susceptibility A is proportional to $T \operatorname{Ln} \frac{t}{\tau_0}$:

$$A = M_a'(H_0)\, P(0)\, kT \operatorname{Ln} \frac{t}{\tau_0} \quad (5)$$

in the low temperature limit. The coefficient B of the quandratic terms is independent of $T \operatorname{Ln} \frac{t}{\tau_0}$ in the same limit

$$B = M_a'(H_0)\, P(0)/2\, \overline{M}_g . \quad (6)$$

Notice the classical results [15] known as Rayleigh's laws : the response is quadratic in the field variation (1st law) ; the coefficient of the quadratic term is twice as large during the first application of the field than in any subsequent decrease (2nd law). An illustration of this behaviour is shown in the figure 6.

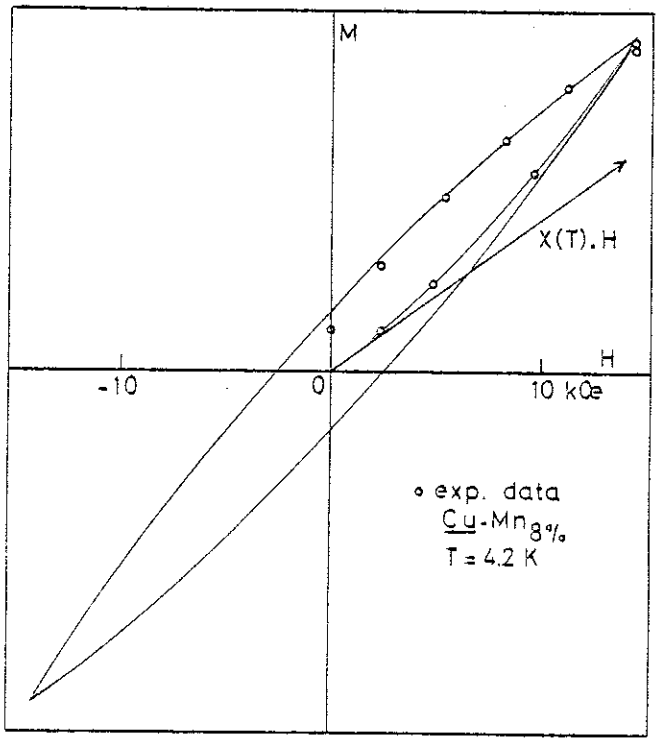

Fig. 6. — The magnetization of a CuMn 8 at. % in the Rayleigh domain at 4.2 K. The deviations to an ideal behaviour (solid line) noticed in zero field are accounted for by the relaxation of the magnetization during the time necessary to increase and decrease the field.

Out of the Rayleigh domain, when $\overline{M}_g \Delta H_F$ becomes larger than the maximum height $W_{max} - W_c$ of the effective barriers the integration has to be extended over the whole distribution $P(W)$. We have then :

$$M(H_0 + \Delta H) = M_a(H_0 + \Delta H) - \int_{W_c}^{\infty} P(W)\, dW \int_{H_0 - \Delta H - \frac{W - W_c}{\overline{M}_g}}^{H_0 - \Delta H} M_a'(H)\, dH \simeq$$

$$\simeq M_a\left(H_0 + \Delta H - \int_{W_c}^{\infty} P(W) \left(\frac{W - W_c}{\overline{M}_g}\right) dW\right). \quad (7)$$

The magnetization tends therefore towards a limiting curve which is obtained by translating the equilibrium curve along the field axis by the quantity :

$$\delta H = \frac{1}{\overline{M}_g} \int_{W_c}^{\infty} P(W)\,(W - W_c)\,\mathrm{d}W\,. \qquad (8)$$

6. **Case of a constant density of energy barriers.** — Let us assume

$$P(W) = P(0) = \frac{1}{W_{max}} \quad \text{for} \quad W < W_{max}$$
$$= 0 \qquad \text{for} \quad W > W_{max}\,.$$

This simplification allows us to obtain expressions which, despite the crudeness of the model, give a fairly good qualitative description of the phenomena.

Defining :

$$W_{max} = \frac{1}{P(0)} = kT_G \,\mathrm{Ln}\,\frac{t}{\tau_0} = \overline{M}_g\, H_g \qquad (9)$$

and using reduced units $\theta = T/T_G$ and $\eta = H/H_g$ we have :

a) In the Rayleigh domain i.e. for $\eta < 1 - \theta$

$$\Delta M(\eta_F - \eta_R) = m'_a \left\{ (\eta_F - \eta_R)\,\theta + \frac{\eta_F^2}{2} - \frac{\eta_R^2}{4} \right\} \qquad (10)$$

if η_F corresponds to the initial increase and η_R to the subsequent decrease of the field and where we have introduced

$$m'_a = \frac{\mathrm{d}M_a(\eta)}{\mathrm{d}\eta} = H_g\; M'_a(H)\,.$$

b) Beyond the Rayleigh domain (i.e. for $\eta > 1 - \theta$) from (8) the limiting curve is obtained by a translation $(1 - \theta)^2/2$ of the equilibrium curve

$$M_a(\eta) \to M_a\left(\eta \pm \frac{(1-\theta)^2}{2}\right). \qquad (11)$$

These two expressions (10) and (11) allow a simple description of the behaviour of the magnetization below the glass temperature T_G of the system.

7. **Description of the magnetization.** — The equilibrium curve $M_a(\eta)$ is given by experiment.

— The limiting hysteresis cycle $M_a\left(\eta \pm \frac{(1-\theta)^2}{2}\right)$ is obtained by translating $M_a(\eta)$ by $\pm \frac{(1-\theta)^2}{2}$ along the field axis (Fig. 7).

— By cooling the sample in zero field we start from an equilibrium point with zero magnetization. The first application η_F of a field then allows, starting from equilibrium, the ascending branch of the limiting hysteresis cycle to be reached, for $\eta \geqslant 1 - \theta$, through a Rayleigh parabola $m'_a\,\eta_F\left(\theta + \frac{\eta_F}{2}\right)$. One thus describes the first magnetization curve. Notice the presence of a reversible thermodynamic initial susceptibility $m'_a\,\theta$ $\left(\text{proportional to } T\,\mathrm{Ln}\,\frac{t}{\tau_0}\right)$.

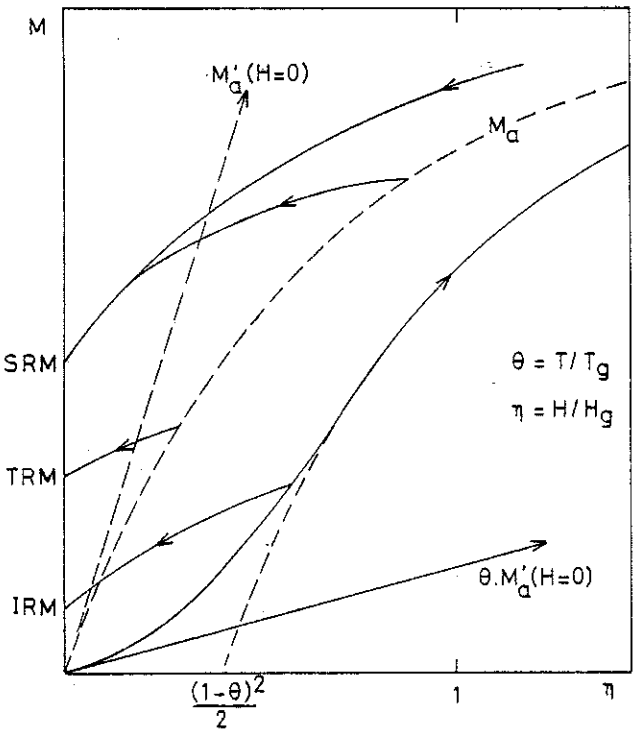

Fig. 7. — Schematic representation of the predicted behaviour of the different magnetizations below T_G. The limiting hysteresis cycle is obtained by translating the equilibrium curve $M_a(\eta)$ by $\pm \frac{1}{2}(1-\theta)^2$ along the field axis. Starting from $M_a(\eta)$, a field variation opposite and equal to the cooling field η yields the *T.R.M.* The first magnetization curve is obtained by a field variation η, starting from $M_a(0)$. The *I.R.M.* is the result of a field decrease starting from the first magnetization curve. Notice the presence of a reversible susceptibility proportional to θ.

Starting now from the ascending branch, the descending branch of the limiting cycle can be reached through a Rayleigh parabola $m'_a\,\eta_R\left(\theta + \frac{\eta_R}{4}\right)$ (for $|\eta_R| \leqslant 2(1-\theta)$) by decreasing the field.

The agreement with experiment is discussed in chapter 11. There are two features which the model fails to describe.

1. It does not account for the presence of a large reversible susceptibility at $T = 0$.

2. Experimentally the ascending and descending branches of the hysteresis cycle join in large fields. They can not be deduced from each other by a simple translation. We will discuss later the natural interpretations that one can make of these discrepancies.

8. **The remanent magnetization.** — Particular interest is attached to the remanent magnetization obtain-

ed after the applied field has been removed, because it inevitably affects the results of measurements in low fields (and the susceptibility).

— The thermoremanent magnetization, *T.R.M.* is obtained by cooling in a magnetic field and removing the field at low temperatures. It is therefore (on our definitions) the result of a first application η_F equal and opposite to the field in which the sample has been cooled.

— The isothermal remanent magnetization (*I.R.M.*) is obtained by a retrogression from the first magnetization curve. Both the *T.R.M.* and the *I.R.M.* saturate to the value *S.R.M.* where the descending branch of the limiting hysteresis cycle cuts the magnetization axis (Fig. 7).

Inasmuch, therefore, as one can neglect the curvatures of $M_a(\eta)$ over the range $0 < \eta < 2(1 - \theta)$ one obtains easily from equations (10) and (11) :

$$S.R.M. = m'_a \frac{(1-\theta)^2}{2} \tag{12}$$

$$T.R.M. = m'_a \eta \left(1 - \theta - \frac{\eta}{2}\right) \quad \text{for} \quad \eta \leqslant 1 - \theta \tag{13}$$

$$= S.R.M. \quad \text{for} \quad \eta \geqslant 1 - \theta$$

$$I.R.M. = m'_a \frac{\eta^2}{4} \quad \text{for} \quad \eta \leqslant 1 - \theta$$

$$= S.R.M. - m'_a \frac{(2(1-\theta) - \eta)^2}{4} \quad \text{for} \quad 1 - \theta \leqslant \eta \leqslant 2 - \theta \tag{14}$$

$$= S.R.M. \quad \text{for} \quad \eta \geqslant 2 - \theta .$$

The comparison of figure 8 with figures 15 and 19 shows that those predictions are, considering the roughness of the assumptions, in good agreement with the experimental results. In particular it is found, in agreement with experiment, that the remanent magnetizations are more easily saturated the higher the temperature. For a given field $\eta \ll 1$ there always exists a regime in the vicinity of T_G where $\theta + \eta > 1$ and the *T.R.M.* is saturated. Below this regime the *T.R.M.* is a linear function of the temperature in agreement with the experimental results (Fig. 8*b*).

Notice however that the model does not account for the occurrence of a maximum in the dependence of the *T.R.M.* on the magnetic field η (see Fig. 15 and previous data from Tholence [4]).

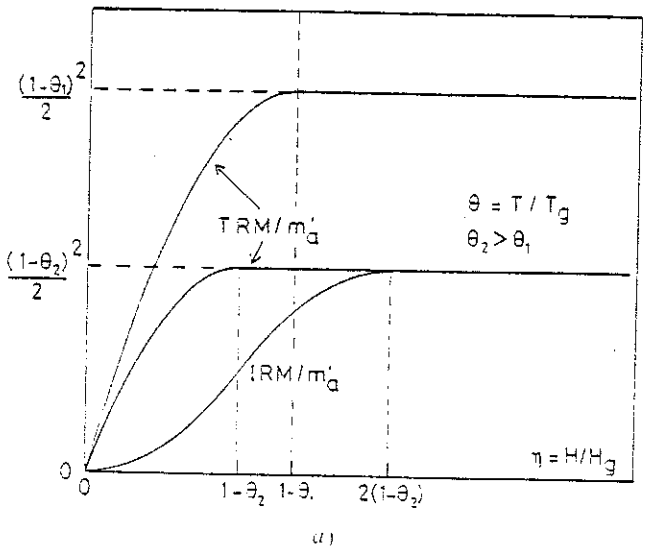

a)

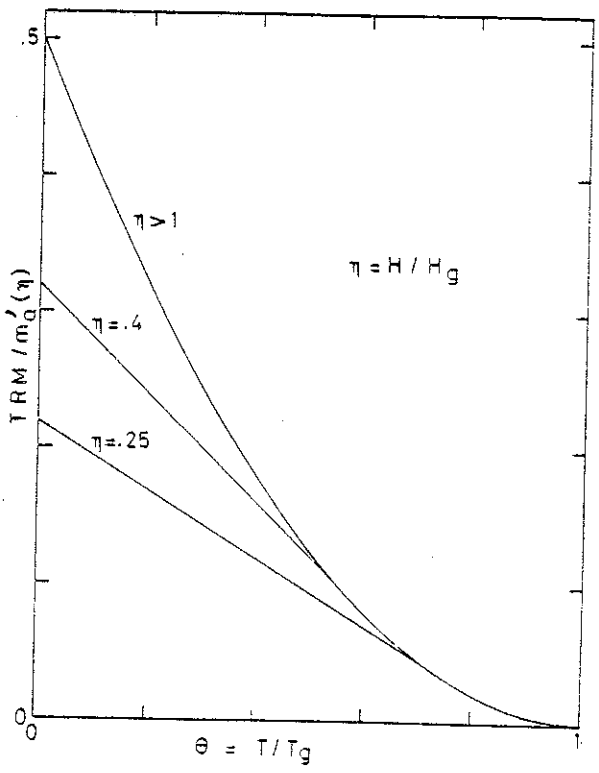

b)

Fig. 8. — (*a*) The predicted variation of the *T.R.M.* and the *I.R.M.* in terms of the reduced field η at fixed values of the reduced temperature θ. (*b*) The predicted variations of the *T.R.M. vs.* θ for different values of the reduced field η. For $\eta > 1$, the *T.R.M.* is saturated and follows a parabola $\left(S.R.M. = M'_s \frac{(1-\theta)^2}{2}\right)$. For $\eta < 1$, the *T.R.M.* is linear in θ for $\theta < 1 - \eta$ and reaches the saturated regime as soon as $\theta > 1 - \eta$.

9. **Susceptibilities.** — By cooling the sample in a small field η we obtain $M_a(\eta) \simeq m'_a \eta$. When the field η is withdrawn at low temperature we are left with the *T.R.M.* in the field η. *By definition of the low temperature reversible susceptibility* χ_{rev} *we have therefore* :

$$\chi_{rev}\,\eta = m'_a\,\eta - T.R.M. = m'_a\,\eta\left(1 - \frac{T.R.M.(\eta)}{M_a(\eta)}\right) \tag{15}$$

from which we get

$$\chi_{rev} \simeq m'_a\left(\theta + \frac{\eta}{2}\right) \quad \text{for} \quad \theta \leqslant 1 - \eta$$

$$= m'_a\left(1 - \frac{(1-\theta)^2}{2\,\eta}\right) \quad \text{for} \quad 1 - \eta \leqslant \theta \leqslant 1\,. \tag{16}$$

One would obtain the same result by defining $\chi_{rev}\,\eta$ as the first magnetization decreased from the *I.R.M.* in the same field. This result is made of two parts. $m'_a\,\theta$ is the thermodynamic contribution due to those barriers $W < W_c$ which are at thermal equilibrium at temperature T in the time of the measurement. The other contribution, which is anomalous, is due to those barriers $W > W_c$ over which the applied field can induce transitions. This magnetization, initially proportional to η^2, is responsible for a susceptibility which is proportional to η for small values of η.

The figure 9 shows the expected variation of $\chi_{rev}(\eta)/m'_a(\eta)$ as a function of θ for different values of η between 0 and 1. The increasing curvatures which are expected for increasing fields account reasonably well for the experimental observations of for example Sarkissian *et al.* [19]. See also on figure 20 our results on CuMn 8 at. %. For η fixed however small it may be, there always exists a domain in the vicinity of T_G where $\theta + \eta > 1$ and deviations from linearity in θ are observed.

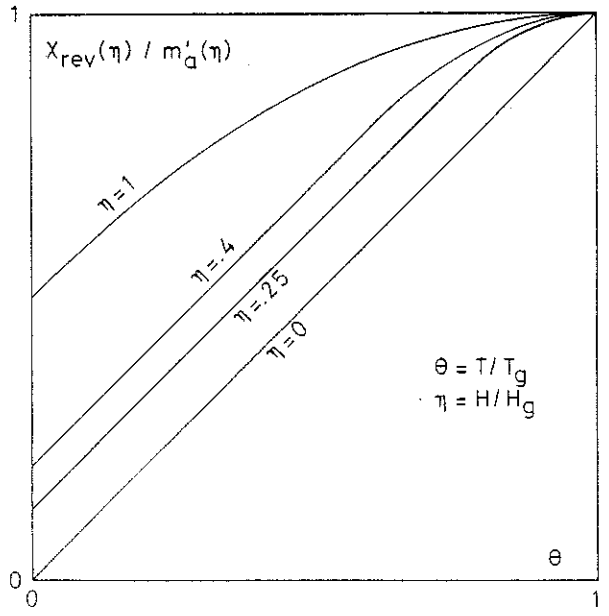

Fig. 9. — Evolution of the predicted reversible susceptibility *vs.* the reduced temperature θ for increasing values of the reduced field η.

We have expressed our data in terms of $m'_a(\eta)$, the susceptibility of the equilibrium magnetization. Figure 9 represents the actual susceptibility variations in systems like CuMn (or AuFe, AgMn, ... at low concentrations) where m'_a does not depend too much on the temperature. We show in figure 10 *a* and *b* the expected behaviours of χ_{rev} when m'_a is given by a Curie-Weiss and by a Curie law respectively. If, as in PtCo [18] and other exchange-enhanced or cluster-enhanced systems, the equilibrium susceptibility evolves from Curie like to Curie-Weiss like behaviour, the susceptibility maximum can appear at a temperature T_{max} different from T_G where the remanences vanish. Obviously in such cases, T_{max}, is a totally irrelevant quantity.

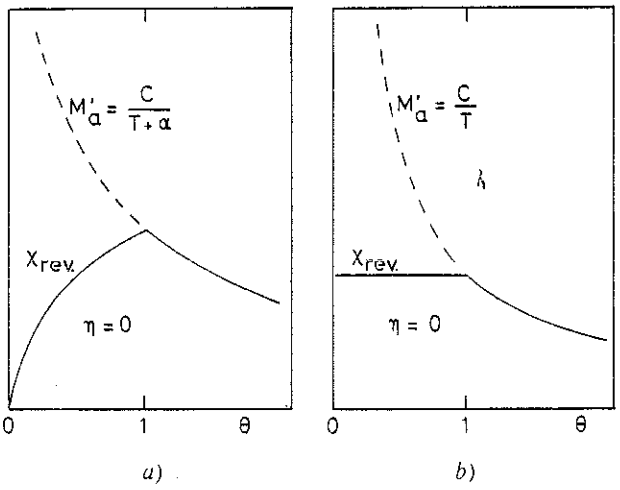

a) *b)*

Fig. 10. — Predicted behaviour of the low field susceptibility when the equilibrium susceptibility M'_a follows a Curie-Weiss law (Fig. *a*) and a Curie law (Fig. *b*).

10. **Edwards and Anderson's** q **parameter.** — We have seen above that the reversible susceptibility can be expressed as $m'_a\left(1 - \frac{T.R.M.(\eta)}{M_a(\eta)}\right)$. This expression allows to identify in the limit $\eta \to 0$ the ratio $T.R.M.(\eta)/M_a(\eta)$ with the parameter $q(t)$ which measures the average $\langle S(t)\,S(0)\rangle$ of the correlation of the magnetization of a site at time t with the value that it had at time $t = 0$. Physically this formula implies that starting from an unmagnetized sample only those objects for which the correlation has vanished at time t, have acquired their equilibrium magnetization. The correlated objects on the contrary keep the memory of the initially unmagnetized state. Thus the *T.R.M.* in small fields provides a direct measurement of $q(t)$ whose long time limit is the parameter q which Edwards and Anderson proposed to use as the *order parameter* characteristic of an eventual phase transition to a *spin glass phase* [2]. With our assumptions ($P(W) = P(0)$ for $W < W_{max}$) $q(t)$ depends linearly on the temperature and vanishes at $\theta = 1$, i.e. at the temperature $T_G \sim \frac{W_{max}}{\mathrm{Ln}\,\frac{t}{\tau_0}}$ (Fig. 11). In other words $q(t)$ vanishes at

long times and $q = 0$. This conclusion is in agreement with the analysis by Bray and Moore of their Monte Carlo results [20]. For comparison with the experiments, remember that $M_a(\eta)$ does not include the reversible contribution $\chi_0 \eta$ which is not accounted in our model and which will be considered later.

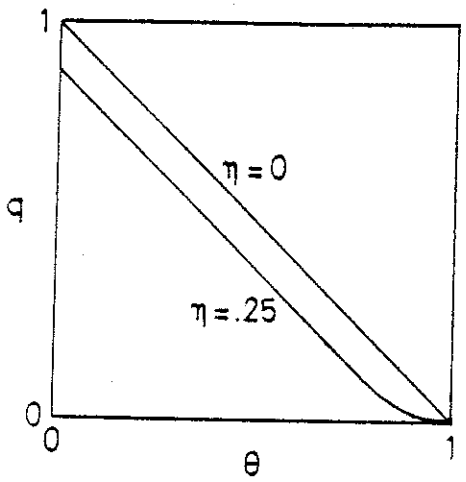

Fig. 11. — Predicted behaviour of the correlation function $q = \langle S(t).S(0) \rangle$ *vs.* the reduced temperature θ for two values of the reduced field η.

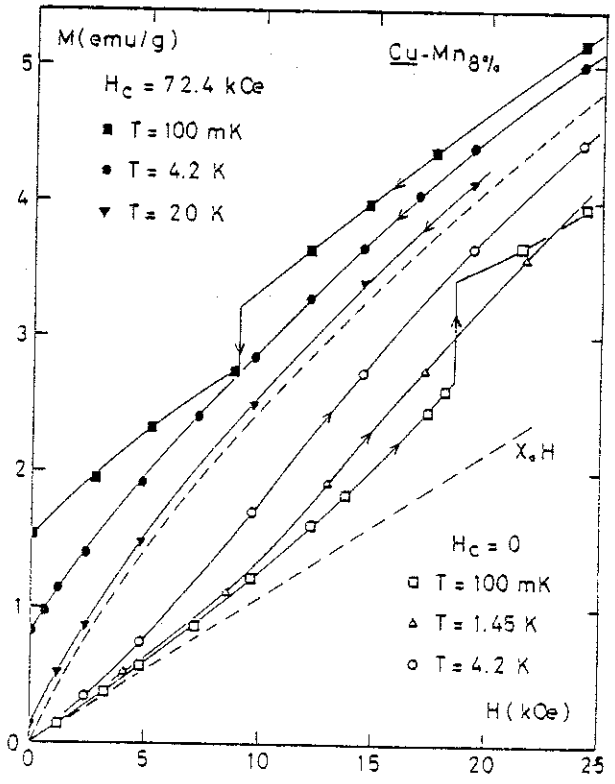

Fig. 12. — The magnetizations of a CuMn 8 at. % *vs.* field at different temperatures below T_G. The dashed curve is the equilibrium magnetization shown in figure 3. The first magnetization curves at 100 mK (□), 1.45 K (△) and 4.2 K (○) are obtained in increasing fields, starting from the zero field cooled sample. The descending branches of the limiting hysteresis curves at 100 mK (■), 4.2 K (●) and 20 K (▼) are obtained in decreasing fields, starting from the field cooled magnetization in 72.4 kOe. Notice the impredicted reversible susceptibility at $T = 0$ (dashed line) and the magnetization jumps at the lowest temperature.

11. **Qualitative comparison with the experiment.** — The equilibrium curve $M_a(H)$ being given, figure 12 shows how the first magnetization curve is obtained by the first application of a field, starting from the point of zero magnetization. There is indeed an initial term quadratic in the field variation as shown on figure 13 but the presence of a large reversible susceptibility χ_0 is not predicted by the model. By translation along this reversible magnetization $\chi(T = 0) H$, the equilibrium curve $M_a(H)$ can be superposed on the ascending branch of the limiting cycle (in small and in moderate fields).

The *T.R.M.* is obtained, starting from $M_a(H)$, when the field variation is equal and opposite to the field applied during the cooling process. For large fields (above the Rayleigh regime) the descending

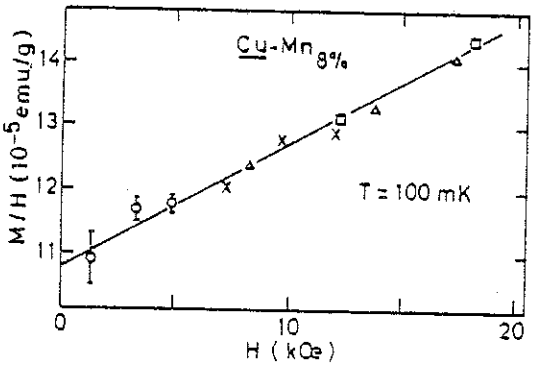

Fig. 13. — The first magnetization curve of a CuMn 8 at. % at 100 mK in a M/H *vs.* H diagram showing the quadratic Rayleigh behaviour and the existence of a reversible susceptibility χ_0 at very low temperature.

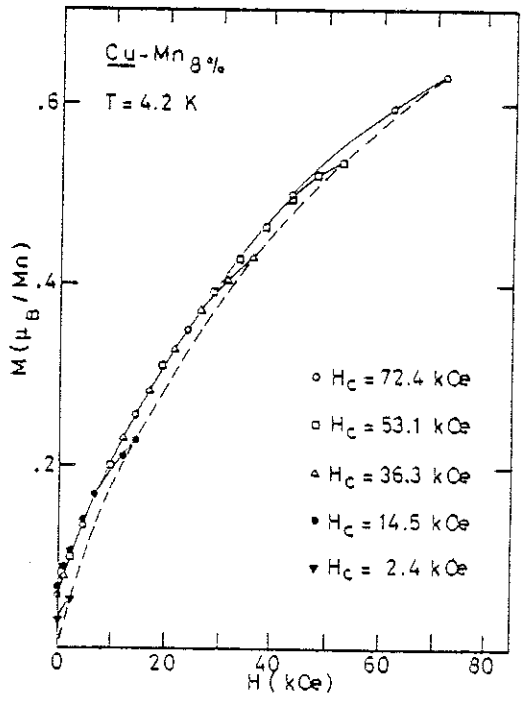

Fig. 14. — The descending branch of the limiting hysteresis cycle is reached through a Rayleigh parabola starting from different points of the equilibrium curve $M_a(H)$ (dashed curve). In small enough fields, the Rayleigh parabola intersects the magnetization axis and the thermoremanent magnetization is not saturated.

branch of the hysteresis cycle is reached (Fig. 14).

The *I.R.M.* is obtained, starting from the first magnetization curve with a decrease in field equal and opposite to the initial increase.

Figure 15 exhibits the experimental behaviour of the *T.R.M.* and of the *I.R.M. vs. H* at different temperatures, and should be compared with the predictions of figure 8. Notice the unexplained maximum of the *T.R.M.*

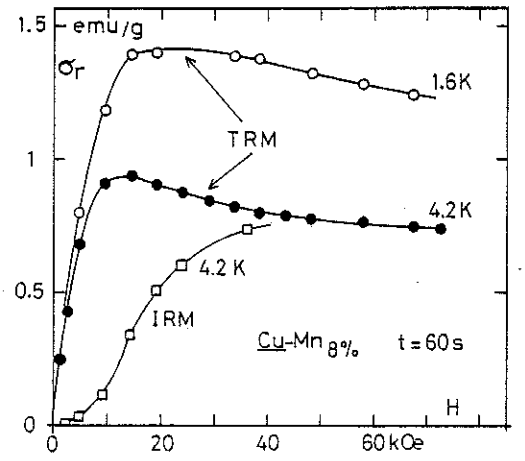

Fig. 15. — The *I.R.M.* and the *T.R.M.* at 4.2 K and 1.6 K *vs.* the field *H* in CuMn 8 at. %. The field was applied during 60 min. The measurements were performed 60 s after the field was withdrawn.

The temperature dependence of the saturated remanent magnetization measured at fixed times in the region of the plateau which follows the *T.R.M.* maximum, departs noticeably from the predicted parabolic behaviour in the vicinity of T_G (compare figures 8 and 18) : the hypothesis of a sharp cut-off at W_{max} is of course very bad in this domain.

A better fit is obtained with an exponential law :

$$S.R.M. \simeq S(0) \exp - \left(\frac{T}{T_0} \ln \frac{t}{\tau_0}\right) = S(0) \left(\frac{t}{\tau_0}\right)^{-T/T_0} \quad (17)$$

between $T_G/3$ and $2\ T_G/3$ (Fig. 16) as was noticed previously [5], [21]. However we observe important deviations from exponential behaviour in both the high and the low temperature range whatever the concentration (see in particular the figure 17 where data at several concentrations have been superimposed in a reduced diagram $S.R.M./S(0)$ *vs.* T/T_G). The agreement with exponential behaviour is made somewhat better but still unsatisfactory if the value of the *T.R.M.* at its maximum rather than in the subsequent plateau is used as the determination of the *S.R.M.* For the time being therefore we believe that the expression (17) can be considered only as an *ad hoc* best fit in a restricted temperature range. More studies would be necessary to decide about its eventual generalization.

12. Determination of τ_0 : validity of the Arrhénius law. — We have used the excellent agreement which is obtained with an exponential behaviour in the range $T_G/3$, $2\ T_G/3$ to make a determination of the characteristic time τ_0 which enters in the Arrhenius law. The parallelism of the straight lines which represent the variations of Log *S.R.M. vs.* T Log t at fixed T and the observed linearity of Ln *S.R.M. vs.* T (Fig. 16) are consistent with a unique expression

$$S.R.M. \sim S(0) \exp - \left(\frac{T}{T_0} \operatorname{Ln} \frac{t}{\tau_0}\right) = S(0) \left(\frac{t}{\tau_0}\right)^{-T/T_0} \quad [21]$$

which describes both the time and the temperature dependences. The value of τ_0 obtained is $\tau_0 \sim 10^{-11}$ s, consistent with other estimates in this and in other systems.

Even in the high and low temperature ranges where deviations from the exponential behaviour have been noticed the *same* value of τ_0 does lead to a good superposition of the data in terms of $T \operatorname{Ln} \frac{t}{\tau_0}$ i.e. in terms of the reduced variable $\theta = T/T_G$ which we have introduced (Fig. 10). This scaling $S.R.M. \simeq f\left(T \operatorname{Ln} \frac{t}{\tau_0}\right) = f(\theta)$ implies the validity of the Arrhenius law and that we are dealing with thermally activated processes.

Figure 19, where the evolution of the remanent magnetizations in different fields is shown *vs.* $T \operatorname{Ln} \frac{t}{\tau_0}$, should be compared with figure 8*b*. Except for the previously considered deviations from parabolic behaviour the qualitative agreement is good. In particular a linear dependence of the *T.R.M.* on $T \operatorname{Ln} \frac{t}{\tau_0}$ is observed in small fields up to the vicinity of T_G where a saturated regime is always reached ($\eta + \theta > 1$).

We have noticed a deterioration of the above picture in *very small fields*. It would then be necessary to introduce values of τ_0 much larger than 10^{-11} s to restore the above mentioned time temperature correspondance. Typically we would need $\tau_0 \sim 10^{-6}$ s in the 10 Oe range. Other authors have also observed the disappearance of any sign of irreversibility if small enough fields are used [22]. We can comment within the framework of our model on some other consequencies of such a change in the characteristic time τ_0. For example we have seen that the error which was made when identifying the field cooled magnetization $M_a(H)$ with the equilibrium magnetization was of the order of $1/Q$ of the maximum desequilibrium which could be reached in this field (i.e. the *T.R.M.*). With $\tau_0 \sim 10^{-6}$ s this error becomes sizeable. We believe it can account for the fact that in many measurements which have been performed with Squid techniques in fields of the order of 1 Oe, the field cooled susceptibility itself does exhibit a weak

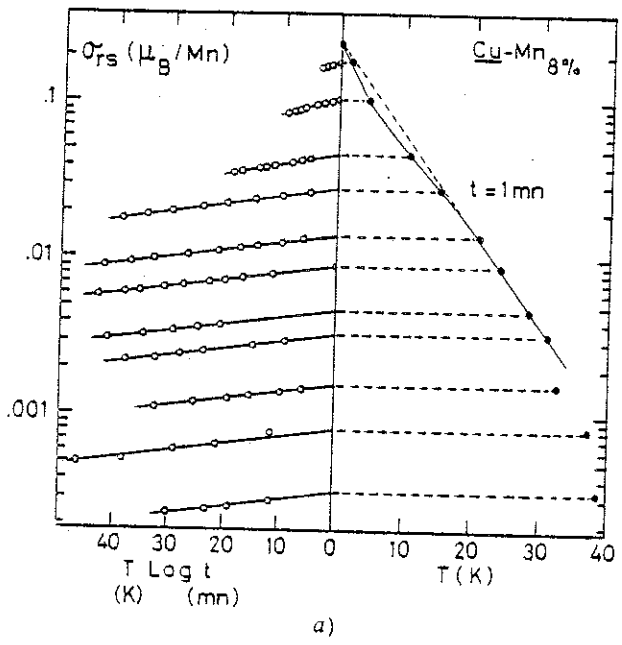

a)

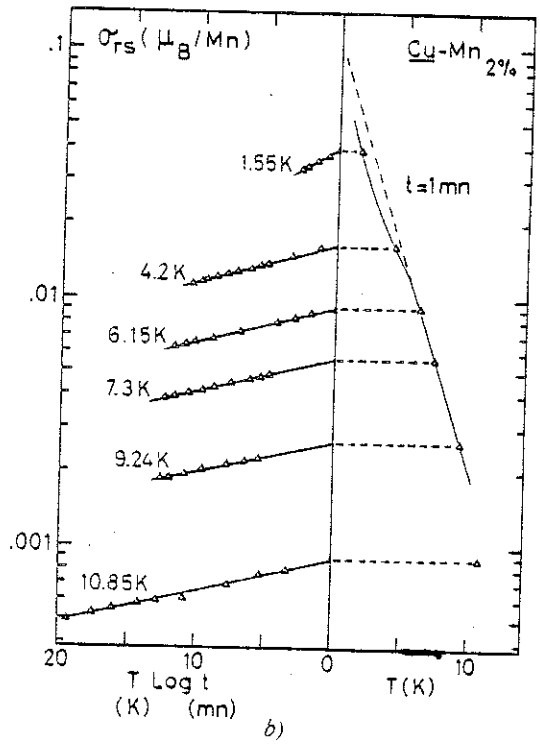

b)

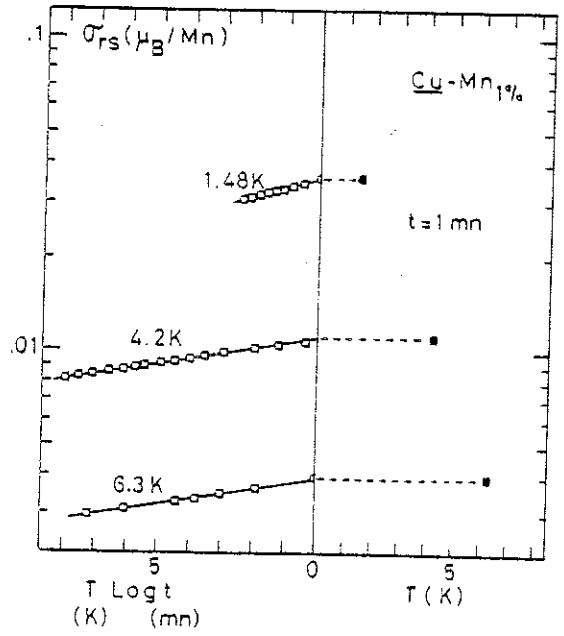

c)

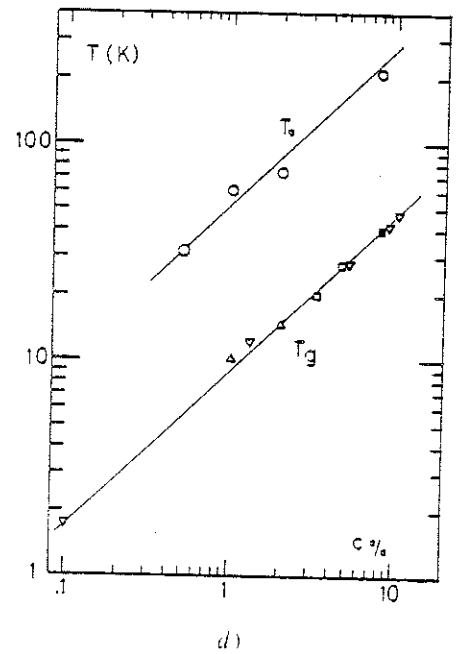

d)

Fig. 16. — The Log of the saturated thermoremanent magnetization $\sigma_{rs}(T, t)$ of a CuMn 8 at. % is shown (Fig. *a*) at different constant temperatures (left side) *vs.* T Log t for times t varying from 1 to 100 min. after the field was removed. The right side shows the temperature dependence of Log $\sigma_{rs}(T, t = 1 \text{ min.})$. For

$$T_G.3 < T < 2\,T_G.3\,,$$

we have (left side) $\text{Ln}\ \sigma_{rs}(T, t) = \text{Log}\ \sigma_{rs}(T, t = 1 \text{ min.}) - \frac{T}{T_0}\,\text{Ln}\ t$ with $T_0 \simeq 210$ K, and (right side)

$$\text{Ln}\ \sigma_{rs}(T, t = 1 \text{ min.}) = \text{Ln}\ \sigma_0 - \alpha\,\frac{T}{T_0}\,.$$

Those results can be condensed in the unique expression

$$\sigma_{rs} = \sigma_0 \exp\left(-\frac{T}{T_0}\,\text{Ln}\,\frac{t}{\tau_0}\right) \quad \text{with} \quad \tau_0 \simeq 10^{-11}\ \text{s}\,.$$

Figures *b* and *c* : same results for CuMn 2 at. % ($T_0 = 84$ K) and 1 at. % ($T_0 \simeq 59$ K) respectively.

Figure *d* : the concentration dependence of T_0 (○) is compared with the concentration dependences of T_G (▽ : [32], △ : [33], □ : [34], ■ : our work and [35]). $T_G \sim 0.2\ T_0$.

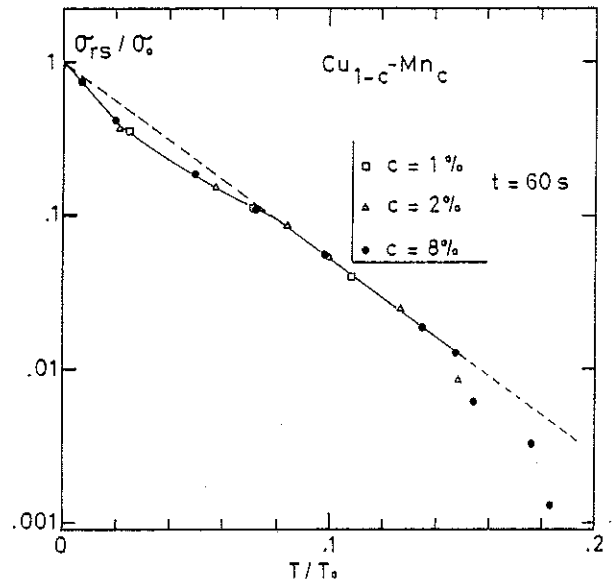

Fig. 17. — The same data as in figure 16 (for $t = 1$ min.) are superimposed in a unique reduced diagram $\sigma_{rs}/\sigma_0 = f(T/T_0)$ including all three concentrations (8 at. %, 2 at. %, 1 at. %) with σ_0 and T_0 defined in figure 16.

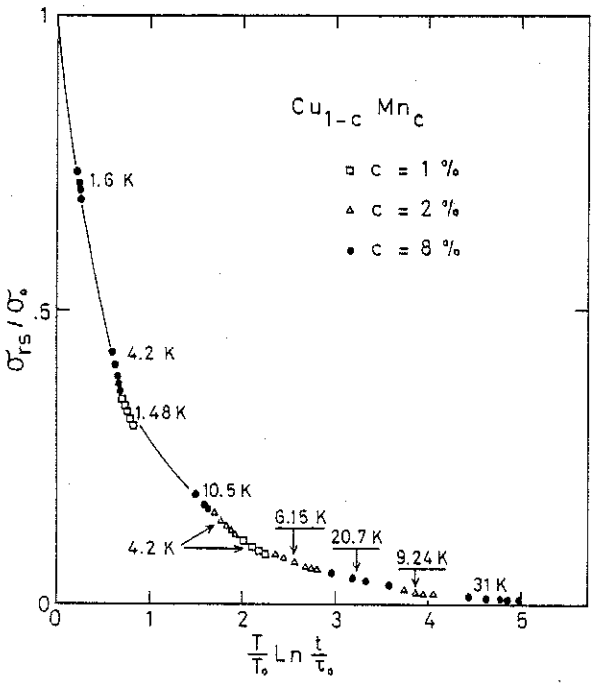

Fig. 18. — The same data as in figure 16 including the time (1 min. $< t <$ 100 min.) and temperature ($T_G/25 < T < T_G$) variations of all three concentrations (8 at. %, 2 at. %, 1 at. %) are shown in a unique *reduced* diagram σ_{rs}/σ_0 *vs.* $\frac{T}{T_0} \text{Ln} \frac{t}{\tau_0}$ with $\tau_0 \simeq 10^{-11}$ s determined as in figure 16.

maximum [23]. This argument suggests a correction of the form :

$$\chi_{eq} = M'_a(H) + \frac{M'_a(H) - \chi_{rev}(H)}{Q}$$

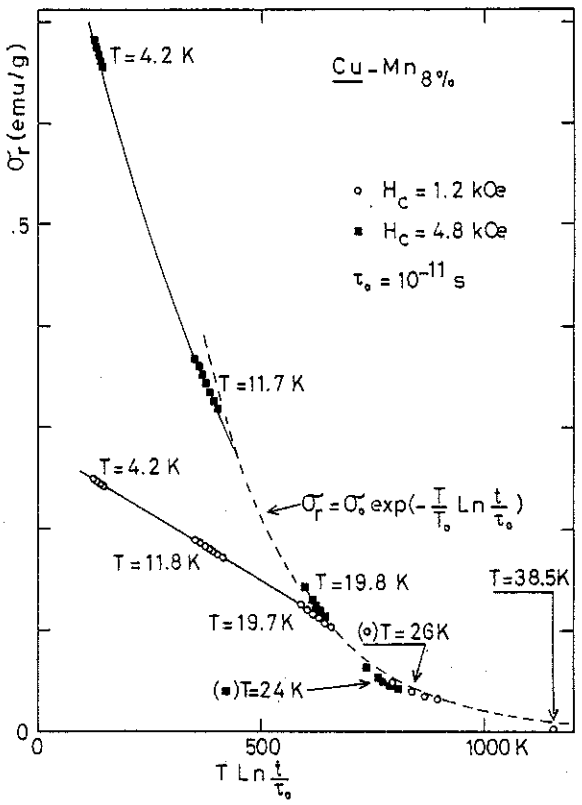

Fig. 19. — The thermoremanent magnetization of CuMn 8 at. % in different constant fields is shown *vs.* $T \text{Ln} \frac{t}{\tau_0}$. Notice the linear temperature dependence in the unsaturated regime at low $T \text{Ln} \frac{t}{\tau_0}$ values.

which seems of the correct order of magnitude to make the small structure noticed on $M'_a(H)$ vanish.

13. **Discussion of some discrepancies.** — We have quoted several features which the model fails to describe. They are :

a) a finite and large reversible susceptibility at $T = 0$,

b) the presence of a maximum in the *T.R.M.*,

c) indications that τ_0 might become larger in small fields,

d) the existence of jumps in the magnetization,

e) another major difficulty is associated with the sharpness of the susceptibility cusps which have been reported in some cases (not all). The last point *e*), to us, is much more important than the others *a*)-*c*) since whatever sharpness which is present in our description is obviously connected with the unphysical cut-off which we have assumed for the distribution $P(W)$ and would vanish with any reasonable assumption on the shape of $P(W)$.

Points *a*), *b*), *c*), *d*), on the contrary could conceivably be amended in a more realistic description. At least the discrepancy would not obviously increase in an attempt to make the model more realistic as in the case of *e*).

Take point *a*) for example. In order to account for the additional large initial susceptibility $\chi(T = 0)$ we would need to introduce an additional density of states $\mathcal{F}'(\varepsilon_0)$ the access to which would not be restricted by an associated distribution $P'(W)$ of energy barriers. We need

$$\frac{\mathcal{F}'(\varepsilon_0)}{\mathcal{F}(\varepsilon_0)} = \frac{\chi(T = 0)}{m'_s(h)}$$

to be of the order of unity. This *ad hoc* modification to the model is *not* contradictory with our initial motivations (see § 2) : we introduced the distribution $P(W)$ in order to account for the observed large relaxation times of the magnetization and of the energy : this does not exclude the presence at the same time of additional reversible responses of other or of the same objects. In particular, the square cycle (shown Fig. 5) traduces the response to a field applied along the *easy axis* of the objects. The response transverse to this easy axis is in fact reversible (dash-dotted line figure 5). In an assembly of objects where the orientation of the anisotropy axis is presumably isotropic, the barriers restrict the response associated with the component of the external field along the easy directions of the objects. But there exists a reversible response of the same magnitude associated with the transverse component.

The fact that the model does not account for the maximum of the *T.R.M.* (point *b*)) may be a consequency of the very unsatisfactory assumption which we made that $P(W)$ and $\mathcal{F}(\varepsilon_0)$ are independent from each other and from the magnetic state of the sample. It would be tempting to introduce a correction on W_{max} proportional to the deformation which has been applied to the system : $W_{max} \to W_{max} - \alpha \Delta M$ where ΔM is the variation of the magnetization starting from the initial equilibrium situation. Thus in the saturated regime the remanent magnetization associated with a larger field would relax faster than a remanent associated with a smaller field and would appear smaller at any finite measurement time.

We do not regard the apparent increase of the magnitude of τ_0 when very small measurement fields are used (point *c*)) as the manifestation of an inadequacy of the model. Physically τ_0^{-1} is related with the curvature of the potential well and it is expected that this curvature increases when W increases [15]. Of course it is reasonable to neglect (as we have done) the effect of the variations of τ_0 as compared with the hudge variations in τ arising from the large distribution of W since W appears in the exponent of the Arrhenius law. When moderate or high fields are used a wide enough range of W is reached and τ_0 can reasonably be replaced by its average value. The small fields however only select those barriers which are small and which correspond to a large τ_0 very different from the average value.

We have stressed from the beginning that this model has no ambition in explaining the occurrence of magnetic jumps (point *d*)) in positive fields (Fig. 12) nor in negative fields as those discussed in reference [16]. Concerning the latter however, provided the interaction which is responsible for $P(W)$ and $\mathcal{F}(\varepsilon_0)$ has the rotational symmetry (like the R.K.K.Y. interaction) the magnetizations which we described are conserved by rotation. In this case it should be possible to align at no cost the remanent magnetization along any direction of space. The results of reference [16] clearly show that the small reverse field which is necessary to abruptly reverse the magnetization of a CuMn alloy must be due to the anisotropy associated with the conduction electron spin flip cross section due to spin orbit coupling. This cross section is particularly small in CuMn but it can be modified by orders of magnitude through the addition of a very small amount of non magnetic impurities (such as Au or Pt) with little, if any, influence on the properties which we have attempted to describe in this paper.

This shows that the existence (or non existence) of magnetic jumps is not a characteristic property of the spin-glass state. On another hand it is clear that the spin-glass state can be constructed with an interaction which has the rotational symmetry. This observation eliminates any explanation which would imply at some stage the necessity of an anisotropic interaction (such as the dipolar interaction) to account for the observed relaxations (i.e. the energy barriers) [25].

14. **What do the magnitudes of Q, W_{max} and H_{max} tell us about the objects ?** — The main parameters of the problem are, apart from the additional initial susceptibility $\chi(T = 0)$, the width W_{max} of the distribution $P(W)$ of the barrier heights, the associated field H_s and the parameter $Q \sim \text{Ln}\,\frac{t}{\tau_0}$ through which the experimental time affects the problem. We have measured $\tau_0 \sim 10^{-11}$ s and $Q \sim 25$. The energy $W_{max} \simeq kT_G\,Q$ is therefore about 25 time larger than the apparent energy kT_G through which it manifests itself in usual measurements ($t \sim 1$ s). This is much larger than the R.K.K.Y. interaction at the average interimpurities distance. This has several consequencies. The first, which has been often stressed, is that the considered objects are large size objects. Comparing

$$\overline{M}_s\,H_s \sim W_{max} \sim QkT_G$$

one gets an estimation of $\overline{M}_s \sim 500\ \mu_B$ in CuMn 8 at. %, 250 μ_B in CuMn 1 at. % (to be compared with 95 μ_B obtained from energy relaxation measurements in AuFe 4 at. % [11]).

This large value implies the association of a large number n of individual moments. This is an important feature which has to be taken into account in the microscopical description of the objects. A picture was proposed by Holtzberg *et al.* [5] who attempted

to extend to spin glasses Néel's ideas on fine antiferromagnetic particles. The suggestion was to attribute the origin of the barriers W to an internal dipolar energy proportional to the volume of the objects (called *magnetic coulds*) ; this volume term is bound to become larger than the interactions with neighbouring clouds increasing presumably with the surface of the cloud for some critical size, even if the magnitude of the R.K.K.Y. is much larger than that of the dipolar interaction. Although the interclouds interactions were thus thought to be determinant on the size of a cloud, their effect was in practice omitted in the description of the time effects which was subsequently performed.

The model which was in fact used was a model of symmetrical double well potentials which like equivalent superparamagnetic descriptions [24] can account for neither the energy relaxations nor the shape of the equilibrium curve $M_a(H)$. The model however succeeded in popularizing the idea of a distribution of potential barriers and the phenomenological discussion of time effects which are associated to this distribution. We have tried to go a step further by introducing phenomelogically the interactions between the objects through the distribution $\mathcal{F}(\varepsilon_0)$ or the equivalent use of the equilibrium magnetization $M_a(H)$.

The main criticism which has been raised against the *clouds model* is that the microscopical mechanism which it proposes for the occurrence of *clouds* relies on the dipolar interaction a speculation which, as we saw, has been ruled out by recent measurements [25, 16]. We escape this criticism because, being less ambitious, we do not attempt any such description of the objects. Let us stress however, that whatever satisfactory it might be to have a static picture of the objects, the important point in the problem is not the objects themselves but the *distributions* and the fact that a reasonably *flat and constant density* of objects can be assumed in the conditions of time, temperatures and fields which we consider. This situation is of course automatically realized when the objects are well characterized material fine particles such as Néel considered [15]. But we *are not restricted* to this description. The deformation of the system associated with an experiment may well modify the initial objects, we need only that the new objects which are defined at each step are again characterized by the same distributions. Recall that there is a strong reason for the distributions to remain a white spectrum an it is that in an amorphous system no special value of the energy should be favoured. The additional requirement upon the constancy of the density probably implies little less than the presence of some typical size or correlation length in the problem which would be reasonably field and temperature independent. We believe that in the absence of obvious geometrical grains in a spin glass such a description in term of say *virtual fine grains* would be appropriate.

15. **Frequency dependent maximum and frequency independent cusp.** — Nothing in this model would account for the sharpness of the susceptibility data which first started the *phase transition* hypothesis. Even when, as in this paper, a sharp unphysical cut-off of the distribution $P(W)$ is assumed at W_{max}, the predicted susceptibility is rather unpathological : neither figures 8 nor 9 exhibit the upward curvatures which have been experimentally reported [1] and which can be seen on figure 20. Further, T_G is expected to be frequency dependent :

$$\frac{1}{T_G} = \frac{kQ}{W_{max}}$$

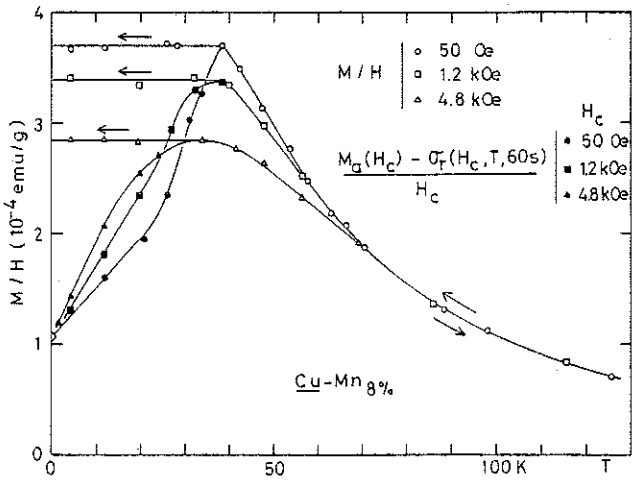

Fig. 20. — The initial susceptibility of CuMn 8 at. % *vs.* temperature in different constant fields. The equilibrium (field cooled) susceptibility does not show any anomaly. The reversible susceptibility $\left(\frac{M_{eq}(h) - T.R.M.(h)}{h}\right)$ shows a rounded maximum in increasing fields.

should be a linear function of Ln t as shown on figure 21, the intercept of the linear variation with the Ln t axis occurring for Ln τ_0. In principle, varia-

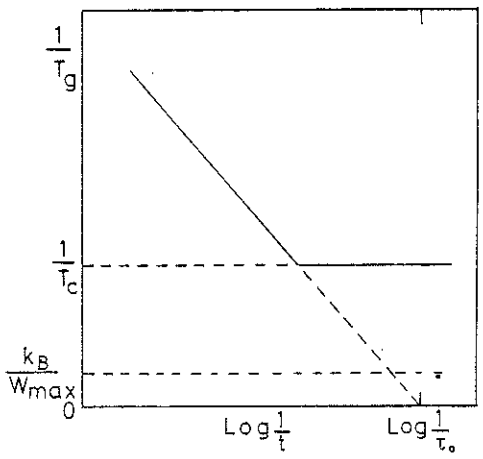

Fig. 21. — Predicted variations of $\frac{1}{T_G}$ *vs.* Ln t · $\frac{1}{T_c} \simeq \frac{k}{\Delta J}$ is the proposed high temperature limit of the variations of T_G (since, over T_c, the cohesion of objects having the necessary size to produce energy barriers as high as W_{max} cannot be maintained).

tions of T_G should be observed over the whole range between the long time limit ($T_G = 0$), and the short time limit ($T_G = W_{max}/k$) which would occur for frequencies of the order of τ_0.

This picture does agree with some of the experimental data which have been reported in insulators like $EuSr_{1-x}S_x$ or true glasses doped with metallic impurities [26] or in systems like $LaAl_2Gd$ [6] which, although an f impurity is involved, are obviously to be classified among the archetypal spin glasses [27].

In low-concentration AgMn in contrast, experiments extended over decades in frequency [8] failed to show any sizeable frequency dependence, a feature which has been confirmed in several other systems [28]. In some cases it was possible, through a heat treatment, to induce a frequency dependence in a sample where no such dependence was present in the initial quenched state [9].

These contradictions we believe, raise the all important question of the validity range of our speculations. Remember that the experimentally determined values of W_{max} are very large : much larger than the average magnitude $\Delta J = \sqrt{\langle J^2 \rangle}$ of the R.K.K.Y. interaction at the average interimpurities distance. This prompted us into considering the above discussed large size objects for which it is not unreasonable to argue that their rearrangements will involve energies much larger than ΔJ. Inasmuch as such objects exist it is possible to justify a $W_{max} \sim 25\ \Delta J$ and a T_G whose higher limit is W_{max}/k. It is however obvious that the model collapses at temperatures of the order of $T_c \sim \Delta J/k$ when the system becomes paramagnetic and the R.K.K.Y. interaction is no longer able to sustain the necessary cohesion of the objects which are the basis of our model. This temperature T_c sets the higher frontier to the validity range of our model.

More precisely, consider an hypothetical alloy which would be built up with impurities in the same positions than in the real alloy and where the interaction would everywhere be positive and identical to the modulus of the real interaction. This alloy has a ferromagnetic transition at $T_c \sim \Delta J/k$. We may now construct the *associated Mattis alloy* by flipping (when necessary) the spins to their actual orientation in the real alloy : provided that for each spin we flip, we flip at the same time all its interactions with the $N - 1$ other spins, we conserve a *flat* model which still exhibits long range order below T_c. (This alloy differs from our real alloy by the fact that any closed loop of bonds contains an even number of antiferromagnetic bonds and frustration is absent.) We know (in particular from numerical experiments) [31] that this long range order is destroyed by the frustration effect [30] (and we enter the spin glass state) when a sufficient fraction of the bonds are flipped to their actual sign in the real alloy. There must be a qualitative difference between the situation over T_c where the temperature in any case prevents the occurrence of long range order and the situation below T_c where the frustration prevents the occurrence of an otherwise infinite cluster. Only below T_c we can speculate about objects of the required (reasonably temperature independent) size to justify the magnitude of $W_{max} \sim 25\ T_G$. T_c therefore would limit the temperature range where the glass behaviour characterized by a scaling in terms of $\theta \sim T/T_G$ (with $T_G \sim (\ln t)^{-1}$) can be observed. In a similar way, we believe the fusion temperature of say crystalline silica sets the higher limit where vitreous silica can be observed and the Curie temperature of the magnetic material sets the limit where fine grains behaviour can be observed in an alloy with this metal.

We have represented in the figures 22, 23 the predicted variations of the susceptibility (assuming an equilibrium susceptibility M_a' given by a Curie-Weiss law and forgetting about $\chi(T = 0)$) and of the parameter $q(t) = \dfrac{T.R.M.}{M_a}\ (h \to 0)$ *vs.* T at different times and *vs.* time at different temperatures. We simply assume in this rough picture that the distribution $P(W)$ is unaffected up to temperatures of the order of $\Delta J/k$ where it suddenly vanishes. We expect a transi-

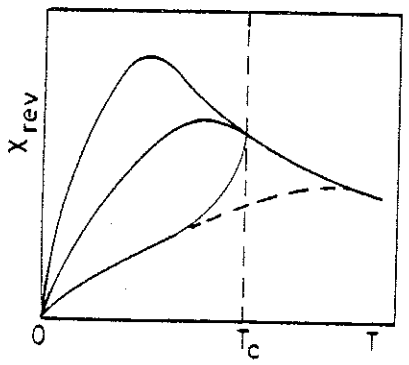

Fig. 22. — Schematic representation of the expected features of the reversible susceptibility *vs.* temperature for different measurement times. The scaling T/T_G (yielding a time dependent maximum) vanishes at T_c where the system becomes paramagnetic.

tion from a *glass regime* where all the properties scale with T/T_G (with T_G being frequency dependent) to a regime where T_G being larger than $T_c \simeq \Delta J/k$ the transition to the paramagnetic regime occurs at T_c (Fig. 22) with a sudden inversion of the curvature of the susceptibility. It is remarkable that reasonable estimations of ΔJ have been made in the past on the basis of the temperature of the susceptibility maximum : this implies that $kT_G \sim W/Q$ and ΔJ are actually of the same magnitude at the usual frequencies i.e. $W_{max} \sim 25\ \Delta J$. This can be checked using independent estimations of ΔJ which can be made very accurately from the magnetization curve in the vicinity of its saturation [29]. It is therefore not unexpected if, depending on the system, W_{max}/Q can be found to be slightly larger than ΔJ (AgMn), or slightly smaller ($LaAl_2Gd$) for usual values of Q.

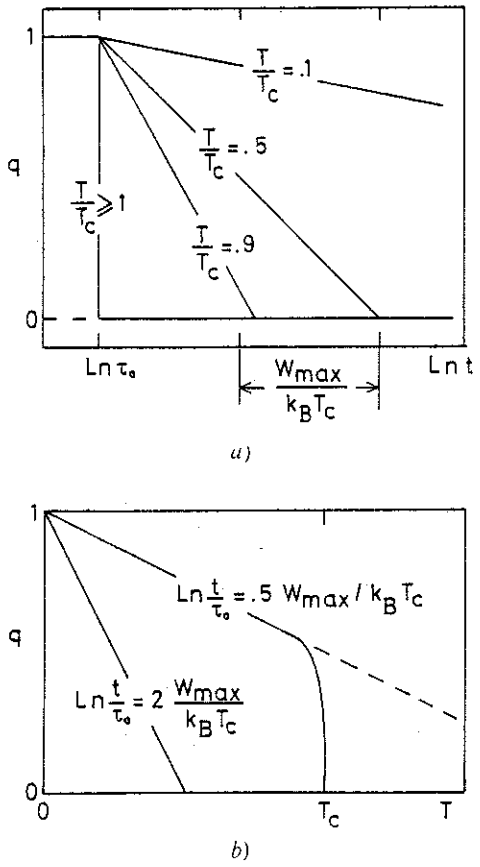

Fig. 23. — Predicted behaviour of the autocorrelation function $q = \langle S(0)\, S(t) \rangle$ *vs.* time for different temperatures (Fig. *a*) and *vs.* temperature for different measurement times (Fig. *b*).

This is supported by the fact that when a straight line is drawn through the experimental data showing the frequency dependence of T_G (like in Fig. 21) it very seldom provides a value of τ_0 (by extrapolation to the Log t axis) in agreement with the low temperature data on the same samples, or even a value which can be easily justified on physical grounds ($\tau_0 \sim 10^{-20}$ s in $LaAl_2Gd$ *vs.* 10^{-11} s from remanent data at low temperatures). This suggests that this straight line was incorrectly drawn through data which are already in the cross-over regime.

16. **Conclusions.** — We have discussed the consequencies of a model of a distribution of asymmetrical, thermally activated double well potentials and found that such a model gives a satisfactory description of the properties of spin glasses.

Some discrepancies would probably be explained by a modified model which would use more realistic distributions and would account more properly for the correlations. The consideration of the magnitudes of the characteristic energies which are required, implies the necessary existence of two regimes : a glassy regime $T < T_c$ where the properties can be expressed in terms of a reduced variable $\theta = T/T_G$ where T_G decreases as $(\text{Log } t)^{-1}$ and a regime $T > T_c$ where the system is truly paramagnetic or superparamagnetic. It is in the transition towards paramagnetism that the pathological effects, which eventually would need the definition of new phase, occur.

The model which has been used is very general since it is justified essentially on the basis that the structural disorder inherent in the system does not favour a particular value of the energy. This generality implies similarities between the magnetic properties of spin glasses and the properties of other disordered systems (for example the elasticity of rubbers). This justifies the name *spin glass* given to this type of magnetic system and also the application to spin glasses of a more practical definition which was established for glasses namely : systems which react like liquids at long times like solids at short times.

Acknowledgments. — We thank Dr. A. Briggs, W. A. Phillips, R. Rammal, J. L. Tholence, R. Tournier and P. Monod for many fruitfull discussions and for critical readings of the manuscript.

References

[1] Cannella, V., Mydosh, J. A., *Phys. Rev.* **B 6** (1972) 4220.
Cannella, V., Mydosh, J. A., *AIP Conf. Proc.* **18** (1973) 651.

[2] Edwards, S. F., Anderson, P. W., *J. Phys. F* **5** (1975) 965.

[3] For a review of theoretical work on the problem of spin glasses see for example :
Blandin, A., LT 15 (1978, Grenoble), *J. Physique Colloq.* **39** (1978) C6-1499.

[4] Lutes, O. S., Schmidt, J. L., *Phys. Rev.* **125** (1961) 433.
Tournier, R., Thesis, Grenoble (1965).
Ishikawa, Y., Tournier, R., Philippi, J., *J. Phys. Chem. Solids* **26** (1965) 1727.
Tholence, J. L., Thesis, Grenoble (1973).

[5] Tholence, J. L., Tournier, R., *Physica* **86-88b** (1977) 873 and
Holtzberg, F., Tholence, J. L., Tournier, R., *Amorphous Magnetism II* (Plenum Press, New York and London) 1977, p. 155.

[6] Von Lohneysen, H., Tholence, J. L., Tournier, R., LT 15 (1978), *J. Physique Colloq.* **39** (1978) C6-922.

[7] The parallelism of the properties of spin glasses and other substances for ex. insulating $EuSr_{1-x}S_x$ is now sufficiently known by everybody so that the extension of the name *spin glass* to those systems does not make any problem despite the differences in the nature of the interactions : this extension is very much in the line of our Model-Frequency dependent maxima of the susceptibility were reported in this system by :
Tholence, J. L., Holtzberg, F., Godfrin, H., Von Lohneysen, H., Tournier, R., LT 15 (1978, Grenoble), *J. Physique Colloq.* **39** (1978) C6-928 ;
Maletta, H., Felsch, W., Tholence, J. L., *J. Magn. Magn. Mat.* **9** (1978) 41 and
Maletta, H., Felsch W., LT 15 (1978, Grenoble) *J. Physique Colloq.* **39** (1978) C6-931.

[8] Dahlberg, E. D., Hardiman, M., Souletie, J., *J. Physique Lett.* **39** (1978) L-389.
Dahlberg, E. D., Hardiman, M., Orbach, R., Souletie, J., *Phys. Rev. Lett.* **42** (1979) 401.

[9] KORN, D., SCHILLING, D., ZIBOLD, G., LT 15 (1978, Grenoble), *J. Physique Colloq.* **39** (1978) C6-899.
ZIBOLD, G., KORN, D., ICM (1979, Münich), *J. Magn. Magn. Mat.* **15-18** (1980) 143.

[10] NIEUWENHUYS, G. J., MYDOSH, J. A., *Physica* **86-88B** (1977) 880.

[11] BERTON, A., CHAUSSY, J., ODIN, J., RAMMAL, R., SOULETIE, J., TOURNIER, R., *J. Physique Lett.* **40** (1979) L-391 ; see also *C.R. Hebd. Séan. Acad. Sci.* **289B** (1979) 49.
BERTON, A., CHAUSSY, J., ODIN, J., PREJEAN, J. J., RAMMAL, R., SOULETIE, J., TOURNIER, R., I.C.M. (1979, Münich), *J. Magn. Magn. Mat.* **15-18** (1980) 203.

[12] ANDERSON, P. W., HALPERIN, B. I., VARMA, C. M., *Phil. Mag.* **25** (1972) 1.
PHILLIPS, W. A., *J. Low Temp. Phys.* **7** (1972) 351.

[13] RAMMAL, R., Thesis, Grenoble (1977).
VOLKENSTEIN, M. V., PTITSYN, S. B., *J. Techn. Phys.* (USSR) **26** (1956) 2204.

[14] SOULETIE, J., *J. Physique Colloq.* **39** (1978) C2-3.

[15] Among the numerous contributions of L. Néel to those problems, see for instance :
Cah. Phys. **12** (1942) 1.
J. Physique Radium **11** (1950) 49
for the theory of Lord Rayleigh's laws in massive substances and :
Ann. Geophys. **5** (1949) 99
Phil. Magn. Suppl. **4** (1955, in english) 191
for the aspects of the magnetism of fine grains and their application to rock magnetism.

[16] MONOD, P., PREJEAN, J. J., LT 15 (1978, Grenoble) *J. Physique Colloq.* **39** (1978) C6-910.
MONOD, P., PREJEAN, J. J., TISSIER, B., *Magnetism and Magnetic Materials* (New York, 1979) *J. Appl. Phys.* **50** (1979) 7324.
PREJEAN, J. J., JOLICLERC, M. J., MONOD, P., *J. Physique* **41** (1980) 427.

[17] WENGER, L. E., KEESOM, P. H., *Phys. Rev.* **B 9** (1976) 4053.

[18] SOULETIE, J., TISSIER, B., ICM (1979, Münich) *J. Magn. Magn. Mat.* **15-18** (1980) 201.

[19] SARKISSIAN, B. V. B., *J. Phys. F.* **7** (1977) L-139.

[20] BRAY, A. J., MOORE, M. A., REED, J., ICM (1979, Münich) *J. Magn. Magn. Mat.* **15-18** (1980) 102.
See also
STAUFFER, D., BINDER, K., ICM (1979, Münich) *J. Magn. Magn. Mat.* **15-18** (1980) 113.

[21] PREJEAN, J. J., LT 15 (1978, Grenoble) *J. Physique Colloq.* **39** (1978) C6-907.

[22] GRAY, E. M., ICM (1979, Münich) *J. Magn. Magn. Mat.* **15-18** (1980) 177.
HOWATH, W., as mentioned by Gray, E. M., *J. Phys. F* **9** (1979) L-167.
KRUSIN-ELBAUM, L., RAGHAVAN, R., WILLIAMSON, S. J., *Phys. Rev. Lett.* **42** (1979) 1762.

[23] An early work of
GUY, C. N., *J. Phys. F* (1975) L-242 draws attention to the time dependence of the susceptibility and its evolution towards some limit which could be the field cooled susceptibility. The effects of very small fields have been considered by the same author in some details in *J. Phys. F.* **7** (1977) 1505 and *ibid.* **8** (1978) 1309. See also *Magn. Magn. Mat. Conf.* (1979, New York), *J. Appl. Phys.* **50** (1979) 7308.

[24] WOHLFARTH, *Phys. Lett.* **70A** (1979) 489.

[25] ALLOUL, H., *Phys. Rev. Lett.* **42** (1979) 603.
ALLOUL, H., MMM Conference (1979, New York) *J. Appl. Phys.* **50** (1979).
MONOD, P., BERTHIER, Y., ICM (1979, Münich), *J. Magn. Magn. Mat.* **15-18** (1980) 149.

[26] CHAPPERT, C., BEAUVILLAIN, P., RENARD, J. P., KNORR, K., ICM (1979, Münich) *J. Magn. Magn. Mat.* **15-18** (1980) 117.
FERRE, J., POMMIER, J., RENARD, J. P., KNORR, K., *J. Phys. C* (1980) to be published.

[27] VON LÖHNEYSEN, H., THOLENCE, J. L., STEGLICH, F., *Z. Phys.* **B 29** (1978) 319.
VON LÖHNEYSEN, H., THOLENCE, J. L., *Phys. Rev.* **B 19** (1979) 5858.

[28] MULDER, C. A. M., VAN DUYNEVELDT, A. J., MYDOSH, J. A., ICM (1979, Münich) *J. Magn. Magn. Mat.* **15-18** (1980) 141.

[29] LARKIN, A. I., KHMEL'NITSKII, D. E., *JETP* **31** (1970) 958.
SMITH, F. W., *Phys. Rev.* **B 14** (1976) 241.
MATHO, K., NUNEZ-REGUEIRO, M. D., ICM (1979, Münich) *J. Magn. Magn. Mat.* **15-18** (1980) 135.

[30] TOULOUSE, G., *Commun. Phys.* **2** (1977) 115.
VANNIMENUS, J., TOULOUSE, G., *J. Phys. C* **10** (1977) L-537.

[31] BIECHE, I., MAYNARD, R., RAMMAL, R., UHRY, J. P., *J. Phys. A : Mat. Gen.* **13** (1980) 2553.
RAMMAL, R., SUCHAIL, R., MAYNARD, R., *Solid State Commun.* **32** (1979) 487.

CHAPITRE III

LA CORRELATION TEMPS-TEMPERATURE DANS LES RELAXATIONS D'AIMANTATION ET LA DETERMINATION DE τ_o DU SYSTEME CuMn A $T < T_g$ (COMPLEMENT)

INTRODUCTION

Nous avons résumé dans le chapitre II les principales propriétés magnétiques caractéristiques des verres de spins à $T < T_g$ et utilisé un modèle simple capable de les décrire qualitativement.

Dans le présent chapitre nous voulons revenir sur les problèmes concernant la relaxation des aimantations et la détermination de τ_o. En effet, l'estimation de la valeur de τ_o donne lieu à de nombreuses controverses et certains auteurs, selon les méthodes expérimentales employées, indiquent, sur un même système, des valeurs allant de 10^{-40} s (ce qui est difficilement explicable physiquement) à 10^{-6} s.

Après une présentation de résultats expérimentaux montrant comment on peut ralentir ou accélérer une relaxation d'aimantation selon le traitement thermique imposé au système, nous nous intéresserons à un phénomène encore non expliqué : la dépendance en température de l'aimantation rémanente est liée étroitement au processus expérimental utilisé (cependant la valeur estimée de τ_o est unique).

Puis nous préciserons les différentes méthodes de détermination de τ_o et le domaine de validité de cette estimation expérimentale.

1. EFFET D'UN TRAITEMENT THERMIQUE A CHAMP CONSTANT SUR LA RELAXATION DE L'AIMANTATION

Si les processus d'activation thermique sont à l'origine du franchissement des barrières de potentiel dans les phénomènes de relaxation des aimantations, pour une même hauteur de barrière W_{eff}, le temps de relaxation associé $\tau = \tau_o \exp(W_{eff}/k_B T)$ est fortement dépendant de la température et on s'attend à pouvoir expérimentalement accéler la relaxation par une augmentation de température et ralentir la relaxation par une diminution de la température.

C'est ce que nous vérifions ici en présentant des résultats expérimentaux portant sur l'aimantation thermorémanente saturée.

Celle-ci, créée à la température T, subit à l'instant t_1 après coupure du champ, une modification de température portant le système à la température $T + \Delta T$. L'aimantation résultante des moments dont la relaxation est gouvernée par la même barrière W_{eff} est donnée par l'expression :

$$m = m_i \exp(-\frac{t_1}{\tau_1}) \exp(-\frac{t-t_1}{\tau_2})$$

m_i étant l'aimantation initiale, $\tau_1 = \tau_o \exp(W_{eff}/k_B T)$,
$\tau_2 = \tau_o \exp\left[W_{eff}/k_B(T+\Delta T)\right]$ (fig. 1).

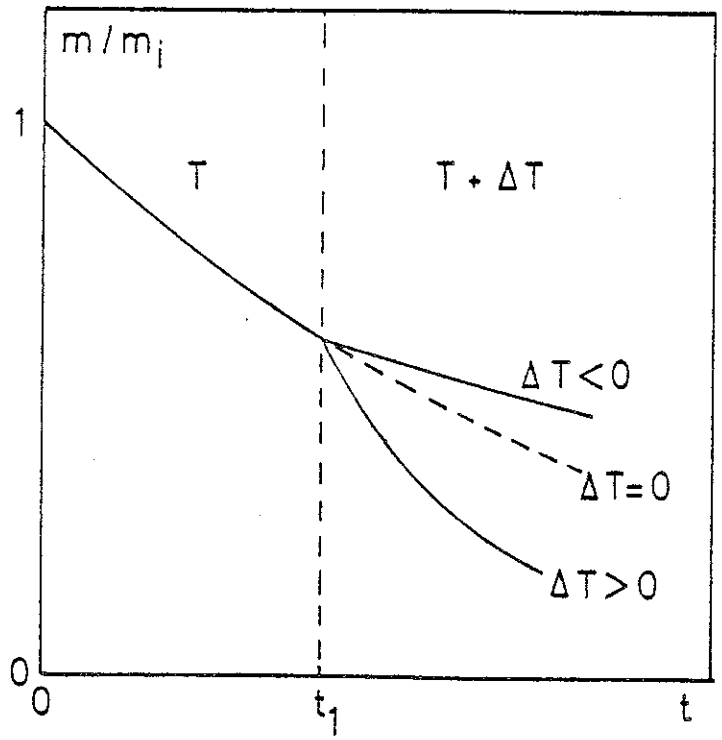

Fig. 1

En utilisant l'argument de coupure à $W_c = kTLnt/\tau_o$, déjà justifié dans le chapitre II, l'aimantation totale à l'instant t_1 est :

$$\sigma_r = \int_{W_{eff} > W_{c_1} = kTLnt_1/\tau_o} M_g$$

a) Si ΔT est positif, l'aimantation devient :

$$\sigma_r = \int_{W_{eff} > k(T+\Delta T) Ln \frac{t-t_1}{\tau_o}} M_g$$

dont la relaxation est aussi de nature logarithmique, la nouvelle origine des temps étant à prendre à t_1.

La figure 2 montre l'évolution en temps à 1,48 K de l'aimantation thermorémanente saturée obtenue en refroidissant sous un champ de 25 kOe un échantillon d'AuFe 4 at.% de $T > T_g$ à $T = 1,48$ K. L'origine des temps est prise à l'instant où le champ a été ramené à 0. Après une vingtaine de minutes, le système est porté, le champ restant nul, à la nouvelle température $T_1 = 1,82$ K. La relaxation reste de nature logarithmique mais avec pour nouvelle origine des temps l'instant t_1 où la température T_1 a été stabilisée. Le procédé est répété un certain nombre de fois dans l'expérience dont les résultats sont portés figure 2.

b) Si ΔT est négatif, l'aimantation restera stable tant que :

$$k_B \left[T - |\Delta T| \right] Ln \frac{t-t_1}{\tau_o} < k_B T \; Ln \frac{t_1}{\tau_o} \quad .$$

La figure 3 représente la dépendance en température de l'aimantation thermorémanente saturée du système CuMn 8 at.% obtenue par refroidissement sous un champ de $T > T_g$ à $T = 20.8$ K. Puis le système est chauffé jusqu'à $T_1 = 25$ K , l'aimantation étant mesurée tout au long de cette excursion de température. Lors du cycle thermique $T_1 \rightarrow 4,2$ K $\rightarrow T_1$, l'aimantation mesurée reste constante et stable dans le temps. Dans une nouvelle augmentation de température au-delà de T_1, l'aimantation suit la loi de décroissance observée antérieurement.

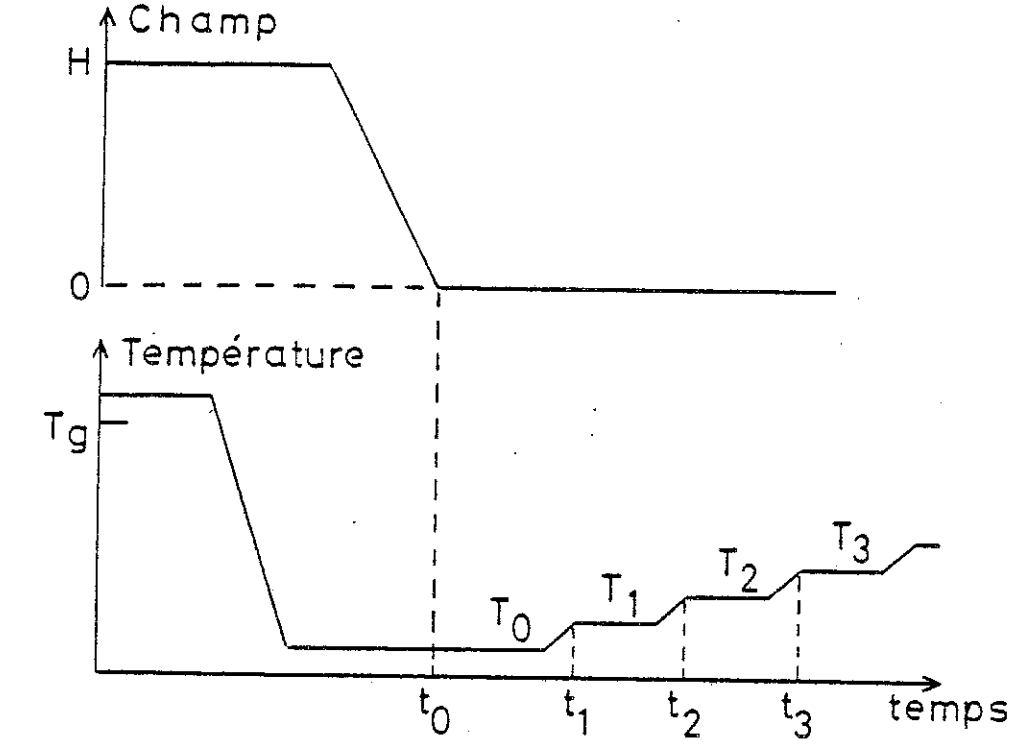
Champ
H
0
Température
Tg
T0
T1
T2
T3
t0
t1
t2
t3
temps

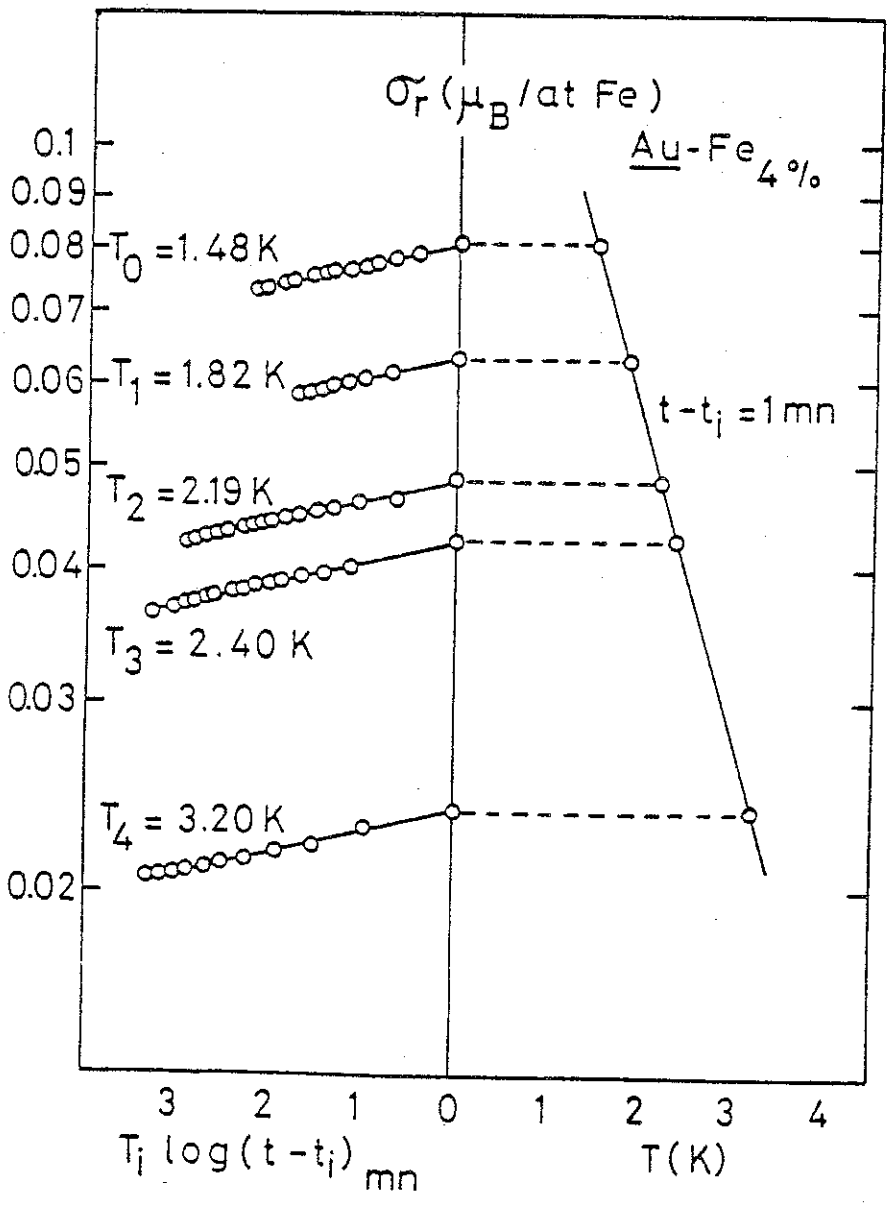
σr (μB/at Fe)
Au-Fe 4 %
0.1
0.09
0.08
0.07
0.06
0.05
0.04
0.03
0.02
T0 = 1.48 K
T1 = 1.82 K
T2 = 2.19 K
T3 = 2.40 K
T4 = 3.20 K
t - ti = 1 mn
3
2
1
0
1
2
3
4
Ti log (t - ti) mn
T(K)

Fig. 2

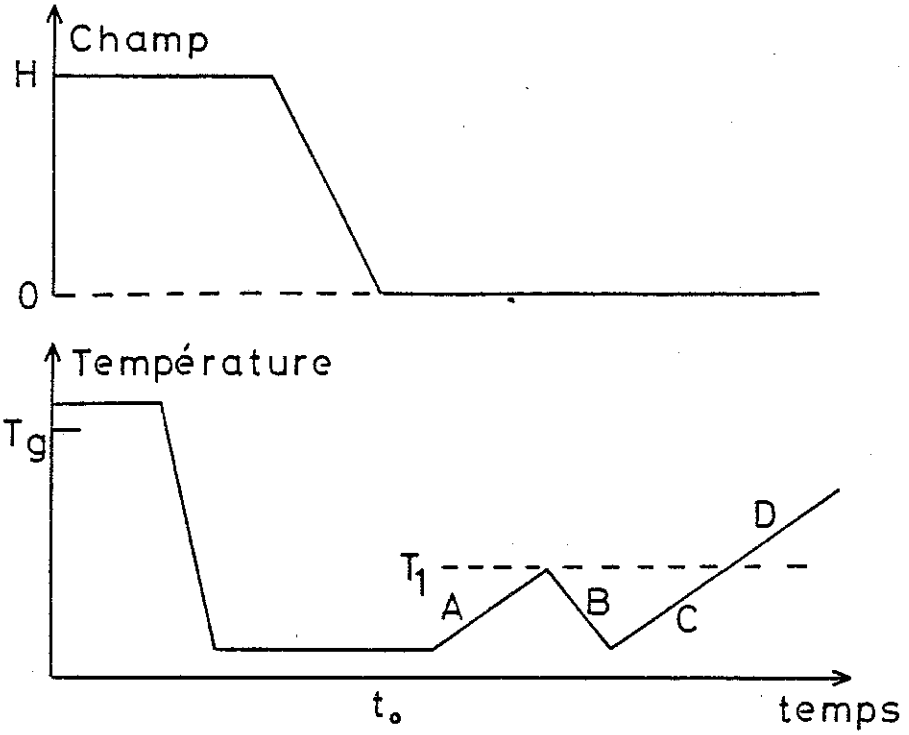
Champ
H
0
Température
Tg
T1
A
B
C
D
t₀
temps

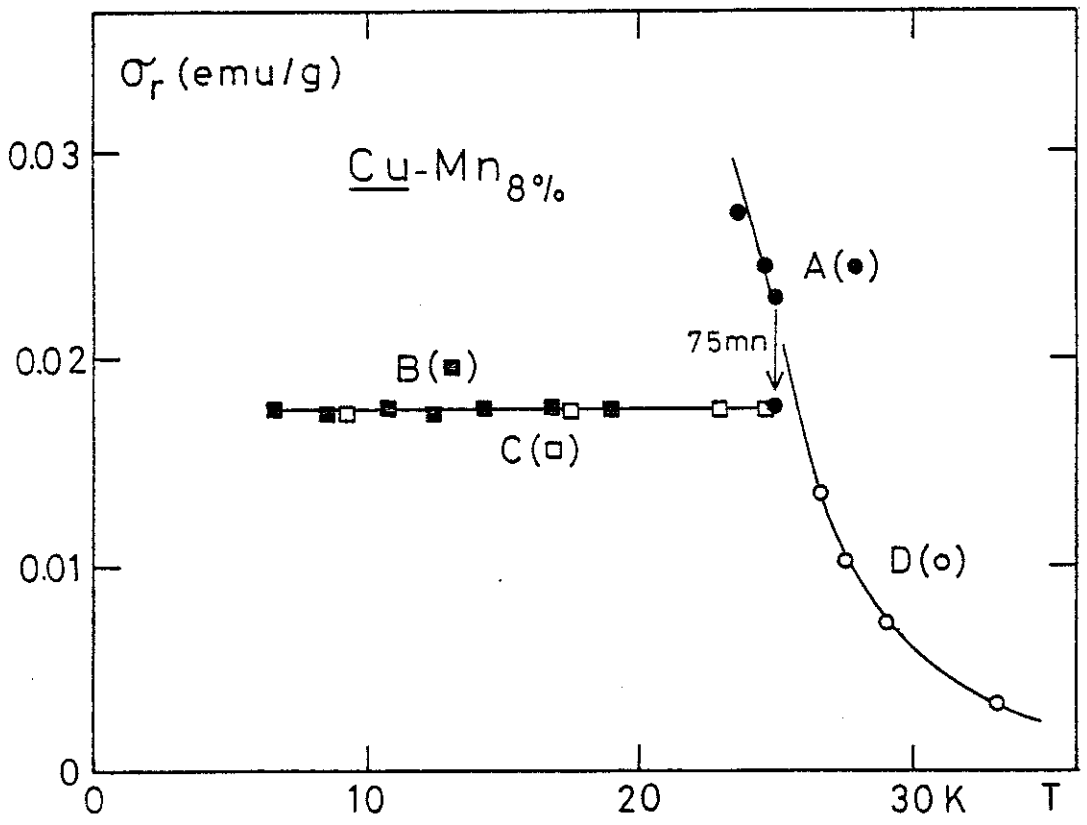
σr (emu/g)
Cu-Mn 8%
0.03
0.02
0.01
0
A(●)
75mn
B(■)
C(□)
D(○)
0
10
20
30 K
T

Fig. 3

c) Cas d'un pulse de chaleur

La dépendance en temps de l'aimantation thermorémanente saturée est représentée sur la fig. 4. A l'instant t_1 = 100 mn un pulse de chaleur est envoyé pendant δt sur l'échantillon (ΔT positif suivi du même ΔT négatif). L'aimantation diminue brusquement de

$$\sigma_r = \int_{W_{eff}>kTLnt/\tau_o} M_g$$

à

$$\sigma_r = \int_{W_{eff}>k(T+\Delta T)\,Ln\,\frac{\delta t}{\tau_o}} M_g$$

et va de nouveau relaxer dès que $T\,Ln(\frac{t-t_1-\delta t}{\tau_o}) > (T+\Delta T)\,Ln\,\frac{\delta t}{\tau_o}$. Ce traitement thermique employé a "vieilli" l'échantillon de $\Delta t = t_1$ = 100 mn, la nouvelle relaxation suivant une loi en $T\,Ln(\frac{t-t_1-\delta t}{\tau_o}) \simeq T\,Ln(\frac{t-t_1}{\tau_o})$.

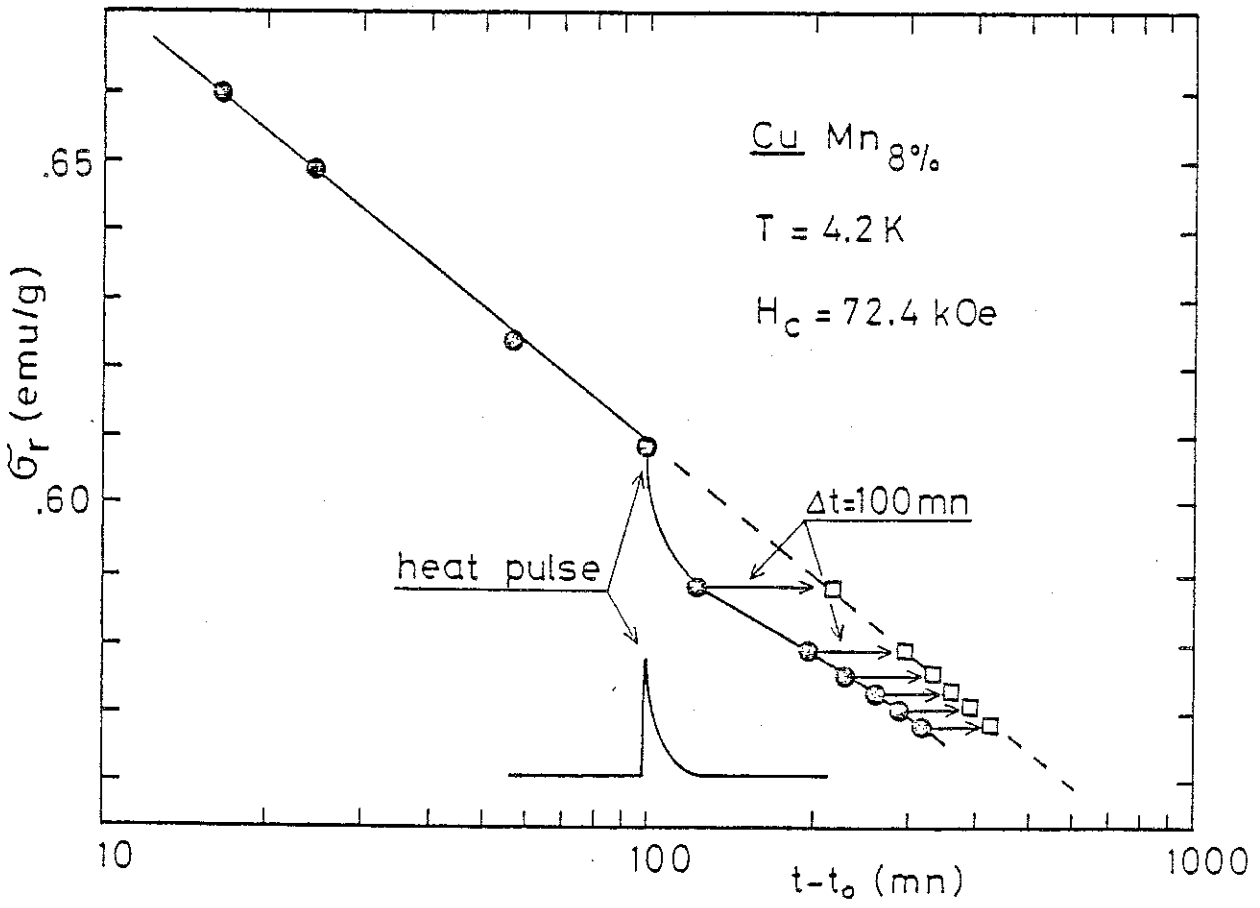

Fig. 4

2. EFFET DU PROCEDE EXPERIMENTAL EMPLOYE SUR LA VALEUR DE L'AIMANTATION REMANENTE SATUREE

Nous avons décrit sur la figure 2 le procédé utilisé pour l'étude comparée de l'évolution en température de l'aimantation thermorémanente saturée du système AuFe 4 % et de l'énergie associée (cf. la publication "Magnetization and energy relaxation in spin glass $AuFe_{4\%}$ below T_g"). Ce procédé, également utilisé pour l'obtention des résultats représentés fig. 3 et fig. 6 (courbe (a)) dans le système CuMn, conduit à des valeurs de l'aimantation rémanente saturée $\sigma_{rs}(T,t)$ très différentes de celles observées à partir de la méthode classique utilisée chapitre II. Résumons celle-ci (figure 5) : Le système, ayant été refroidi sous champ de $T > T_g$ à T_1, l'aimantation est mesurée après coupure du champ en fonction du temps de mesure. Puis le système est réchauffé à $T > T_g$ et refroidi sous champ jusqu'à une nouvelle température T_2. L'aimantation rémanente est observée après coupure du champ.

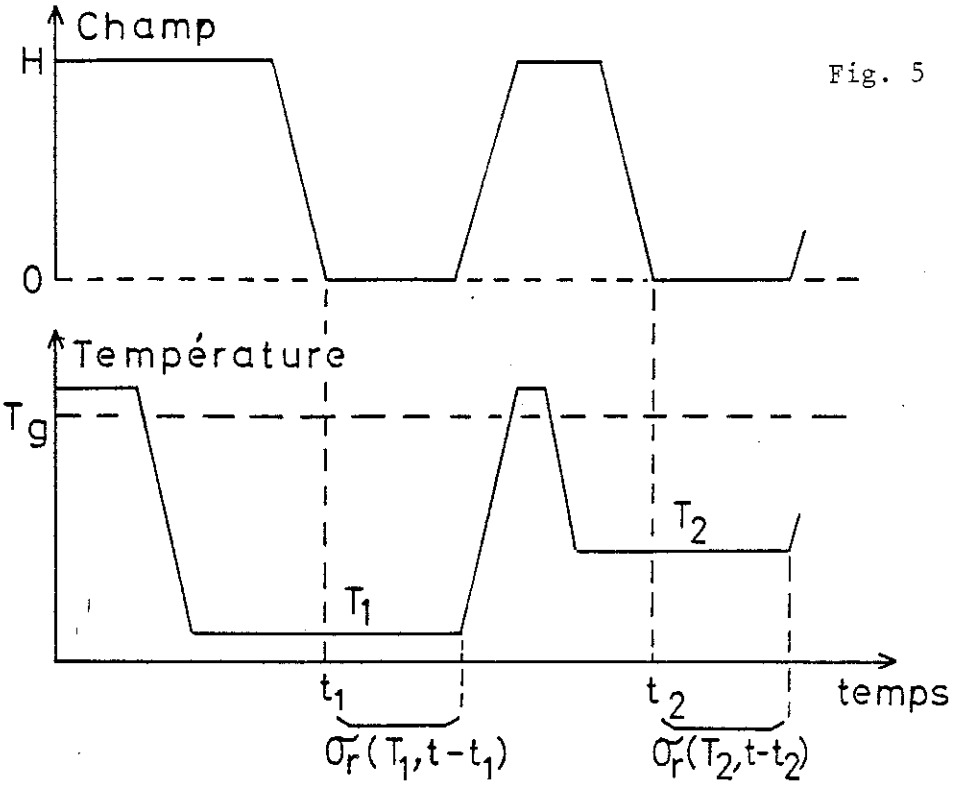

Fig. 5

Les résultats obtenus (figure 6, courbe (b)) montrent que, dans un diagramme $Ln\sigma_{rs} = f(T, t=1\ mn)$, la pente diffère sensiblement de celle obtenue à partir des valeurs observées dans la première méthode. Cette différence a été aussi observée par nous dans le système AuFe et par Tholence dans $Eu_{1-x}Gd_xS$.

Cependant, les valeurs de τ_o déterminées par chaque méthode sont identiques (10^{-13} à 10^{-11} s).

La mise en évidence de cette différence de comportement en fonction du processus expérimental utilisé (et pour laquelle nous n'avons pu jusqu'à présent apporter aucune explication) est nécessaire pour percevoir l'importance dans la littérature de la définition de l'histoire thermique du système avant la mesure.

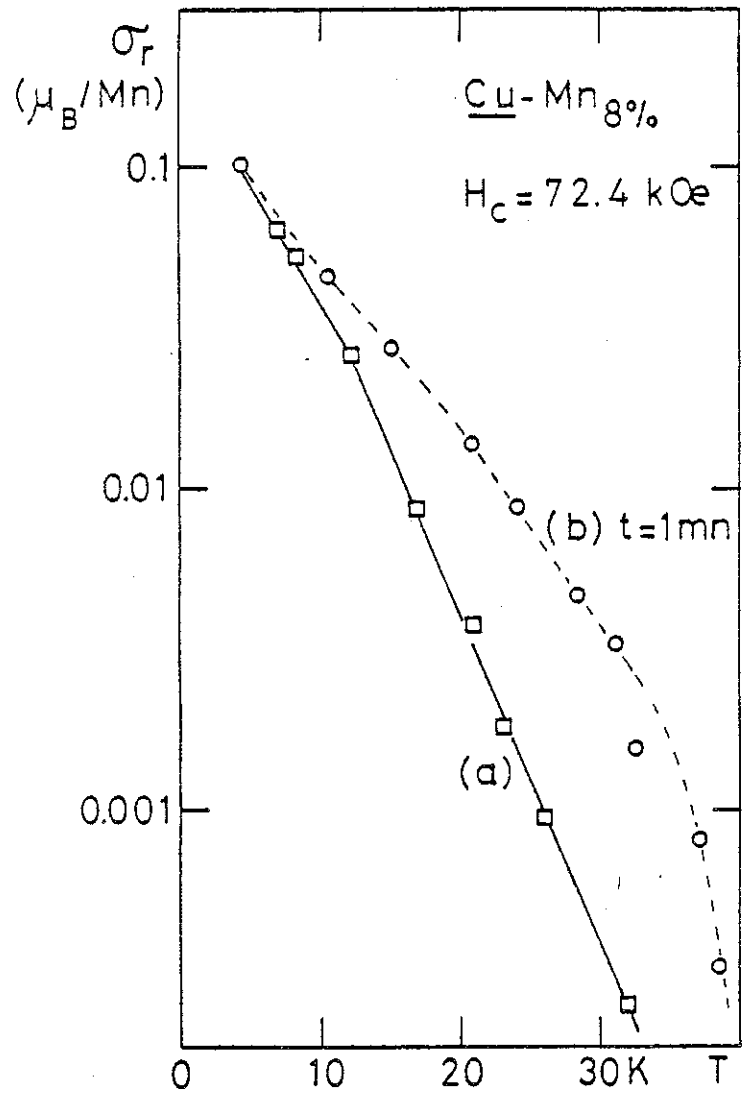

Fig. 6

3. DETERMINATION DE τ_o EN CHAMP NUL

Nous avons pu estimer précédemment la valeur de τ_o ($\sim 10^{-11}$ s) dans la gamme des champs utilisés pour construire les aimantations. Cette estimation n'est pas aisée et nécessite des résultats expérimentaux nombreux et précis. En effet, si on se limite à la zone de température ($T_g/3<T<2T_g/3$), la relaxation de l'aimantation rémanente saturée suit une loi puissance du temps avec un exposant proportionnel à la température.

$$\sigma_{rs}(T,t) = \sigma_{rs}(T,t=1)\ (t)^{-T/T_o}$$

$$= \sigma_{rs}(T,t=1)\ \exp(-\frac{T}{T_o}\ \mathrm{Lnt})\ .$$

C'est la pente de $\mathrm{Ln}\ \sigma_{rs}(T,t=1) = f(T)$ qui détermine τ_o : En effet, dans cette zone de température, $\sigma_{rs}(T,t=1) = \sigma_o \exp(-\alpha T)$, et $\mathrm{Ln}\ \tau_o$ est déterminé par $\alpha = \frac{1}{T_o}\ \mathrm{Ln}\ \frac{1}{\tau_o}$.

La loi puissance du temps est suffisamment précise pour déterminer T_o à 10 % près. Il est nécessaire d'être soigneux dans la détermination de α : si on assimile par exemple les résultats obtenus à basse température ($T < T_g/3$) et ceux obtenus pour $\frac{T_g}{3} < T < \frac{2T_g}{3}$ en une même variation de σ_{rs} "quasi" exponentielle en température, on peut faire une erreur pouvant aller jusqu'à 30 % dans la détermination de $\mathrm{Ln}\ \tau_o$ et ainsi estimer des valeurs de τ_o de 10^{-8} s dans l'exemple présenté figure 7.

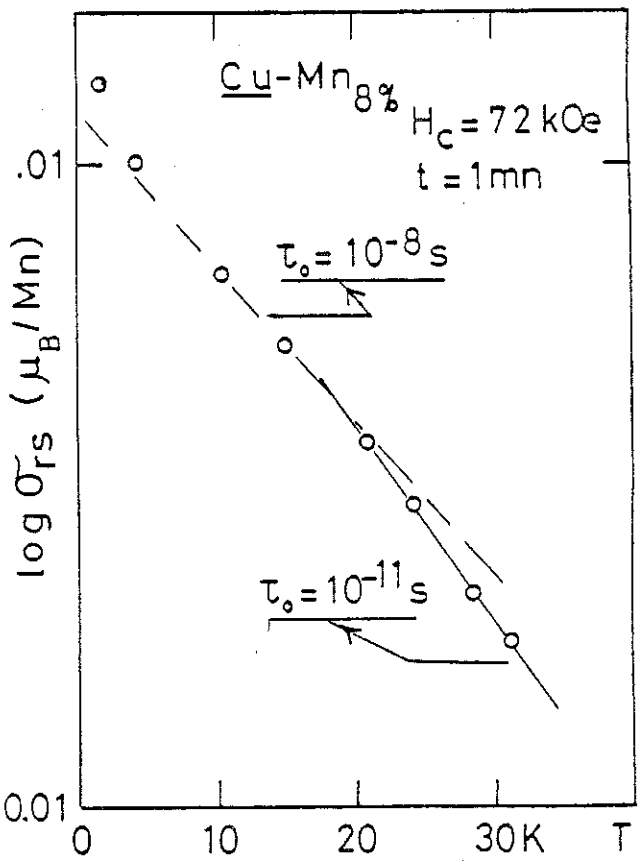

Fig. 7

Il est évident que, même en tenant compte de cette question, la précision obtenue sur τ_o (un facteur 10 à 100 près) ne peut permettre de déterminer par exemple une dépendance en concentration c d'impuretés magnétiques dans les systèmes que nous avons étudiés (c = 0.5 à 8 %).

Il est nécessaire de tester la valeur de τ_o trouvée précédemment dans des régions plus étendues en température et pour des champs de refroidissement différents. Nous avons été ainsi capable (chapitre II) de présenter les dépendances en temps et température de l'aimantation rémanente (saturée ou non) dans un diagramme en $TLnt/\tau_o$ où τ_o est la valeur déterminée précédemment. A basse température ($T \lesssim T_g/10$), l'aimantation thermorémanente, même obtenue à partir du champ H_c suffisant pour la saturer, est quasi linéaire en température.

$$\sigma_{r_{(H_c,T,t)}} \simeq \sigma_o(H_c) - \beta T \qquad (1)$$

et pour chaque température est linéaire en Logt. La fig. 8 représente $\frac{\partial \sigma_r}{\partial Logt}$ à T = 4,2 K en fonction du champ de refroidissement H_c, la variation de σ_r étant mesurée pendant 2 décades de temps. $\partial\sigma_r/\partial Logt$ croît avec le champ, passe par un maximum et rejoint un plateau, comme l'a déjà observé Sarkissian dans le système ScGd.

A l'aide de ces résultats et connaissant la valeur de σ_r mesurée 1 mn après coupure du champ H_c, on peut, comme le montre la figure 9, extrapoler la variation de $\sigma_r = f(H_c)$ à un temps de mesure de 2.10^{-6} s. La courbe en pointillé représente la dépendance en H_c de l'aimantation thermorémanente obtenue en refroidissant le système sous le champ H_c de $T > T_g$ à T = 1.6 K et mesurée 1 mn après coupure du champ. Quel que soit H_c, on peut écrire :

$$\sigma_r(H_c, T=1.6\ K, t=1\ mn) = \sigma_r(H_c, T=4.2\ K, t=2.10^{-6}\ s) .$$

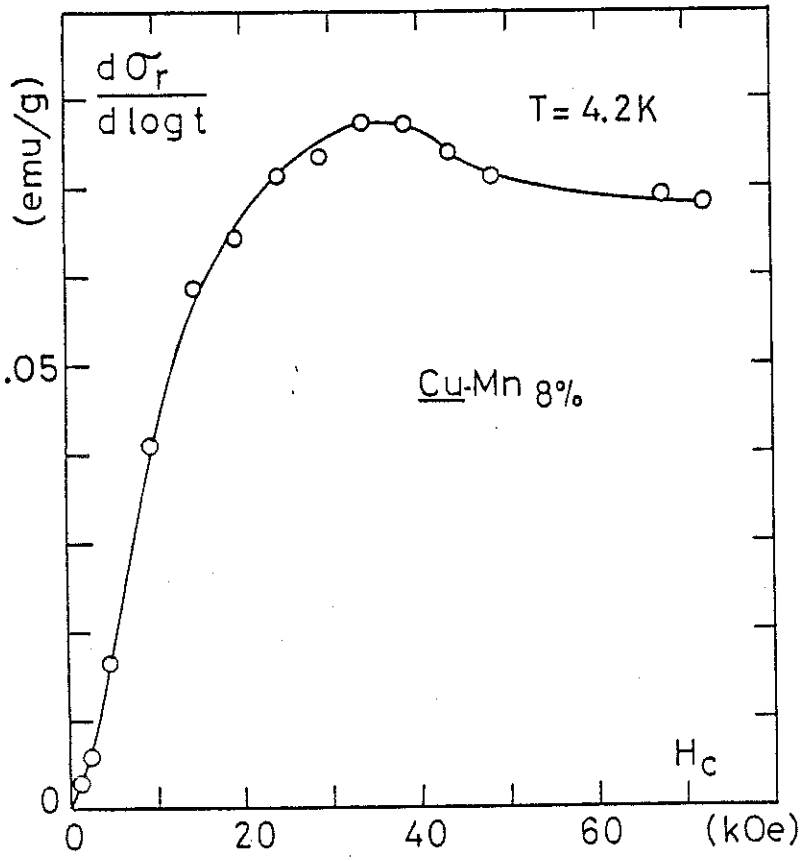
dσr/dlogt
T= 4.2K
(emu/g)
.05
0
Cu-Mn 8%
Hc
0
20
40
60
(kOe)

Fig. 8

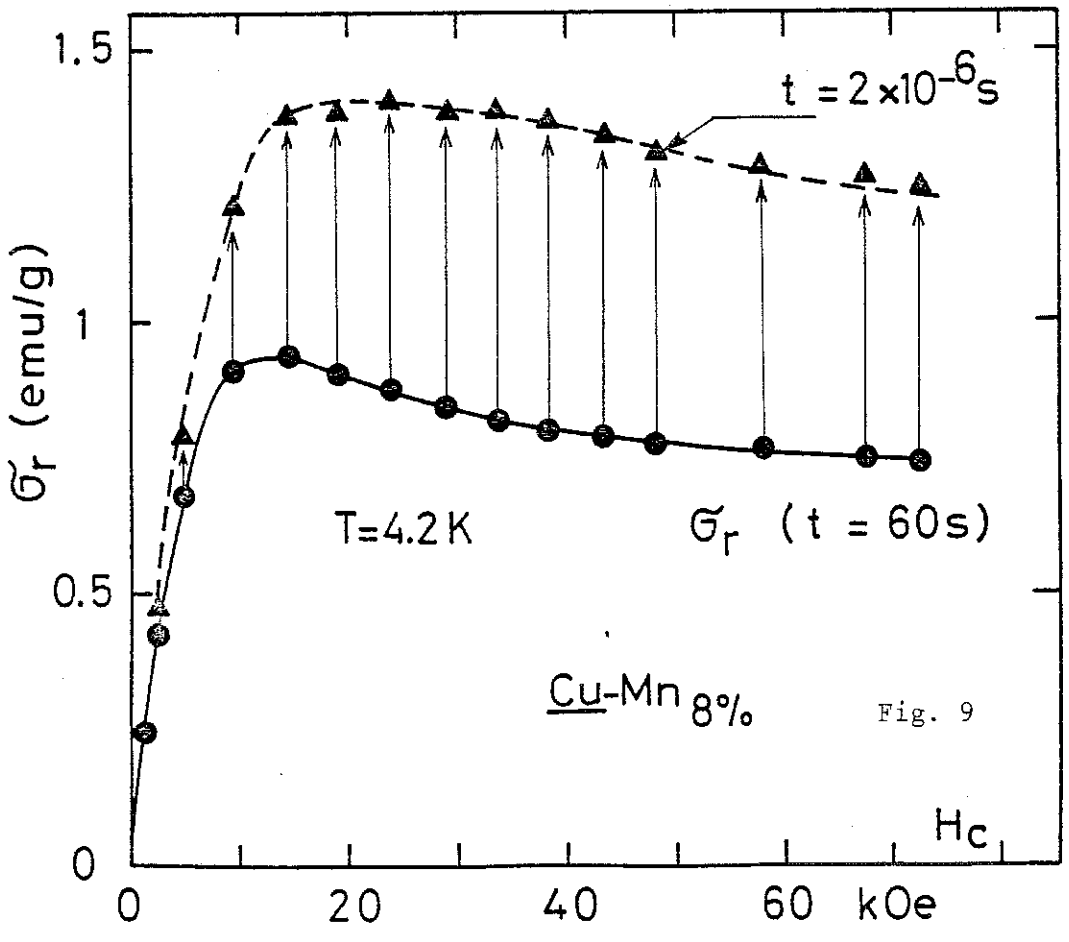
1.5
1
0.5
0
σr (emu/g)
t = 2x10-6s
T=4.2K
σr (t = 60s)
Cu-Mn 8%
Hc
0
20
40
60 kOe

Fig. 9

La généralisation de l'expression (1)

$$\sigma_r(H_c,T,t) = \sigma_o(H_c) - \beta(H_c)\ T\ \mathrm{Ln}\ t/\tau_o \quad ,$$

permet, par identification des résultats à (T = 4.2 K, t = 2.10^{-6} s) et (T = 1.6 K, t = 1 mn), de déterminer Ln $1/\tau_o$. Nous trouvons par cette méthode $\tau_o = 10^{-10}$ s.

4. DETERMINATION DE τ_o EN PRESENCE DE CHAMP MAGNETIQUE

L'application isotherme d'un champ H sur un système préalablement refroidi en champ nul produit une aimantation M dépendant du champ et de la température et évoluant dans le temps avec une dépendance logarithmique.

A suffisamment basse température ($T_g/10$), cette dépendance est linéaire en Logt, l'origine des temps étant prise à l'instant où le champ a atteint la valeur H.

Nous présentons sur la figure(10) la variation M(H) mesurée 1 mn après l'établissement du champ pour deux températures (4.2 K et 100 mK) et sur la fig. (11) la variation relative en temps $\frac{dM(H)}{dLogt}$ de l'aimantation mesurée à 4.2 K. En supposant que la variation de M(H) en temps peut s'exprimer linéairement en Logt, nous pouvons extrapoler à $t = \tau_o = 10^{-11}$ s, c'est-à-dire pour $T\mathrm{Lnt}/\tau_o = 0$, la valeur de l'aimantation M(H,4.2 K). Ces valeurs extrapolées sont peu différentes de celles obtenues expérimentalement à T = 100 mK si H $\leqslant$ 10 kOe.

Il est possible d'en conclure que, pour cette gamme de champs :

$$M(H,T,t) = M(H,T\ \mathrm{Ln}\ \frac{t}{\tau_o}) + \gamma(H)\ T\ \mathrm{Ln}\ \frac{t}{\tau_o} \ .$$

τ_o est donc peu dépendant du champ et sa valeur précédemment estimée permet de rendre compte des processus de relaxation sous champs.

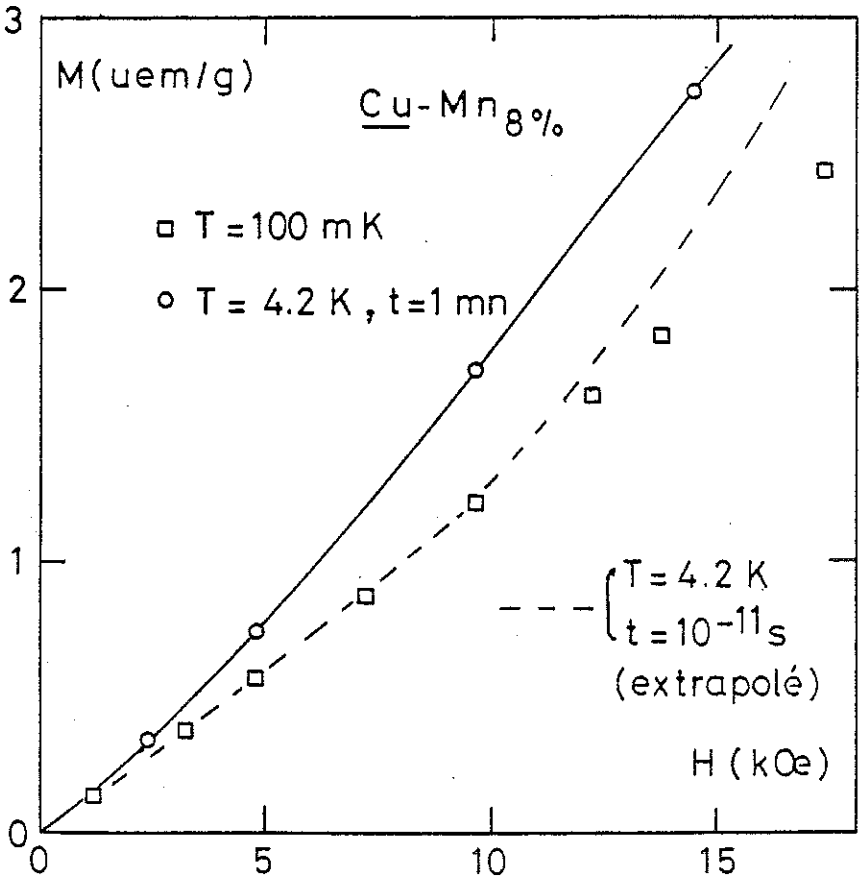
M(uem/g)
Cu-Mn 8%
T = 100 mK
T = 4.2 K , t=1 mn
T = 4.2 K
t = 10⁻¹¹s
(extrapolé)
H (kOe)
0
1
2
3
0
5
10
15

Fig. 10

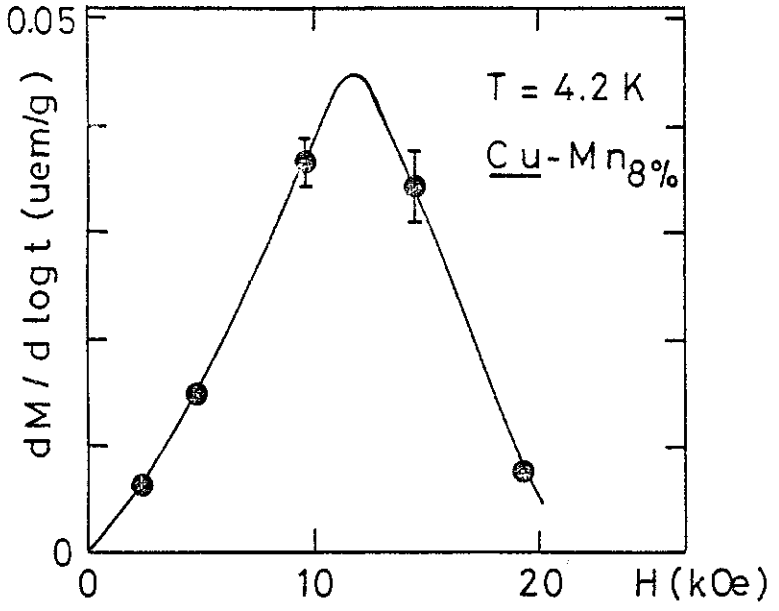
dM / d log t (uem/g)
T = 4.2 K
Cu-Mn 8%
H (kOe)
0.05
0
0
10
20

Fig. 11

5. CAS D'IMPOSSIBILITE DE DETERMINATION D'UNE VARIABLE UNIQUE TLn $\frac{t}{\tau_o}$

a) Grandes valeurs de τ_o :

Dans les chapitres 1 et 2 nous présentons des résultats exprimés en fonction de la variable unique TLn $\frac{t}{\tau_o}$, ce qui nous permet de conclure que les processus d'activation thermique sont responsables du franchissement des barrières. Pour des valeurs de τ_o suffisamment grandes pour que $k_B T$ Ln $\frac{t}{\tau}$ soit de l'ordre de quelques $k_B T$, on ne peut plus faire l'approximation de la transition brusque de 0 à 1 de exp $-\frac{t}{\tau}$ à $W=kTLnt/\tau_o$.

La relaxation des aimantations ne peut plus s'exprimer en fonction de la variable T Ln $\frac{t}{\tau_o}$, même si la loi d'Arrhénius est toujours valable.

C'est apparemment le problème en très bas champs (voir chapitre II).

b) Soit T_c la température (fixe dans le temps) au-dessus de laquelle l'échantillon est paramagnétique. On peut supposer, par analogie avec un ferromagnétique que l'aimantation du système est d'abord une fonction de $\frac{T}{T_c}$ qui dépend peu de la température tant que $T \ll T_c$. Cette aimantation chutera brusquement vers une valeur nulle à T_c. σ_r s'écrit sous la forme d'un produit :

$$\sigma_r = M_g(\frac{T}{T_c}).f(T \text{ Ln } \frac{t}{\tau_o})$$

qui fait intervenir deux variables $\frac{T}{T_c}$ et T Ln $\frac{t}{\tau_o}$. Il est possible de réécrire σ_r sous la forme d'une fonction de T Ln $\frac{t}{\tau_{o\,app}}$ au voisinage de T_c. La valeur apparente $\tau_{o\,app}$ ainsi estimée sera fonction de la température T et surtout pourra atteindre des ordres de grandeur qui n'ont aucune signification physique (10^{-40} s par exemple).

L'extraction de τ_o à partir de l'évolution temporelle de σ_r, nécessite de prendre des précautions :

- à $T \ll T_c$ $\quad M_g(\frac{T}{T_c}) \simeq$ constante et τ_o est bien défini
- à $T \lesssim T_c$ $\quad M_g(\frac{T}{T_c})$ évolue avec T et $\tau_{o\,app}$ ne nous renseigne pas sur une éventuelle échelle de temps τ_o.

C H A P I T R E I V

BREF BILAN PROVISOIRE DES PROPRIETES GENERALES DES VERRES DE SPINS

1 - Les résultats expérimentaux concernant la construction et la relaxation des aimantations dans les verres de spins nous ont permis de conclure à un comportement vitreux au-dessous d'une certaine température T_c. Au-dessus de T_c, le système semble devenir simplement paramagnétique. Les propriétés générales de ces aimantations, valables pour tous les verres de spins, sont susceptibles de décrire le comportement de la susceptibilité $\chi(T,t)$ dont la mesure alternative est à l'origine du regain d'intérêt pour ces systèmes.

2 - Les lois d'échelle en concentration c d'impuretés magnétiques sont observées[1], à condition de prendre certaines précautions : les températures caractéristiques T_o, T_g, T_c ne sont pas strictement proportionnelle à c dans le domaine de concentrations étudiées (fig. 1).

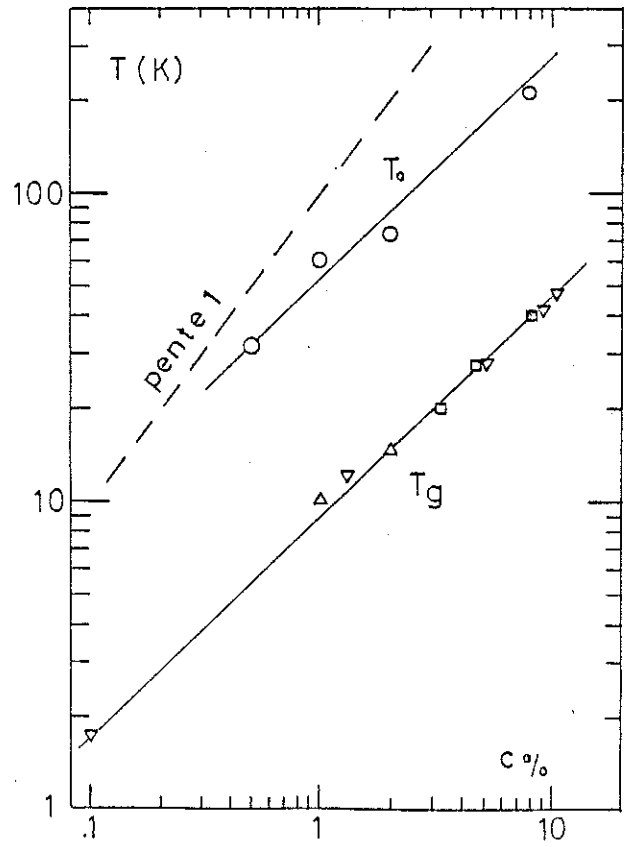

Fig. 1

Si l'interaction RKKY entre impuretés gouverne les propriétés verres de spins au-dessous de T_c, il faut tenir compte du libre parcours moyen λ des électrons libres pour décrire les lois générales observées plus haut. Le facteur $e^{-r/\lambda}$ (où r est la distance entre impuretés) que l'on introduit dans le potentiel J_{ij} d'interaction RKKY ($J_{ij} \sim \cos(2k_F r_{ij})/r_{ij}^3$) ne permet plus d'exprimer $\langle J \rangle$ et les températures associées en fonction de $\frac{1}{r^3} \sim c^{(1,2)}$.

D'autre part, la valeur de l'aimantation des entités magnétiques, mises en évidence précédemment, est très sensible à une éventuelle tendance au ferromagnétisme dans le cas des fortes concentrations. Les valeurs de σ_o (aimantation rémanente saturée à 0 K) (fig. 2) montrent une déviation notable à un comportement linéaire en concentration. De même, la dépendance en concentration du maximum de susceptibilité (χ_m) et, dans une moindre mesure, de la susceptibilité réversible à 0 K (χ_o), ne présentent pas le caractère constant auquel on s'attend dans le cas des lois d'échelle strictement observées.

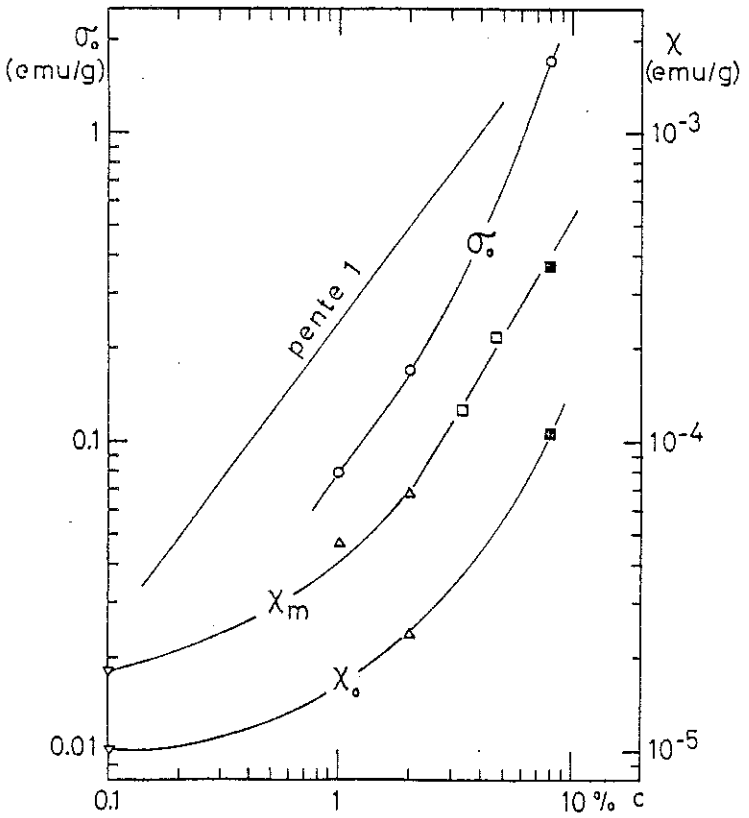

Fig. 2
Les différents symboles correspondent à des auteurs différents (cf. référence Ch. II)

C'est pour tenir compte de ces difficultés que nous avons introduit des diagrammes réduits du type $\frac{\sigma r}{\sigma_o} = f(T\ Lnt/\tau_o/T_o)$ et non de la forme $\sigma_r/c = f(T/c)$ dans l'étude de l'aimantation rémanente σ_r.

On peut également superposer (fig. 3) les courbes d'aimantation à temps constant $\frac{M}{\sigma_o} = f(\frac{H}{T_o},\frac{T}{T})$ pour diverses concentrations, à condition de se limiter à des champs ne détruisant pas le caractère initial des entités magnétiques. Pour des valeurs bien supérieures du champ, des diagrammes réduits $\frac{M}{c} = f(\frac{H}{T_o},\frac{T}{T_o})$ pourrait être en meilleur accord avec les résultats expérimentaux.

Fig. 3

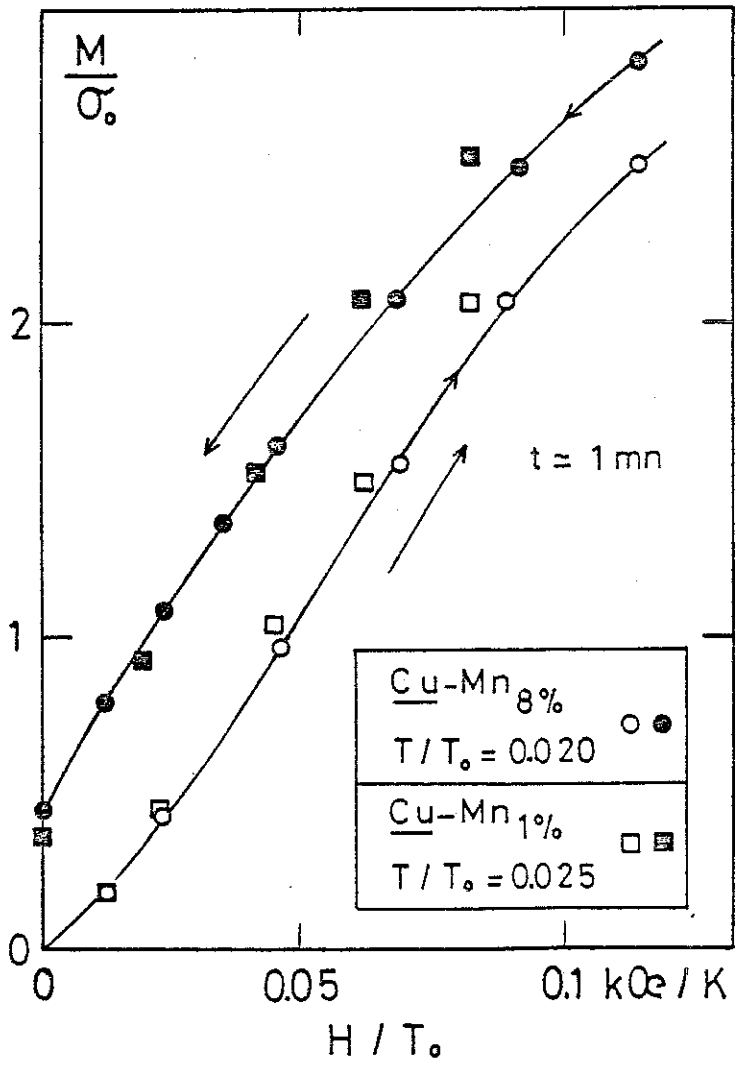

3 - L'observation expérimentale des relaxations de l'aimantation rémanente saturée et de l'énergie associée nous a conduit à utiliser un modèle de systèmes à 2 niveaux asymétriques.

Pour décrire l'ensemble des cycles d'hystérésis, il devrait être possible de prolonger en champ inverse ce modèle qui s'est révélé capable de rendre compte qualitativement des propriétés, générales à tous les verres de spins, de construction et relaxation des aimantations à $T < T_c$.

Nous nous heurtons alors à une contradiction avec l'expérience : il a été en effet observé que la forme du cycle d'hystérésis en champ inverse est très dépendante du système.

La compréhension de ce qu'est l'état verre de spins pose déjà des problèmes complexes, mais une nouvelle question apparaît maintenant : quels sont les processus supplémentaires responsables de la différenciation des cycles d'hystérésis ?

Pour essayer d'apporter une réponse, nous avons procédé à une étude détaillée et comparé des cycles pour différents systèmes.

Les résultats sont présentés dans les deux chapitres suivants.

REFERENCES

(1) Souletie, J., Thèse (1968) - Université de Grenoble.

(2) Larsen, U., Solid State Comm. 22 (1977) 311.

CHAPITRE V

CYCLES D'HYSTERESIS DANS L'ETAT VERRE DE SPINS

L'examen du cycle d'hystérésis du système AuFe (fig. 1) ne montre aucune discontinuité : en champ négatif croissant, la destruction progressive de l'aimantation rémanente positive et la construction d'une aimantation négative peuvent être décrites de manière continue avec le modèle utilisé précédemment en champ positif.

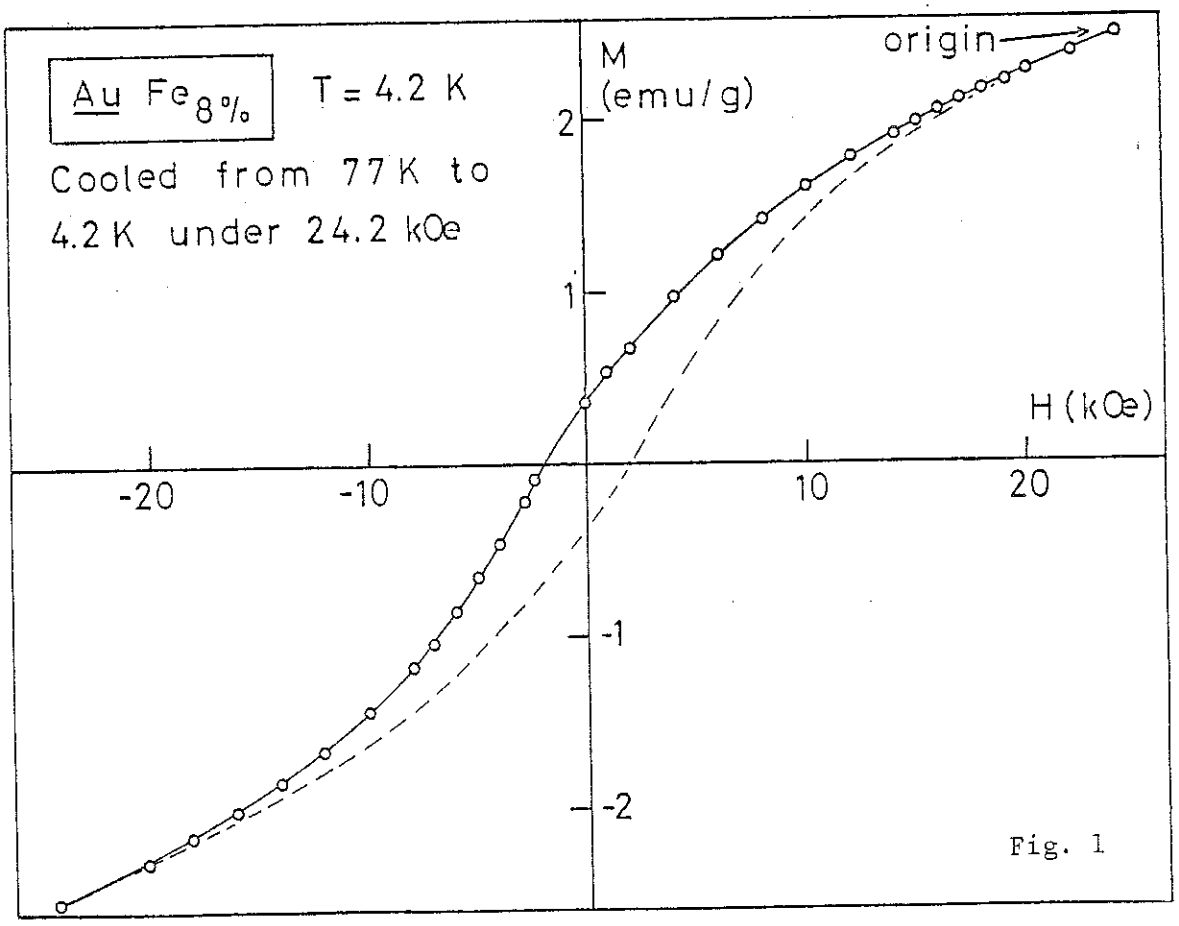

Fig. 1

Alors que la construction et la relaxation de l'aimantation en champ positif sont identiques dans CuMn et AuFe, la figure 2 montre que l'aimantation rémanente du système CuMn préfère se retourner globalement en faible champ négatif.

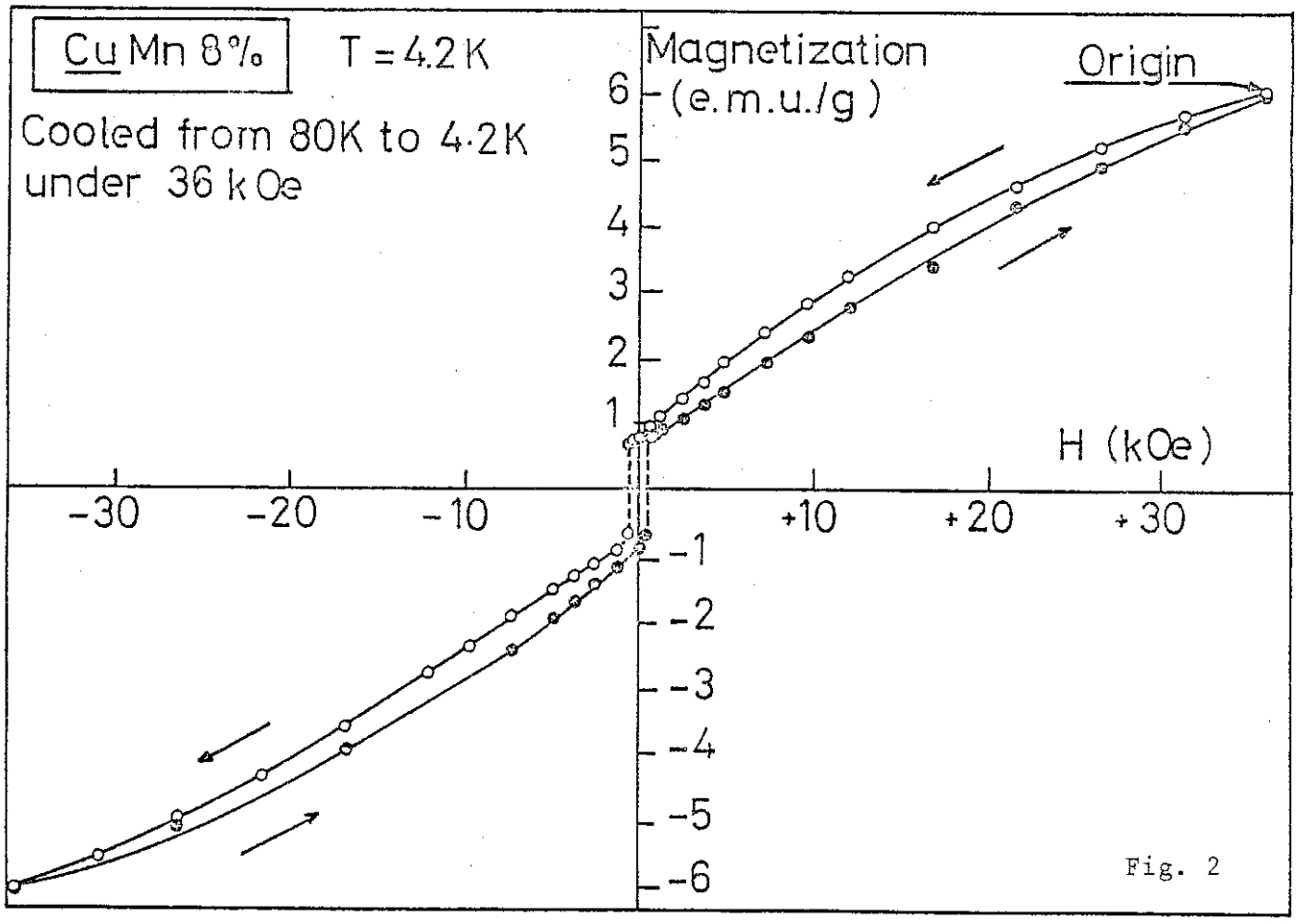

Fig. 2

Cette propriété spécifique du système CuMn n'est pas en soi surprenante. Nos résultats expérimentaux précédents ne nous ont pas permis de déterminer précisément si un seul type d'interactions entre impuretés est responsable des barrières de potentiel et des états différents d'énergie. Si l'interaction dominante dans le problème des verres de spins est isotrope par symétrie de rotation, l'aimantation rémanente, une fois construite dans une certaine symétrie, peut répondre comme un moment unique à toute sollicitation de champ extérieur dont la symétrie est différente. Il suffit pour cela que le réseau n'exerce pas sur l'aimantation un couple suffisant pour empêcher cette réponse et que les temps impliqués dans les sollicitations de champ extérieur soient courts devant le temps de vie de l'aimantation rémanente.

On conçoit dès lors l'importance d'une étude détaillée des cycles d'hystérésis du système CuMn pour avancer dans la compréhension microscopique des propriétés de la phase verre de spins.

Des résultats expérimentaux déjà anciens (Kouvel) de cycles d'hystérésis et de réponse en champ transverse de l'aimantation rémanente existent pour des concentrations de manganèse supérieures à 5 % at.

Nous avons prolongé cette étude pour des concentrations variant de 600 ppm à 2 %at. de manganèse dans le cuivre.

Dans une première publication ("observation of magnetization reversal and macroscopic domains in CuMn spin glass"), nous mettons en evidence que le système, une fois l'aimantation rémanente σ_r construite, se comporte comme un grain monodomaine :

- En faible champ inverse, la susceptibilité $\chi(T)$ est conservée.
- Le système garde en champ négatif croissant la mémoire de la symétrie de σ_r jusqu'à un champ seuil H_r, où l'aimantation rémanente s'inverse brusquement.
- H_r a une valeur faible en comparaison de l'ordre de grandeur des champs nécessités pour construire σ_r.

Les lois générales de la magnétostatique d'un monodomaine sont observées lorsqu'on superpose au champ inverse un champ transverse (astroïde de Stoner). L'énergie d'anisotropie associée est peu dépendante de la température, varie comme le carré de la concentration de manganèse et dépend de l'état métallurgique de l'alliage. Ces résultats sont exposés dans une seconde publication : "Magnetic hysteresis of CuMn in the spin glass state".

Ces données expérimentales laissent à penser que c'est l'interaction RKKY qui est dominante dans les propriétés verre de spins du système CuMn. En effet, cette interaction est symétrique par rotation : Si rien ne couple magnétiquement l'aimantation rémanente au réseau, l'ensemble constitué par les impuretés magnétiques et les électrons de conduction est disponible pour toute rotation collective.

Le problème qui se pose à ce stade de l'étude est de comprendre pourquoi le système AuFe ne présente pas une telle propriété. Nous reviendrons dans le chapitre VI sur cette question essentielle.

JOURNAL DE PHYSIQUE *Colloque* C6, *supplément au n°* 8, *Tome* 39, *août* 1978, *page* C6-910

OBSERVATION OF MAGNETIZATION REVERSAL AND MACROSCOPIC MAGNETIC DOMAINS IN Cu Mn SPIN GLASS

P. Monod*, and J.J. Prejean

Centre de recherches sur les très basses températures, C.N.R.S. 166 X, 38042 Grenoble Cedex, France.

Résumé.- L'étude du cycle d'hystéresis d'alliages Cu Mn dilués (< 2 % at.) révèle un comportement "carré" de l'aimantation rémanente : les deux branches du cycle sont reliées par un saut d'aimantation. Dans le cas d'un renversement partiel de l'aimantation, on observe deux domaines magnétiques macroscopiques ce qui implique l'existence de corrélations à longue distance des propriétés dynamiques de l'aimantation.

Abstract.- The hysteresis cycle of dilute Cu Mn alloys (less than 2 % at.) well below the spin glass temperature is observed to be "square" like i.e. : the two branches of the cycle are connected by a single magnetisation jump. By allowing only a partial magnetization inversion, two macroscopic magnetic domains are observed, implying along range correlation in the magnetization dynamics.

A number of investigations of hysteresis in dilute magnetic alloys have revealed on the one hand the phenomena of shifted hysteresis loop /1/ in Cu Mn and Ag Mn and on the other hand magnetization instabilities giving rise to large amplitude magnetization jump at low temperature /2/ in Au Fe and Cu Co. However, no systematic study of hysteresis has been carried so far for impurity concentration less than a few atomic per cent. We show that for Cu Mn (0,5 %) at low temperature both phenomena occur and in certain cases large scale magnetic domains are in fact being observed. Our magnetization measurement are made by integration of the magnetic flux variation induced by the passage of the sample between two counter-wounded pick up coils /2/. This method is a D.C. method (measurements are made point by point as a funtion of the static magnetic field) but allows to measure any rapid magnetization change within the sample at any time between two measurements. The sample is in the form of a cylinder 0.5 × 0.5 × 2 cm. It has been made from high purity copper and manganese /3/ by a crucible less, semi levitation, induction melting. It was quenched from the melt, then cold rolled to final dimensions and annealed at 950° C for 1 hour in Ar + H_2 atmosphere.

As quite similar results have been observed in 0.3 % and 2 % alloys, we will only report here the observations on a 0.5 % atomic alloy which we consider as "typical". For this alloy the spin glass temperature is about 8 K. As the static magnetization of this system has been amply described /4/ in high fields, we will focus on the low field behaviour (forward and reverse). However, it should be remembered that the measured magnetization corresponds to a very weak remanent moment per Mn atom of the alloy typically of the order of 0.05 Bohr magneton /Mn or less due to the high degree of spin disorder present below Tg.

In order to perform a complete hysteresis loop, we start from high field situation by cooling the sample from 4.2 K to 1.35 K in a field of 3.2 kgauss The main effect of field cooling is to give to the sample a non zero remanent magnetization in zero field as is apparent at point A of figure /1/. When the field is reversed, the magnetization decreases linearly from A (h=0) to B (h= -150 gauss). This variation is reversible i.e. bringing back the field to zero the magnetization takes a value close to the starting point A but somewhat less due to the always present logarithmic time decay of the remanent magnetization /4/. The slope of this linear variation is identical to that observed in positive fields (this is the reversible part of the susceptibility). At point B (h= -150 gauss) a sudden "jump" occurs towards point C with a time constant less than 0.1 second. The amplitude of the jump corresponds to nearly 90 %reversal of the remanent magnetization. After this jump the same linear slope towards D is observed and no further jumps. Coming back to zero field the same slope is followed upwards and a reverse remanent magnetization measured at E (h=0). At point F (h= +30 gauss) a reversed jump happens bringing back the magnetiza-

* Permanent address : Physique des solides Université Paris Sud 91405 Orsay FRANCE

tion at G, close to it's initial value, but somewhat less.

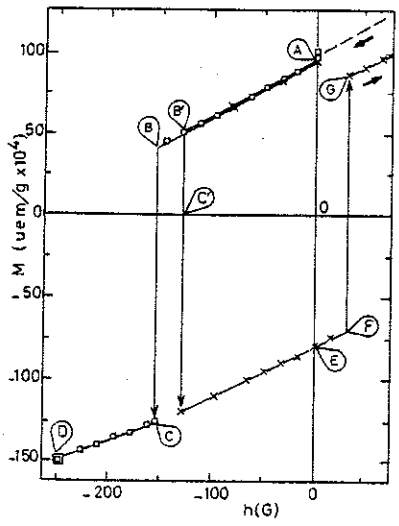

Fig. 1 : Hysteresis cycle for Cu Mn 0.5 % after cooling from 4.2 K to 1.35 K in 3.2 kgauss. Arrows indicate the path followed.

Thus, the entire cycle can be described as two reversible linear parts connected by two almost complete magnetization jumps occuring at non symmetrical values of the field with respect to zero field.
We have tried to characterize these facts more precisely and we will only state here our observations :

- the value of the remanent magnetization and the reversible slope do not depend on the sample metallurgical state (i.e. annealed or cold worked),
- the amplitude of the jump is largest for the best annealed samples,
- the jumps occur spontaneously after a few minutes if the reversed field is applied slowly and left constant (point B'). It can be triggered by an external perturbation such as a mechanical shock,
- the temperature dependance of the cycle is such as to leave the cycle area roughly constant (within a factor 2) between 0.1 K and 2.5 K,
- the jump occurs in all cycles in that range of temperature.

At certain occasions (for a field slightly less than the threshold field), a partial jump is observed i.e. only 50 % of the magnetization is reversed. When this state is achieved, the overall magnetization of the sample is close to zero (point C' on figure 1). However, the magnetization density is observed to be inhomogeneous on a large scale : as the sample is being removed from one of the measuring coils a voltage corresponding to one direction of the magnetization is first recorded and the opposite direction is then observed when the sample leaves the coil. Thus, it appears that at least two macroscopic domains "head on" have been formed. This state is unstable against a small increase of the reversed field. However, letting the field decrease leave the domain configuration "frozen in" as evidenced from the asymmetry of the recorded signals. A number of puzzling questions are raised by these observed facts among which the more important are :

- Is the magnetization instability observed as a characteristic of the spin glass state ?
- What fraction of the spins are involved in the reversal process ?
- What is the nature of the domains ?
- Does the observation of domains imply long range order in a spin glass ?

We wish to acknowledge essential discussions for our understanding with J.L. Tholence and R. Tournier.

References

/1/ Kouvel, J.S., J. Phys. Chem. Solids 21 (1961) 57.
Knitter, R.W., Kouvel, J.S. and Claus, H., J. Mag. and Mag. Mat. 5 (1977) 356.

/2/ Tournier, R., thèse, Université de Grenoble (1965)

/3/ A.S.A.R.C.O. 5 "9" and Johnson Mattey high purity grade

/4/ Lutes, O.S. and Schmitt, J.L. Phys. Rev. 125 (1962) 433
Lutes, O.S. and Schmitt, J.L. Phys. Rev. 134 (1964) A676
Souletie, J. and Tournier R., J.Low Temp. Phys. 1 95 (1969)
Tholence, J.L. and Tournier, R. Physica 86-88B (1967) 873

7324 J. Appl. Phys. 50(11), November 1979 0021-8979/79/117324-06$01.10 7324

Magnetic hysteresis of CuMn in the spin glass state

P. Monod,* J. J. Préjean, and B. Tissier**

CRTBT CNRS 166 X38042 Grenoble (France)

We present a series of measurements of the magnetic hysteresis properties of alloys of CuMn in the concentration range 0.06% at. to 4.7% at. when these are cooled well into the spin glass state i.e. $T/Tg < 0.3$. Previous studies (1) made at higher concentrations have revealed the occurrence of a complete reversal of magnetisation in a narrow range of coercive fields and a shifted hysteresis loop. Quite unexpectedly we find that going to lower Mn concentration increases the cooperative nature of the magnetisation reversal to the point where the hysteresis becomes square and that complete, spontaneous (less than 0.1 second time constant) magnetisation jumps are observed in low magnetic field (typically 150 gauss) together with a shifted square center. We report on the effect on the hysteresis of a number of variables: the magnetisation, the concentration, the temperature, the metallurgy, the time and the application of a static transverse magnetic field. These observations lead to the existence of a well defined anisotropy field in the spin glass state.

PACS numbers: 75.30.Hx, 75.60.Ej, 75.60.Nt

I - INTRODUCTION

Among the magnetic measurements carried out on dilute alloys of magnetic impurities in the spin glass state relatively little attention has been given to the properties of the magnetisation along a complete hysteresis loop. Kouvel(1) has reported a systematic investigation of the system CuMn between 5% to 28% at Mn and AgMn between 12% to 24% at.Mn at helium temperature. His observation of very narrow cycles displaced towards negative fields led him to analyse these systems in a way similar to NiMn alloys with a mixture of ferromagnetic and antiferromagnetic regions giving rise to exchange anisotropy(2).Beck et al(3) have studied as a function of temperature the properties of CuMn 25% and scattered work, assembled in Table 1, has reported some information about hysteresis of CuMn but not in a systematic way. On the other hand Tournier(5) has investigated the hysteresis properties of AuFe 8%, AuCo 6% and CrFe 15% down to 0.1°K. He observed very broad (Kgauss) cycles interrupted by large scale magnetic instabilities or "jumps".

TABLE 1

HYSTERESIS DATA ON Cu Mn

Concentration (at %)	Température (°K)	Ref	Sample
24.1	4.2	a	also AgMn, same concentration
5.5, 8.9, 14 18.9, 24.1, 28.6	1.8	b	also AgMn, same concentration
1.8	4.2	c	remanent magnetisation cycle
0.34	1.6	d	
17.7	20	e	Single crystal Torque hysteresis
25	4.2	f	cold worked
25	4.2, 15, 29.8, 60	g	Quenched
9	4.2	h	
1.89	0.06	i	
0.5	1.35	j	
14	4.9	k	

REFERENCES OF TABLE 1

a - Kouvel J.S.J.Appl.Phys.31, 142 S(1960).
b - Kouvel J.S,J.Phys.Chem.Solids 21,57(1961).
c - Jacobs I.S. and Schmitt R.W., Phys.Rev.113 459(1959).
d - Franz J. and Sellmyer D.J.Phys.Rev.B8 2083 (1973).
e - Iwata T, Kai K., Nakamichi T. and Yamamoto M.J.Phys.Soc. Jap.28, 582 (1970).
f - Tustison R.W. Solid St.Comm.19 1075(1976).
g - Beck P.A.Prog.Mat.Science 23, 1, (1978).
h - Knitter R.W., Kouvel J.S. and Claus H., J.Magnetism Magnetic Mat.5 356 (1977).
i - Careaga R., Thèse de 3ème cycle, Université de Grenoble (unpublished)(1968).
j - Monod P.and Préjean J.J., J.Phys.C6 910 (1978).
k - Schwink C. § Schulze U.J.Magnetism Magnetic Mat.9,33 (1978).

The purpose of our study is to investigate systematically the properties of CuMn dilute alloys at concentrations below 5% in the spin glass state and, from the simple behaviour found(6) to investigate the effect of a number of variables on the hysteresis. In order to understand what this kind of work can tell about the nature of the spin glass state we have to recall first the properties of the magnetisation. According to Tholence and Tournier(7) the magnetisation in the spin glass state is the sum of the reversible magnetisation and the irreversible, or remanent, one. The reversible magnetisation is linear with field at low fields, and independant of temperature below the spin glass temperature Tg defined by the susceptibility cusp(8), it is best compared to the perpendicular susceptibility of an antiferromagnet. The remanent magnetisation appears progressively below Tg. It can be induced either by cooling the alloy below Tg in a fixed field(Thermo-Remanent Magnetisation TRM) or by exposing for a short time the spin glass(previously cooled in zero field)to a somewhat larger field at fixed temperature(Iso thermal magnetisation IRM). The qualitative properties of the remanent magnetisation are quite similar in all known spin glass systems(9). They have been best described in terms of the theory of rock magnetism by Néel(10) as an average over a collection of independant magnetic particles, implying that the spin glass state is inhomogeneous by nature. Such a model is particularly well suited to account for the slow time dependance observed and has very definite predictions about the hysteresis properties. The principle of such an analysis has been carried out, starting from the magnetostatic equilibrium of each magnetic particle by Stoner and Wohlfarth(11). As we shall see, our major conclusion (which was already noticed by Jacobs and Schmitt(1959) (ref c table 1)) is that an independant particle picture is basically inadequate to represent the collective magnetisation reversal observed on macroscopic samples which, on the contrary seem to imply the existence of correlations at large distances for the dynamic of the spins in the spin glass state of CuMn.

II - EXPERIMENTAL CONDITIONS

The alloys(4.7%, 2%, 0.5%, 0.3% and 0.06% at Mn) were prepared by melting the constituents(12) in an induction furnace and casting the melt into a cold copper cylinder 7mm diam.from which a length of 20mm was machined. As the as quenched 0.5% alloy was suspected to be inhomogeneously strained by the casting procedure a systematic anneal at 900°C in $Ar+H_2$ atm.for 1 hour was given after an initial cold rolling of less than 50%. This resulted in highly polycristalline samples with grains $\sim$ 1 mm. The magnetisation was measured by the extractions method(13). The sample is moved between the centers of two counter-wounded coils($\sim$ 7000 turns) 4 cm apart in a constant magnetic field. The induction

pick up is sent into an integrating galvanometer whose deviation is recorded. The sensitivity is limited by the mechanical vibrations in presence of the field or by thermal emf in zero field and is of the order of 10^{-4} emu well beyond our needs. It should be noted that due to the finite integrating time of the galvanometer circuit of $\sim$10 seconds this system can be left continuously integrating and so is able to record not only the magnetic flux change associated to the extraction but also any magnetisation change occuring within the sample, at any time, provided that the time constant of this change be somewhat less than 10 seconds. The temperature ranged from 4.2°K down to 0.07°K achieved by adiabatic demagnetisation. The field was produced by a nitrogen cooled copper coil and was about 3.2 Kgauss max. ensuring that no hysteresis is associated with the field as might be the case with superconducting coils.

III - RESULTS

a) *Description of the elementary cycle.*

We will be mainly concerned at first by the description of the hysteresis properties of the 0.5% at Mn alloy. For this alloy Tg$\sim$8°K(14). It is cooled from 4.2°K to 1.25°K in 3.2 Kgauss. As the magnetic field is being decreased to zero at this temperature the first branch of the hysteresis cycle is measured(point by point) arriving in zero field at A on Fig 1. At this point some time dependance of the remanent magnetisation can be easely observed over the first minutes as is well known(15). As the field is reversed the same slope of magnetisation is observed in negative fields as in the positive part due to the reversible magnetisation (and indeed coming back to zero field at this stage leaves the remanent magnetisation unchanged, to within the unavoidable logarithmic time decrease effect). At point B($\sim$ - 150 gauss) a sudden reversal of the magnetisation occurs going to point C on Fig 1. The amplitude of the magnetisation reversal as measured by integrating the magnetic flux change is within 1% equal to the difference between the magnetisation measured by extraction just before (B) and right after the reversal(C): this means that all the magnetisation change has occured in less than 1 second. In the best cases this amplitude amounts to a reversal of 95% of the initial remanent magnetisation(but can be sometimes less)without ever exceding this value, independantly of the value of the reversible magnetisation which appears simply"superposed" to the remanent magnetisation.Going beyond point C the slope of magnetisation towards D is again that of the reversible magnetisation. In cases where only a partial reversal of the remanent magnetisation is observed at B, one or a few more smaller jumps are observed upon further increasing the negative field until the total remanent magnetisation is inverted.

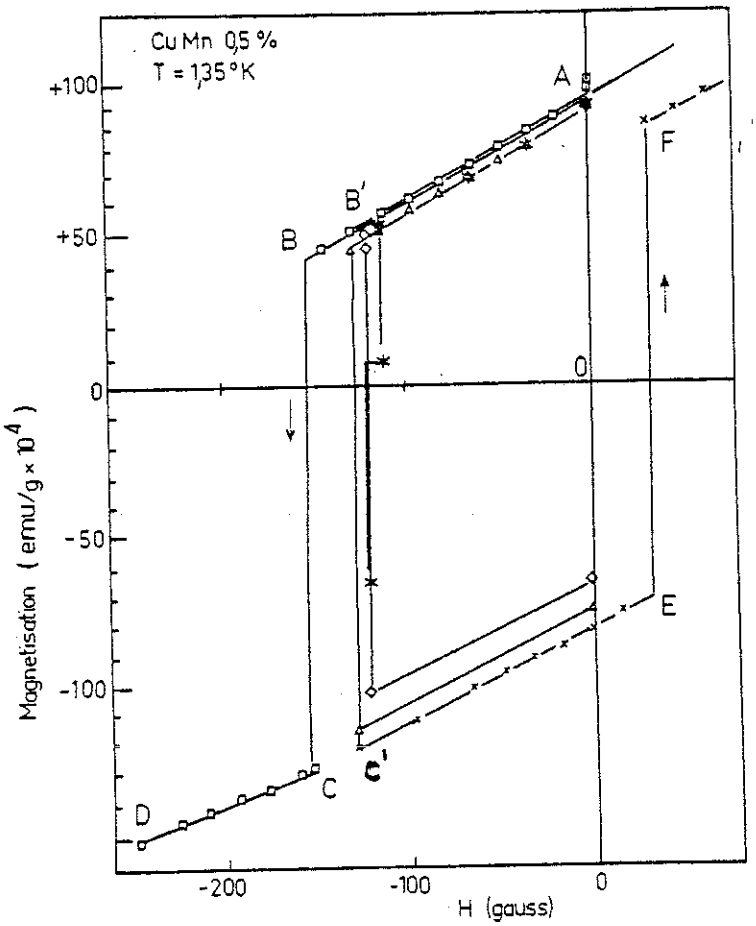

Fig 1: Hysteresis of CuMn 0.5% at 1.35°K with saturated remanent magnetisation. Different symbols are used for different runs.

At point D essentially all the remanent magnetisation is now reversed and a choice is possible:

i) to continue into larger negative fields until a more or less symmetrical magnetic state from the starting point is reached or:

ii) to come back towards zero field.

We have systematically operated with the second choice for the following reason: by going to large negative fields we will simply build up a magnetisation of the sample in inverse fields by the IRM process. The returning branch of such a cycle is by definition the mirror image of that in positive field and does not provide a new physical information. Such a symmetrical loop is found in ref h(table 1)(16). Coming back from D towards zero field the same reversible slope of the magnetisation is followed until point E(+ 20 gauss) is reached. (When passing by zero field the inverse remanent magnetisation is measured accompanied by an inverse time dependance i.e. leading to a net decay in amplitude). At E(not symmetrical to C) again a sudden reversal of the magnetisation takes place bringing the magnetisation

close to, but somewhat less than, the original branch of the cycle. Again if the jump at E is incomplete it is immediately followed by a discrete serie of smaller jumps. Thus the entire cycle at low fields can be caracterised by a square loop of width 170 gauss displaced from the origin by - 80 gauss and superposed to a constant slope due to the reversible magnetisation. This behaviour, although reminiscent of the overall observation of Kouvel and Tournier, is quite unexpected a priori in a dilute alloy as the cycle appears more square than for the more concentrated alloys reported(1). We have studied in great detail the magnetisation reversal at point B: it is a genuine macroscopic magnetisation instability: it is possible to leave the system at B', within a few gauss of point B and wait, sometime a few seconds, sometime a few minutes, until the system spontaneously reverse to point C'. The time constant inferred for this reversal is about 0.1 sec but might be limited by the eddy currents within the sample. It is noted that the logarithmic time dependance of the decay of the magnetisation is present as well at B(or B') and is found (if measured while waiting for the instability to occur) to correspond to the same rate as in zero field. Thus the instability phenomena cannot be attributed to a catastrophic acceleration of this process. We have noted also that it is possible to trigger the instability at B' with a mechanical shock(in fact applied to the whole apparatus!). Finally it should be noted that the reproducibility of both instabilities is good to no better than 20 gauss from an average position in field although the reproducibility of the remanent magnetisation and reversible slope can be better than a few percent from run to run.

b) *Transverse Magnetostatic.*

In order to understand more fully the kind of magnetostatic involved we have studied the influence of a transverse field on the occurence of the instability. Such experiments have been briefly reported by Arrott(17) however we seriously question his interpretation.

The experiment now consists in cooling the sample in the original field, now labelled H_Z, and once the remanent magnetisation is obtained at $H_Z = 0$, we apply a small transverse static field H_X of different strength up to 95 gauss. We then invert H_Z and slowly increase it and we note the value for which the magnetic inversion takes place, for each value of H_X (See insert of fig(3))(18). With this procedure we could produce a set of couples of points (H_Z, H_X) at which the instability occured near point B and another set of values for the reverse jump near point E. These points appear on Fig 2 together with the best fit to the astroid of Stoner and Wohlfarth(11) or Landau and Lifchitz(19):

$$H_X^{2/3} + H_Z^{2/3} = H_A^{2/3}$$

characteristic of the existence of an uniaxial anisotropy

energy parallel to the Z axis.

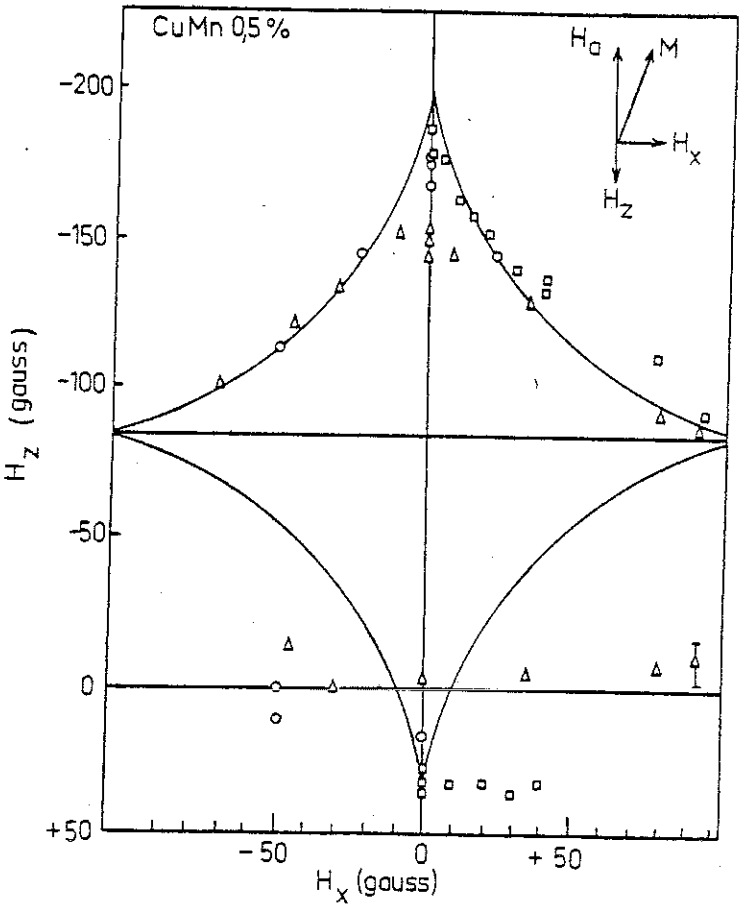

Fig.2: Relation between the longitudinal field H_Z and transverse field H_X at which a magnetisation reversal is observed. The solid line represents a fit to the Stoner-Wohlfarth astroid with H_A=110 gauss centered at -80 gauss. Upper points:"Forward" jump near point B Fig 1. Lower points:Reverse jump near point E Fig 1.

The fit with H_A = 110 gauss can be considered to be fair for the forward jump(upper part) but is out of question for the reverse one(lower part)(20). At this point our partial conclusion is that in as much as a square cycle can serve to define an anisotropy field by it's half width and a displacement field by it's center it should be reminded that the magnetostatic equilibrium is not the same on both sides of the square and that only the forward instability(at B) can be described by a simple uniaxial anisotropy energy. Although we have not tested these transverse properties in different conditions of temperature, concentration etc... we think that they apply quite generally in the other cases of our study as suggested by other work(17,21). Keeping the above mentionned restrictions in mind we will further analyse the cycles only in term of width and shift.

c) *Temperature effects.*

The temperature dependance of the hysteresis cycle is mainly that associated with the temperature dependance of the remanent magnetisation. We see in Fig 3 that upon warming from 1.35°K to 2.28°K the remanent magnetisation decreases by a factor 2 but the hysteresis cycle still contains two complete jumps with fast time constants.

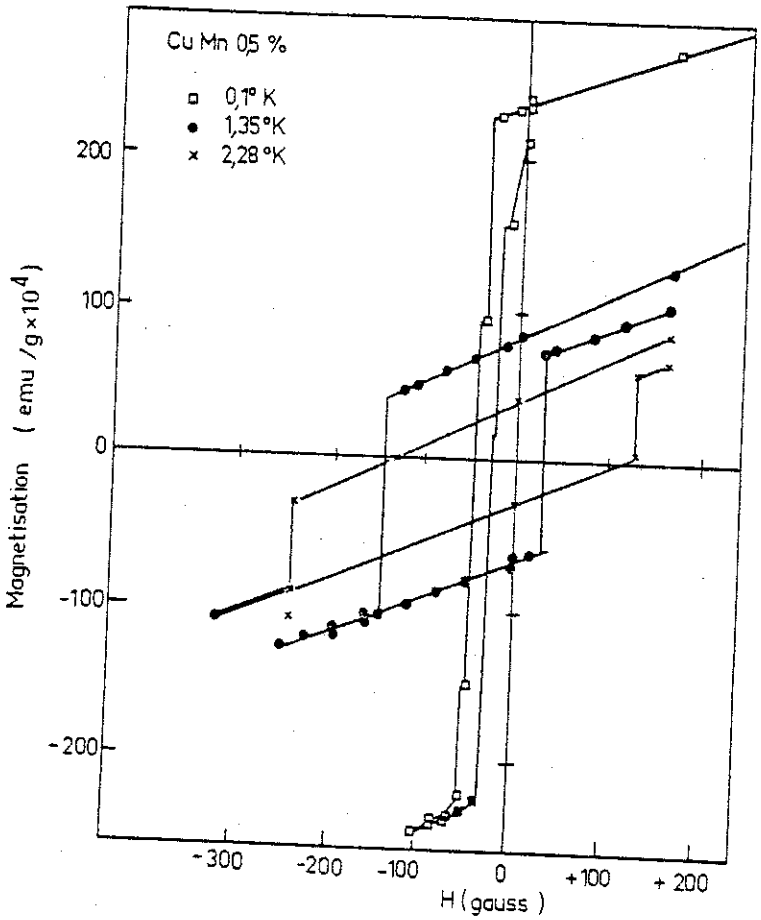

Fig.3: Hysteresis cycle of CuMn 0.5% at three temperatures with saturated remanent magnetisation. The cycle with blackdot is identical to that of Fig 1. Note reduced scales.

However the cycle is now 380 gauss in width and it's center is at -60 gauss. Above 3°K(T/Tg∿0.4)no jump is observed at any value of the negative field and the whole hysteresis becomes "Rayleigh like"- see Fig 18 of ref(3).At temperature lower than 3°K we note that the width ΔH of the square is such as to leave it's area $M_r \Delta H$ approximatively constant. We then define an anisotropy energy K_a by

$$K_a = \frac{1}{4} M_r \Delta H = 10 \pm 5 \text{ ergs/cm}^3$$

for our 0.5% CuMn alloy between 1.35°K and 3°K. When cooling from 1.4° K a choice is possible: 1)Cooling in

zero field, thus obtaining at lower temperature the same remanent magnetisation as has been prepared at 1.4°K The cycle obtained this way is shown in solid lines on Fig 4 where it appears that the width of the cycle is

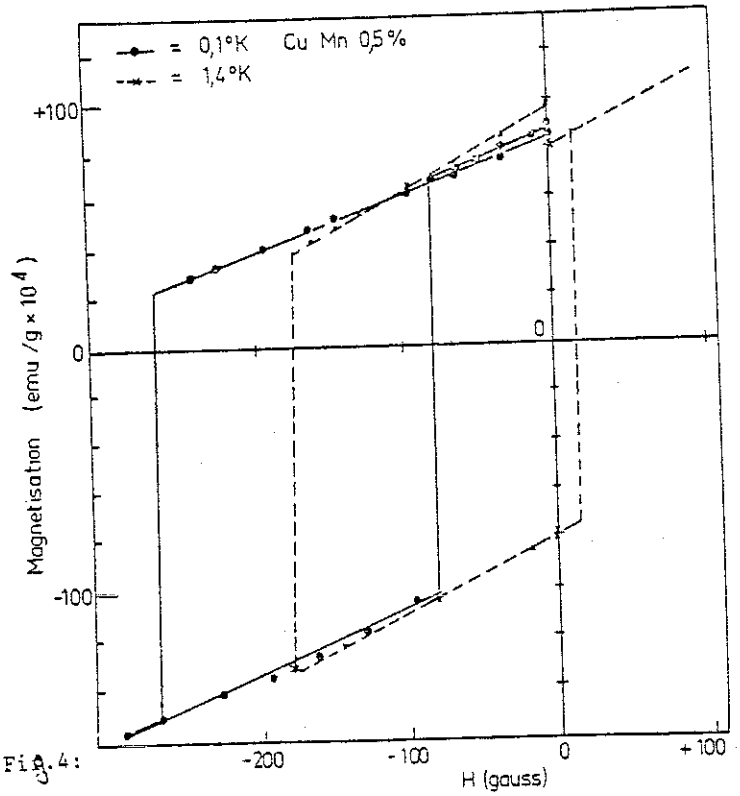

Fig. 4: Temperature effect on hysteresis at constant magnetisation(zero field cooling from 1.4°K).

unchanged and only it's center has been shifted to -170 gauss.It should be noted that the time constant involved in the jumps are short(< 0.1 sec) and that the cycle closes itself nicely as the time dependance is now very long. 2) Cooling in a field of 3.5 Kgauss down to 0.08 K:this will considerably enhance the remanent magnetisation and the cycle of Fig 3 is obtained: the width is now 20 gauss and the displacement - 40 gauss. The time constant for the jump is observed to be much slower(1 to 10 seconds) and a couple of "steps"at intermediate values of M are present. The overall cycle nevertheless scales well with the observation of Kouvel on alloys of 5% or higher at 1.8°K i.e. at temperature such that T/Tg < 30. These observations all indicate that the temperature does not play a role by itself but acts only through the limitation of the possible maximum value of the remanent magnetisation (22).

d) *Concentration.*

We have studied the hysteresis of samples of 4.7%, 2%, 1.35%, 0.3% and 0.06% at temperatures such that T/Tg < 0.2. In this case the scaling properties of the remanent magnetisation with concentration(23) indicate that the remanent magnetisation per Mn atom will be at

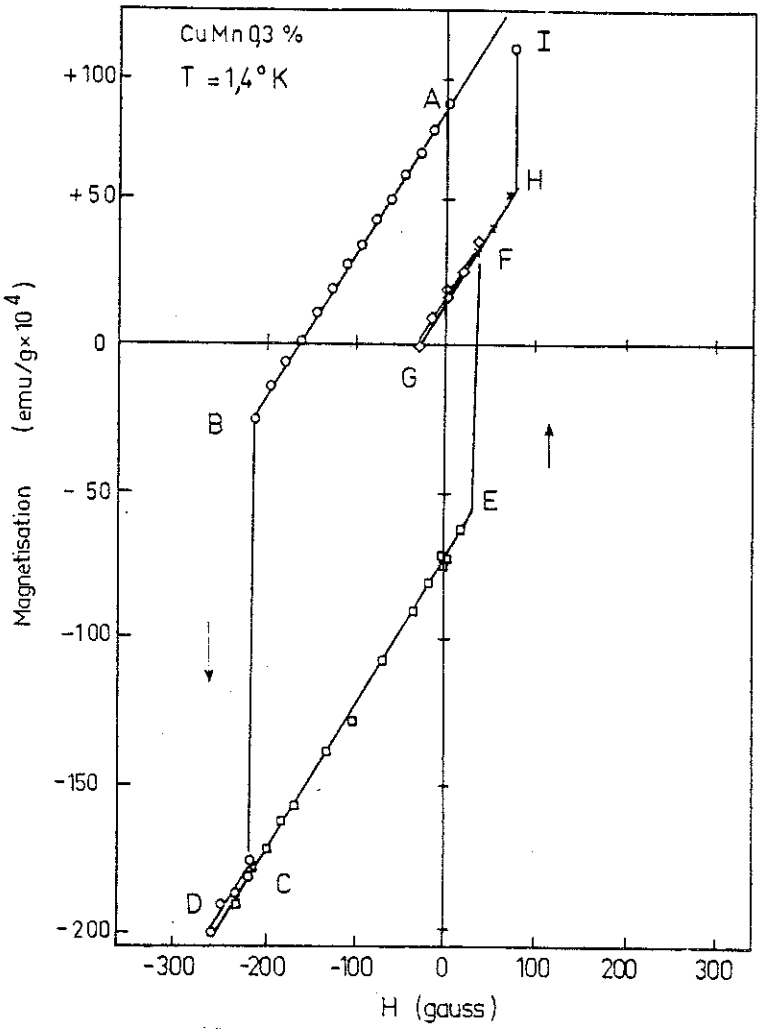

Fig.5: Hysteresis of CuMn 0.3% at 1.4°K. The letters indicate the order followed.

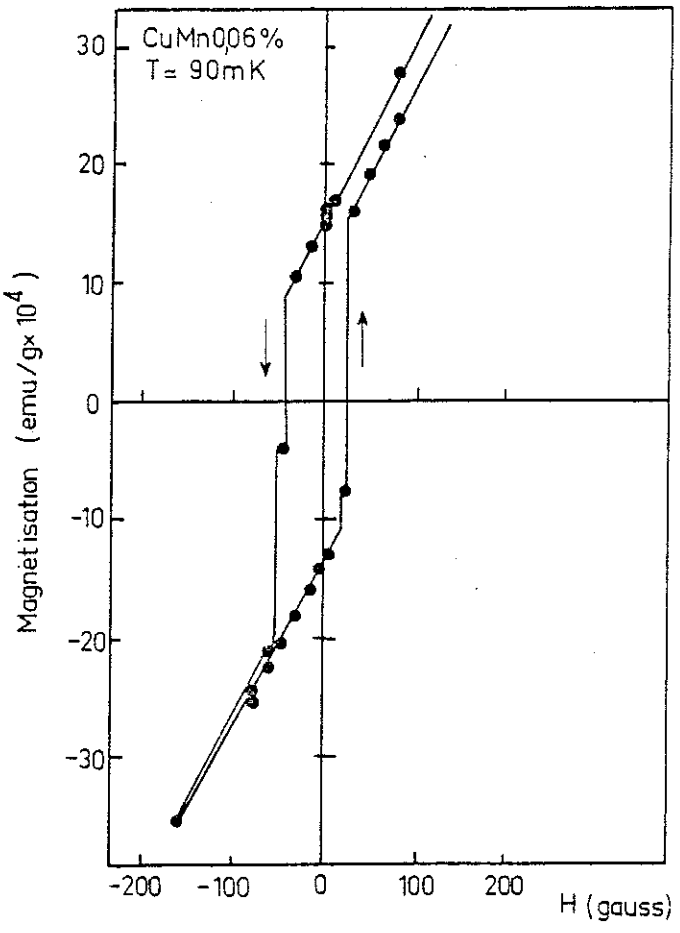

Fig.6: Hysteresis of CuMn 600 ppm at 0.09°K with saturated remanent magnetisation.

least 0.02 μ_B. As can be seen from fig (5) and (6) in these other cases a "square like" hysteresis cycle observed, even in the most dilute samples(600 ppm at., operated at 0.1°K). For the more concentrated alloys (2%,4.7%) the reversal appears less sudden i.e. less cooperative than in the more dilute alloys in the sense that the reversal occured in a small number of discrete jumps rather "sluggish" i.e. their time constant became of the order of seconds or more and began to interfere with the time constant of measurement. That this trend is actually the link between Kouvel's experiments(1,h) and ours is best exemplified by the behaviour of an 8% CuMn alloy studied in the same way. No jump could be detected at 4.2K or 1.4°K(Tg = 40°K) after cooling in 70 Kilogauss and slowly inverting the field. However a very steep slope of the magnetisation existed in a narrow range of fields of 50 gauss centered about -300 gauss where the time constant for the magnetisation change was found to be of the order of 10 minutes. It is thus quite natural to think of that part of the cycle for this alloy as the sum of a large number of small magnetic instabilities having each a rather long time constant. The total change observed corresponds again to a reversal of the initial remanent magnetisation. The natural conclusion from such a picture would be that by diluting the spins one has extended greatly the length characteristic of the magnetic cohesion of the spin glass state until the whole sample behaves like a single magnetic domain.

e) *Scaling*

It is tempting to look for scaling properties for the width and the displacement field of the cycles obtained. Fig (7) represent such an attempt for the elastic energy $K_d = 1/2\ M_r\ h_d$ where h_d is the displacement field of the narrowest cycles measured(at lowest temperature) and Mr the corresponding remanent magnetisation. As noted previously by Kouvel (1), in his limited range of high concentration, K_d varies like the square of the concentration. We see that the same law holds down to our 600 ppm sample. As M_r is proportional to c this scaling simply reflect the fact that the displacement field is linear with concentration with a coefficient of 80 $\pm$ 20 gauss/% at Mn. The width ΔH of the cycle can be simply scaled only if the area of the cycle is temperature independant, which we have tested(within a factor 2) only for the 0.5% alloy. Otherwise we should specify at which value of T/Tg the scaling is done. By noting that in the region $0.02<T/Tg<0.2$ the width of the cycle is of the same order as the displacement it can be safely inferred that the anisotropy energy $K_a = 1/4\ M_r \Delta H$ will also scale in the same way as the elastic energy K_d. However we note that for values of $T/Tg>0.2$ the width becomes larger than the displacement[See Fig(3)] and for

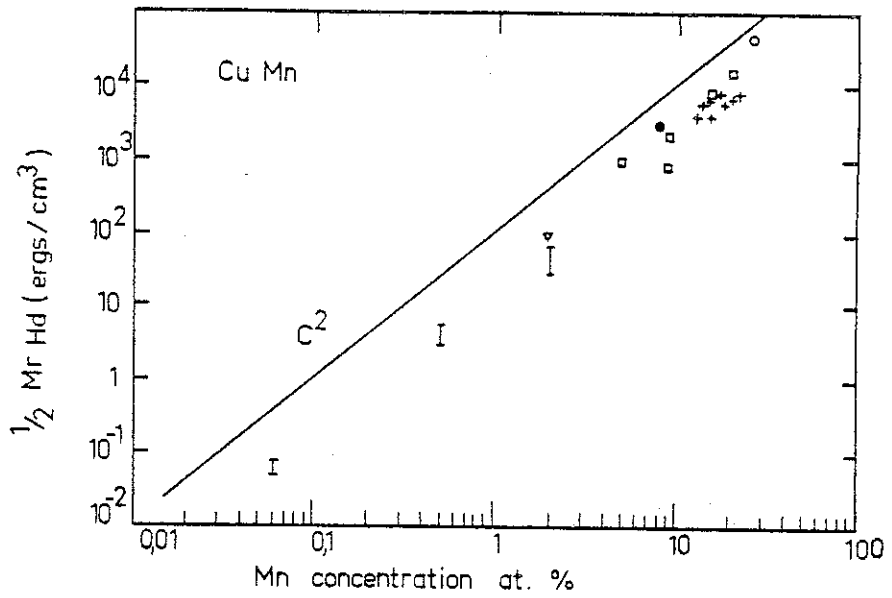

Fig.7: Elastic energy $K_d = 1/2\ M_r h_d$ versus concentration: squares: Kouvel(1) Circle: Beck(3) Triangle:Careaga (i) Crosses: Iwata(e) Bars: Present work.

T/Tg<0.02 the width is smaller than the displacement of the cycle.

f)*Metallurgy*.

In order to understand better the nature of the instability involved in the reversal of the remanent magnetisation we have briefly studied the influence of defects on the hysteresis. Two types of imperfections have been introduced i)by cold working and ii)by diluting a non magnetic impurity. The latter effect will be reported elsewhere(24). Fig(8) shows the effect on the hysteresis cycle of cold working a 0.5% alloy from a diameter of 7mm to a square 5 x 5mm. It is quite remarquable that neither the remanent magnetisation nor the reversible magnetisation slope have changed within a few%, however the single fast jump previously observed at B(dotted line) is now replaced by a serie of smaller steps with a time constant long enough that the whole inversion of magnetisation can be measured point by point for each value of the negative field. As the composition of othe alloy has not been altered it must be inferred that the inversion phenomena is linked to the propagation of the instability which could be pinned by defects. This fact is substantiated by the study of the effect of non magnetic impurities(24) which completely suppress the instability at very low concentrations(0.1% Au in 1% CuMn).

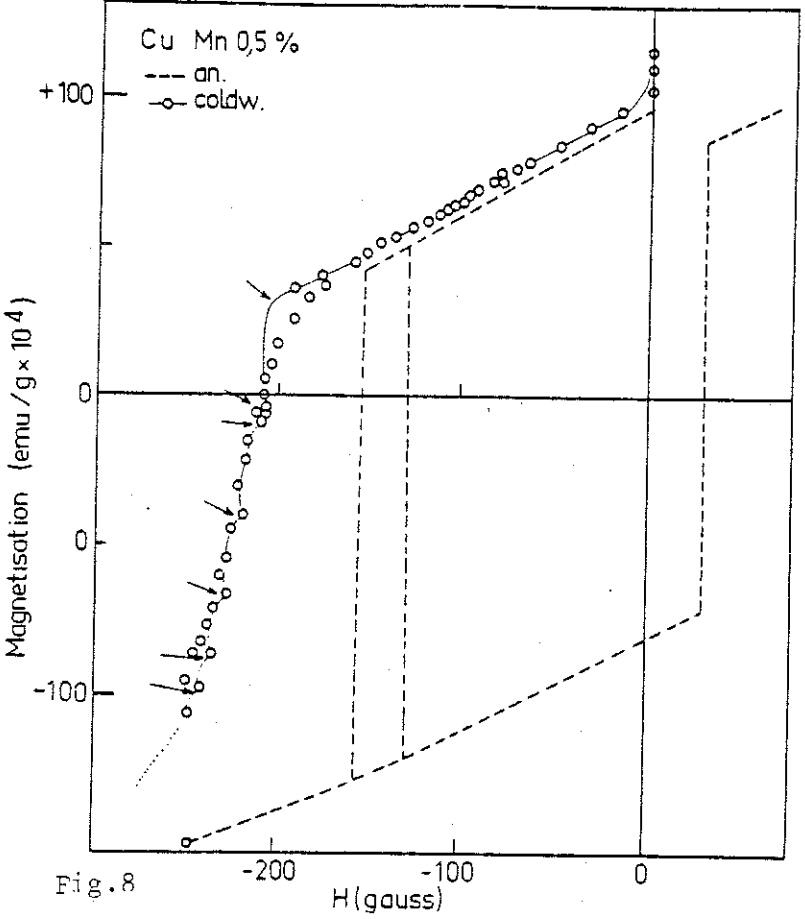

Fig.8

Effect of cold working on the hysteresis of CuMn 0.5% previously annealed(See Fig 1 symbolised by dotted lines).Each arrow present a partial, slow, jump observed with a time constant of a few seconds. The returning branch is also broadened and composed of smaller jumps.

g)*Time dependance*.

A rather puzzling question comes up in the study of the hysteresis of a spin glass, which does not arise in ordinary magnetic materials: in the latter case when the magnetisation is saturated the degeneracy of this state is one but for a spin glass characterised by it's remanent magnetisation(at most 2% of the saturation of all spins) the degeneracy of this state is very high. It is not obvious whether the state reached after a full square hysteresis cycle is the same as the original one or is a "new" state with the same magnetisation. In order to test this we have used the time dependance as a label to distinguish between the old state and the new one after a complete cycle. We have recorded the time dependance of the remanent magnetisation in zero field of the 0,5% alloy at 1.4°K for two hours, after which we could predict with a good accuracy the future time dependance of this particular state at least for the next hour. After running a complete hysteresis cycle in a short time(30 seconds) we measure the time dependance of the achieved state for one hour. The result tells us clearly that to better than 95% there has not been any "reshuffling" of the spins: Indeed the time dependance observed is the one from the "old"state contrary to the initial rapid evolution expected for a completely new state. This implies that the mechanism of reversal involved is adiabatic rather than isothermal.

IV - CONCLUSION

We believe that this ensemble of observations indicate the existence of a macroscopic coherence of the spins of CuMn at low values of T/Tg. However the very question of the relevance of this particular behaviour to the description of the spin glass state must still be considered to be open in the absence of a clear cut explanation of the different behaviour observed in other classical spin glass like AuFe(or AuMn) where no such instabilities are observed in conditions similar to CuMn studied here. With this restriction present one can nevertheless state a few questions raised by our observation: what is the physical origin of the anisotropy field inferred and what is the mechanism of field displacement of the cycles? Is there a threshold in magnetisation for the instability? What is the domain structure corresponding to a partial reversal of magnetisation?

Acknowledgements are gratfully extended to J.L. Tholence and R.Tournier for numerous discussions.

REFERENCES

1. J.S.Kouvel, J.Phys.Chem.Sol.21,57,(1961).

2. I.S.Jacobs and C.P.Bean in Magnetism Vol III,Chap.6 Rado and Suhl Ed.Acad.Press New York 1963.

3. P.A.Beck, Prog.Mat.Sciences 23, 1, (1978).

4. See Table 1.

5. R.Tournier, thèse Université de Grenoble (1965) Y.Ishikawa, R.Tournier and J.Filippi, J.Phys.Chem. Sol.26,1727(1965).

6. P.Monod and J.J.Préjean, J.Phys. 39 C 6,910 (1978).

7. J.L.Tholence and R.Tournier, J.Phys.35C4,229,(1974).

8. V.Cannella and J.A.Mydosh, Phys.Rev.B6,4220,(1972).

9. See Ref(7).

10. L.Néel, Ann.Géophys.5,99,(1949).

11. E.C.Stoner and E.P.Wohlfarth, Phil.Trans.Roy.Soc. London A240, 599,(1948).

12. Copper: American Smelting and Refining C° 5"9" grade Manganèse: Johnson & Matthey high purity grade.

13. J.L.Tholence, Thèse, Université de Grenoble (1973) unpublished.

14. V.Cannella and J.A.Mydosh AIP Conf.Proc.18,651,(1973).

15. J.J.Préjean, J.Phys.39C6, 907,(1978) and Ref(10).

16. In the work of Kouvel(1) the assymetry of the cycles measured, despite a symetric excursion of magnetic field, is due to the fact that the maximum field used(10 Kilogauss) is sufficient to create a large remanent magnetisation by the TRM process but quite insufficient to decrease it by IRM process in negative fields at low temperature(1.8°K) for the high concentration of Mn used. Only the larger fields used in (h) table I are able to symmetrize the whole cycle. For more dilute alloys this limitation is set to smaller negative fields typically ∿ -500 gauss for our 0.5% alloy at 1.4°K.

17. A.Arrott in Magnetism Vol II B chap.4 p.395-396 Rado and Suhl Ed.Acad.Press New York(1963).

18. We were also able to measure the magnetisation change along the transverse axis(with an X axis coil). Our conclusion is that the magnetisation reversal is not exactly 180° but remains slightly tilted towards the transverse field. This is the fact which misled Arrott's interpretation. Very much care was necessary to avoid building up a transverse magnetisation at each cycle. The most efficient procedure found to erase this transverse component was to bring back the longitudinal field to 3.2 Kgauss(with zero transverse field) prior to each cycle. When taking this into account no evidence remains for the "rotation at unison" inferred by Arrott from his findings.

19. L.Landau and E.Lifchitz, Electrodynamics of continuous media Ch V, Moscou 1969.

20. A special test of this reverse jump has been done by first inverting the magnetisation without transverse field then applying a transverse field only on the way back: the same misfit occurred.

21. The Torque analysis of ref e of Table I provides a much better definition of the anisotropy field for a higher concentration alloy.

22. A test done on the 1.35% at Mn alloy sample dramatically stresses this fact: As the same TRM cooling procedure with 3.2 Kgauss was used as for the 0.5% alloy down to 1.4°K an incomplete TRM state was created: For this state no jump and no reversal of the remanent magnetisation is observed whatever the negative field applied down to -3.2 Kgauss. On the contrary cooling the same alloy in a field of 13 Kgauss yields the maximum possible value of the TRM(∿twice larger as our first test) and a well defined square

loop is obtained with jumps at -200 gauss and 0 gauss respectively. From this, a threshold of∿ 0.02 Bohr magneton/Mn appears necessary to have an unstable situation for the magnetisation.

23. J.Souletie and R.Tournier, J.Low Temp.Phys.1,93, (1969).
J.L.Tholence and R.Tournier, Physica 86-88B 875(1977).

24. J.J.Préjean, M.J.Joliclerc and P.Monod, to be published.

C H A P I T R E V I

Nous avons clairement démontré dans le précédent chapitre la possibilité pour l'aimantation rémanente du système CuMn de répondre collectivement et instantanément à des excitations de champ magnétique inverse et transverse. Cette propriétés a été confirmée lorsqu'il s'agit de champ transverse haute fréquence dans les expériences de RMN et de RPE en présence d'aimantation rémanente.

Nous avons émis l'hypothèse que l'interaction RKKY entre impuretés gouvernait les propriétés verres de spins dans ce système : Cette interaction en effet répond au critère de symétrie par rotation.

Il est évident dans ce cas que tout couplage d'ordre magnétique entre les électrons de conduction et la matrice va induire indirectement un couple exercé par le réseau sur l'aimantation rémanente.

C'est ce test que nous allons effectuer en introduisant en faibles quantités, dans le système CuMn, des impuretés non magnétiques connues pour leur fort couplage spin-orbite.

Dans la publication suivante ("Hysteresis in CuMn : the effect of spin-orbit scattering on the anisotropy in the spin glass state), nous mesurons, dans les mêmes conditions d'histoire magnétique et thermique, la largeur du cycle d'hystérésis d'alliages ternaires $CuMn_{1\%}\ I_x$ où l'impureté I est de l'argent, de l'aluminium, de l'or ou du platine. Nous démontrons que cette largeur croît linéairement avec la concentration de ces impuretés à un taux proportionnel à la section efficace du mécanisme de diffusion spin-flip dû au couplage spin-orbite de ces impuretés.

Cet effet est suffisamment important pour que 1 %at d'or ou de platine introduit dans le système CuMn modifie le cycle d'hystérésis pour le rendre équivalent à celui d'AuFe.

Cet effet par ailleurs semble découplé du problème général de la construction et de la relaxation des aimantations qui ne sont pas modifiées en présence de ces impuretés.

J. Physique **41** (1980) 427-435 MAI **1980**, PAGE 427

Classification
Physics Abstracts
75.30 — 75.60

Hysteresis in CuMn : The effect of spin orbit scattering on the anisotropy in the spin glass state

J. J. Prejean, M. J. Joliclerc

C.R.T.B.T., C.N.R.S., BP 166, 38042 Grenoble Cedex, France

and P. Monod

Université Paris-Sud, Physique des Solides, 91400 Orsay, France

(*Reçu le 7 décembre 1979, accepté le 25 janvier 1980*)

Résumé. — L'étude des cycles d'hystérésis à 1,45 K de systèmes ternaires Cu-$Mn_{1\%}$-Au_x dans l'état verre de spins montre que la largeur du cycle est proportionnelle à la concentration d'or avec un taux d'accroissement de 6,2 ± 0,4 kOe/at. % Au. Le fait que ce taux d'accroissement soit beaucoup plus faible pour les systèmes Cu-$Mn_{1\%}$-Ag_x et Cu-$Mn_{1\%}$-Al_x et plus grand pour le système Cu-$Mn_{1\%}$-Pt_x montre sans ambiguïté que le couplage spin orbite est responsable de l'anisotropie macroscopique dans l'état verre de spin. La comparaison est faite avec des alliages similaires étudiés en RPE par Okuda et Date et quelques conséquences sont discutées.

Abstract. — Measurements of the hysteresis cycle of the magnetization of CuMn 1 % in the spin glass state as a function of the concentration of a non magnetic impurity show that the width of the hysteresis is proportional to the concentration of Au at a rate of 6.2 ± 0.4 kOe/at. % Au. A much smaller rate observed for Al and Ag and higher rate observed for Pt demonstrate unambiguously that the spin orbit interaction is responsible for the anisotropy field in the spin glass state. A comparison is made with similar alloys studied by spin resonance by Okuda and Date and some implication are discussed.

1. **Introduction.** — The properties of the magnetization along a complete hysteresis loop in a spin glass have been investigated rather thoroughly for CuMn and AgMn by Kouvel [1] for a range of concentrations above 5 % Mn. Only recently the more dilute alloys of CuMn have been studied by Monod, Prejean and Tissier [2] down to 0.06 % Mn. In this work [2] additional references to previously published hysteresis cycles for CuMn and AgMn are available. Very few other systems have been reported so far, except in a very sketchy manner, from which only qualitative conclusions can be drawn. These concern AuFe [3], CrFe [4], PdMn [5], Mn aluminosilicates [6] and AuCo [3]. One of the major conclusions of refs. [1] and [2] was, however, that despite the very close, almost quantitative, similarity of the magnetization properties of CuMn (and AgMn) on one hand and AuFe on the other hand, there was a striking difference in behaviour between these two systems when a hysteresis loop was measured. In order to emphasize this, a comparison is made in figure 1 of hysteresis cycles for CuMn 8 % and AuFe 8 % ref. [3] measured in similar conditions at 4.2 K. As is evident the system AuFe has a very smooth symmetrical and featureless hysteresis loop. This fact is best interpreted [3] in terms of a distribution of magnetically hard microdomains, stabilized in their own anisotropy field : in this model the width of a few kilogauss of the cycle is a measure of the width of the distribution of the anisotropy field. By contrast the CuMn 8 % alloy shows a complete reversal of the remanent magnetization at low field (typically at — 300 G for this particular alloy at 4.2 K) as if all the spins would collectively reverse their direction. (This difference was already noted in 1959 by Schmidt and Jacobs.) This fact permits the definition of a macroscopic anisotropy field equal to the halfwidth of the cycle. The further discovery of the extreme sensitivity of the hysteresis of CuMn to the presence of mechanical defects (revealed by the difference in hysteresis cycle between samples quenched from the melt, well annealed or deformed mechanically [2]) led us to infer that the collective reversal of magnetization could be observed only if the spins although locked together within the spin glass phase, were *free* to orient themselves as a whole with respect to the lattice. It was noted

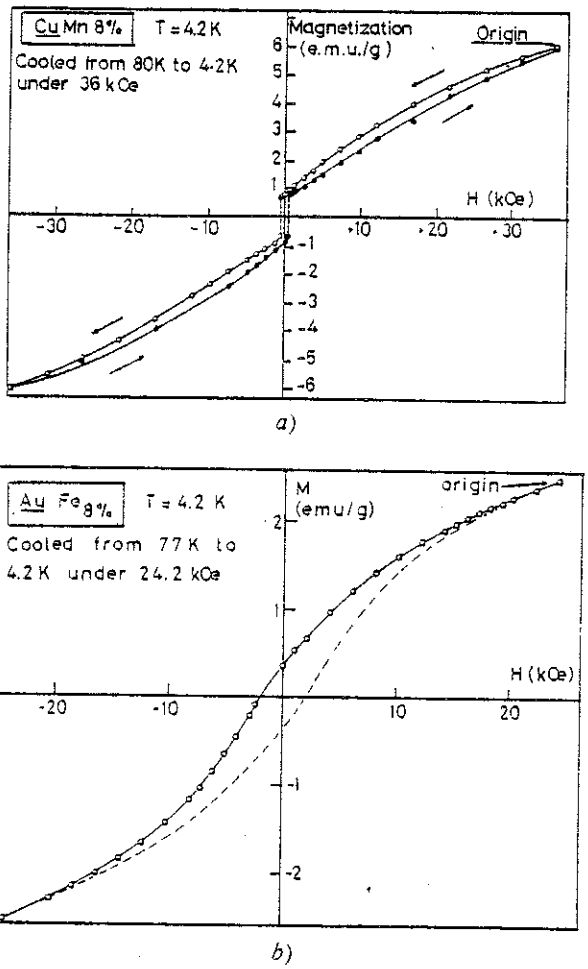

a)

b)

Fig. 1. — Large field hysteresis cycles of $\underline{CuMn}_{8\%}$ (Fig. 1*a*) and $\underline{AuFe}_{8\%}$ [3] (Fig. 1*b*) at 4.2 K. The starting point of the cycle, indicated *origin*, is obtained after cooling the sample from $T > T_g$ (39 K for $\underline{CuMn}_{8\%}$, 29 K for $\underline{AuFe}_{8\%}$) down to 4.2 K in 36 kOe for $\underline{CuMn}_{8\%}$, in 24.2 kOe for $\underline{AuFe}_{8\%}$.

in the same spirit, that only those systems that yield readily observable electron spin resonance in the spin glass state (i.e. CuMn, AgMn and PdMn) had such a very steep magnetization reversal at low negative fields in their hysteresis cycles. This correlation provides a quantitative definition of what is meant by *free* in terms of the width of the electron spin resonance signal. A straight-forward test of this conjecture then consists in measuring the effect on the hysteresis of an impurity already known for its strong spin flip scattering effect. As a first choice we have selected Au as it is supposed to introduce the least electronic disturbance when replacing a Cu atom. The following is an account of our observations and comparison with similar tests made with other impurities with little spin orbit coupling (Al or Ag) or a larger one (Pt).

2. **Experimental results.** — 2.1 SAMPLE PREPARATION AND EXPERIMENTAL TECHNIQUE. — The samples were prepared by melting the constituents with a semilevitation induction furnace and by quenching the melt in a rotating cylindrical copper mold [8].

The copper and non magnetic impurities are first melted under 10^{-6} torr, a second melting under argon is necessary to include the manganese and a third one to insure homogeneity and permit quenching of the melt. The alloys $CuMn_{1\%}Au_x$ were studied first in the *as quenched* condition and subsequently after annealing at 900 °C in Ar + H_2 atmosphere for one hour followed by a slow cooling. The alloys $CuMn_{1\%}Al_x$, $CuMn_{1\%}Ag_x$, $CuMn_{1\%}Pt_x$ were studied only in the quenched condition. For the magnetic measurements the same procedure is used for all samples as follows : the alloy is first cooled under a field of 18 kOe from well above the spin glass temperature (approximately 10 K for $CuMn_{1\%}$) down to 1.45 K. At this temperature the field is removed and the sample is left with a so called (saturated) remanent magnetization [7] σ_r in zero field. To avoid any stray field from the superconducting coil used to create the remanent magnetization, the sample is further lowered into the measuring section of the apparatus where a magnetic field of $\pm$ 3 500 Oe parallel to the cooling field can be achieved by a nitrogen cooled copper coil. As explained in ref. [2] the magnetization is measured by the extraction method : the sample is mechanically moved between the centres of two counterwounded pick-up coils whose flux variation is integrated by a ballistic galvanometer associated with a recorder. The sensitivity of the system is of the order of 10^{-5} emu, and because of the finite time constant of the galvanometer circuit (about 20 s) it can be left integrating at all times. Thus this system will be able to record not only actual flux changes due to the mechanical extraction of the sample but also flux variations due to spontaneous magnetization changes within the sample (without extraction) provided that the time constant of these changes would be somewhat shorter than 20 s.

2.2 $\underline{CuMn}$ RESULTS. — The specific hysteresis properties of $\underline{CuMn}$ (at low concentration) have been described in ref. [2]. We will only recall here how these have been analysed. Figure 2 represents the hysteresis cycles of a $CuMn_{1\%}$ well annealed (solid squares) and as quenched (solid circles) at 1.45 K. Both have common features : the measured magnetization is composed of two parts : the remanent magnetization σ_r and the induced or reversible magnetization which is linear with field. Thus :

$$M = \sigma_r + \chi(T)\, H \qquad (1)$$

where $\chi(T)$ is by definition the reversible susceptibility. It is apparent that this relation is followed for negative values of H until a value H_r (of about $-$ 170 Oe) where a sudden reversal of σ_r in one step (or a limited number of steps) occurs. For small variations of field beyond H_r or coming back towards zero field from this point, the variation of M is represented by :

$$M = -\sigma_r + \chi(T)\, H\,. \qquad (2)$$

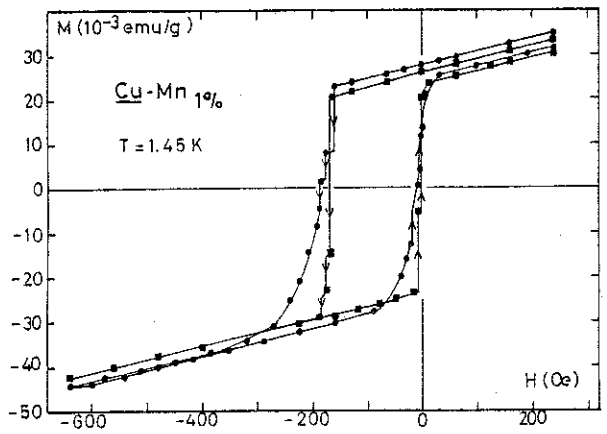

Fig. 2. — Hysteresis cycles in low negative fields at 1.45 K for $\underline{Cu}Mn_{1\%}$ as quenched (solid circles) and after annealing (solid squares). The remanent magnetization is obtained after removing a field of 18 kOe in which the sample was cooled from $T > T_g \sim 10$ K down to 1.45 K.

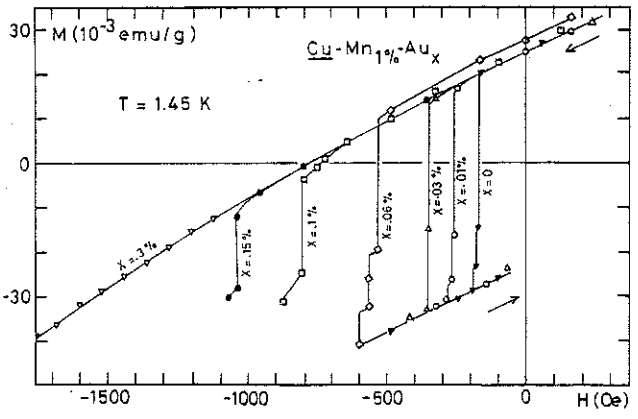

Fig. 3. — Hysteresis cycles in low field of annealed $\underline{Cu}Mn_{1\%}Au_x$. The remanent magnetization is prepared in the same way as described in figure 2 for $\underline{Cu}Mn_{1\%}$. As explained in the text, the time constants associated with the reversal increase with Au concentration from ~ 1 s for the more dilute to over hours for the most concentrated.

However on the way back this is followed only until another threshold field (about 0 Oe in our case) is reached. At this point the remanent magnetization is seen to switch back to a value close to its initial value. This remarkably simple behaviour can be parametrized by the width ΔH of the hysteresis cycle and the position of the centre of the cycle for either the quenched or annealed $CuMn_{1\%}$ in figure 2.

It appears that the only effect of quenching is a broadening of the tail of the cycle. It should be noted however that the initial sharp drop of magnetization occurs at the same field H_r and that neither the reversible susceptibility nor the value of the remanent magnetization have changed in any significant manner in both states of the alloy [9].

2.3 $CuMn_{1\%}Au_x$ SYSTEM. — We have studied the hysteresis of $CuMn_{1\%}Au_x$ with concentrations of $x = 3\ \%$, $1\ \%$, $0.3\ \%$, $0.1\ \%$, $0.03\ \%$ and $0.01\ \%$. When comparing the results of the lowest Au concentration alloys in the as quenched condition and the annealed condition the same qualitative difference appeared in the hysteresis loops when measured as for the $CuMn_{1\%}$ discussed above. That is why we will only present the results of the annealed alloys.

Figure 3 represents the ensemble of magnetization curves measured at 1.45 K along the first branch of the hysteresis cycle for these alloys. As will be made clear, the effect of Au impurities on $CuMn_{1\%}$ is very specific depending upon which property is investigated : this effect is very apparent on what we loosely term *dynamical* magnetic properties, and to the contrary it is not measurable from the static or quasi-static magnetic properties. In order to describe these effects in a systematic way, we first present the properties that are apparently unmodified by the presence of Au and then those that do depend on the presence of Au impurities.

a) *Unmodified quantities.* — The examination of figure 3 and table I reveals that within $\pm$ 10 % (which is the accuracy attributed to the experimental procedure [10]) neither the remanent magnetization σ_r, nor the reversible susceptibility χ are affected by the presence of gold in the concentration range 0.01 %-3 % at 1.45 K. In order to check more precisely this fact, on $CuMn_{1\%}$ and $CuMn_{1\%}Au_{1\%}$, we have compared with much more care the temperature and time dependence of the saturated thermoremanent magnetization $\sigma_r(T, \log t)$ on one hand, and the hysteresis cycle in large fields on the other hand. As shown on figure 4 at $T = 1.48$ K and $T = 4.2$ K we do not

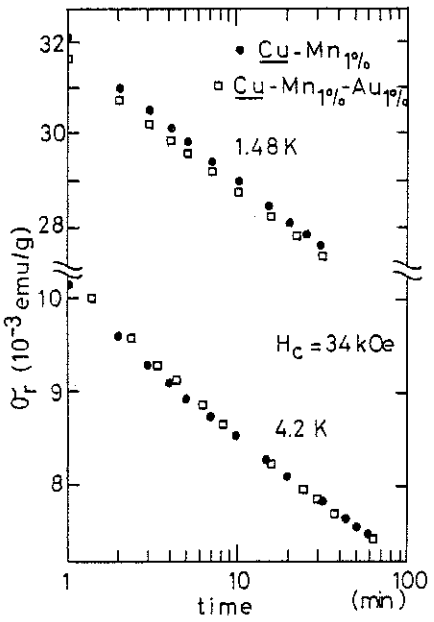

Fig. 4. — Time dependence of the satured thermoremanent magnetization at 4.2 K and 1.48 K of $\underline{Cu}Mn_{1\%}$ (solid circles) and $\underline{Cu}Mn_{1\%}Au_{1\%}$ (open squares). The sample is cooled from $T > T_g \sim 10$ K down to T (1.48 K or 4.2 K) under a field of 34 kOe. The saturated thermoremanent magnetization is obtained by removing the field. The origin of time is taken when the field reaches zero.

Table I.

	$CuMn_{1\%}$	$CuMn_{1\%}Au_x$							$CuMn_{1\%}Al_x$			$CuMn_{1\%}Pt_x$			$CuMn_{1\%}Ag$
x	0	0.01	0.03	0.06	0.1	0.15	0.3	1 3 %	1 %	2 %	3 %	50 ppm	100 ppm	300 ppm	0.5 %
σ_r (emu/g) (a)	26.0	25.0	25.1	28.2	26.5	26.4	27.0	31.6 26.7	30.5	28	28.5	26	24.4	30.6	28.9
χ (10^{-5} emu/g) (b)	2.85	2.84	2.79	2.89	2.95	2.99	2.77	2.74	2.80	3.00	2.94	2.90	2.90	2.72	2.89
H_r (Oe) (c)	− 170	− 256	− 352	− 529	− 802	− 1 043	—	— —	− 281	− 400	− 512	− 411	− 470	− 382 ± 80	− 200
H_r (back) (Oe) (d)	− 8 ± 30	± 16	0 ± 30	− 80 ± 80	—	—	—	— —	− 32 ± 32	− 28 ± 44	− 30 ± 30	− 20 ± 40	− 16 ± 70	—	− 30 ± 30
$K = \frac{1}{2}\sigma_r H_r$ (erg/mole Cu) (e)	70	101	140	237	338	436	—	— —	136	178	232	170	182	430 ± 50	92

(a) Remanent magnetization at $T = 1.45 \pm 0.15$ after cooling in 18 kG.
(b) Reversible susceptibility dM/dH around zero field.
(c) Reversal field for the first step in the magnetization hysteresis (see text) and figures 3, 6*a*, 6*b*.
(d) Back reversal field observed on the negative branch of the hysteresis cycle of the remanent magnetization. The ± sign enclose the range of field over which the major part of the magnetization switch back to the positive (original) branch of the hysteresis cycle. This part of the cycle is present in figure 2 but has been systematically dropped (for sake of clarity) in figures 3, 6*a*, 6*b*.
(e) Anisotropy energy in erg/mole. In order to express this in erg/cm³ : × the figure by 0.14.

detect to within ± 0.5 % any sizeable difference either on the value of σ_r (taken at 1 min. after removing the field), or on the further time dependence of σ_r during the first hour at these two temperatures.

We have also checked that the first magnetization curve $M(H)$ (after cooling in zero field) at 1.45 K is identical for $CuMn_{1\%}$ and $CuMn_{1\%}Au_{1\%}$ to within ± 1 %. In the same way the magnetization $M(H)$ measured in decreasing fields from 20 kOe down to zero is identical for both alloys also within ± 1 %.

b) *Effects of* Au *impurities.* — The main point is the following : the effect of Au impurities in $CuMn_{1\%}$ is a very large increase of the reversal field H_r with Au concentration at a rate of

$$6\,200 \pm 400 \text{ G/\% at. Au}$$

as is shown in figure 5 where the field H_r defined by the initial drop of magnetization in figure 3 is plotted *versus* Au concentration.

Furthermore, the effect of increasing the concentration of Au is observed to considerably lengthen the time constant of the magnetization reversal. This property gives rise to some experimental difficulties. As we pointed out previously [2], the order of magnitude of the time constant of the magnetization jumps is 1 s or less for the $CuMn_c$ system ($c < 2$ %).

For the lowest concentrations of gold ($x < 0.06$ %), we are able to detect the occurrence of the jump, because it is sufficiently rapid to induce a sizeable flux variation in our detection coil. For these samples, as soon as such a flux variation is detected, we keep the magnetic field H_r constant and we measure the magnetization of the sample with time. We observe that $M(H_r)$ after this initial rapid drop continues to decrease with time much faster than the well-known logarithmic time variation of the isothermal and thermoremanent magnetizations.

For higher gold concentration ($x \geqslant 0.1$ %), we could not observe any rapid magnetization drop. In order to still be able to detect such a slow reversal of magnetization, we tested the logarithmic time decay of magnetization for different negative fields. For a given negative field, we notice that the magnetization decreases much faster than the time variation expected. We take this as a criterion for the beginning of a slow reversal of magnetization. For example, we observed that the remanent part of the magnetization of $CuMn_{1\%}Au_{0.15\%}$ is half inverted in 200 min. During the same time, the logarithmic time variation of the isothermal and thermoremanent magnetization is of the order of a couple percent.

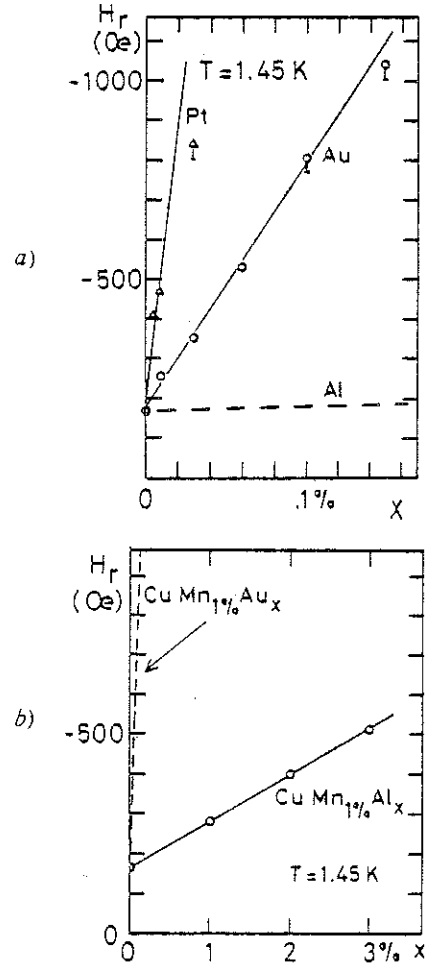

Fig. 5. — H_r *versus* x for Pt, Au, Al, at 1.45 K. H_r is the negative field where we observe an initial drop of magnetization (Figs. 3, 6*a*, 6*b*). On figure 5*a* we represent the effect of Al by a dashed line extrapolated from result of 1, 2 and 3 % Al. See the corresponding cycles in figure 6*a*.

For the highest gold concentrations (0.3 %, 1 %, 3 %), the time constants of a possible reversal of magnetization become of the order of the time constants involved in the ordinary time dependence of the isothermal and remanent magnetization. So it becomes experimentally impossible to determine any reversal of magnetization. In this case it is possible to measure a so called classical remanent magnetization hysteresis cycle [7] as in AuFe [3]. We did not find at 1.45 K any notable difference between the remanence cycles of $CuMn_{1\%}Au_{1\%}$ and $CuMn_{1\%}Au_{3\%}$.

When a magnetization reversal is observed, it is possible to study the dynamics of this reversal with time. It is seen to obey a complex behaviour initially with a time dependence characterized by a logarithmic law (during a time (200 s to 1 000 s) the longer the lower the Au concentration) and then in a second regime following the rapid change the evolution more closely follows an exponential behaviour with a large time constant. So, a long time after the beginning of the reversal of magnetization, it is difficult to distinguish this dynamical feature from the ordinary time variations of the isothermal and remanent magnetization.

The third point we want to emphasize is that, for the alloys where we could detect a reversal of magnetization, when coming back along the second (lower) branch of the hysteresis cycle (not represented on figure 3) there is a tendency to switch back in the same region of field near zero field (see table I H_r (back)). This field depends on the amplitude of the previous excursion made in negative fields (we have not studied this in detail however). We conclude that both the width ΔH and the *displacement* field H_d of the cycle have the same linear Au concentration dependence as H_r.

In good agreement with our earlier findings, we found for $CuMn_{1\%}Au_{0.01\%}$ at 1.45 K and 2.17 K that the product $\sigma_r(T)\, H_r(T)$ is temperature independent and that the switch back of the magnetization occurs for both temperatures at $H \sim 0$. That reflects that for our alloy $\sigma_r\, \Delta H$ is a constant and that the width of the cycle increases as the remanent magnetization decreases.

2.4 $CuMn_{1\%}I_x$ SYSTEMS (I = Ag, Al, Pt). — We have studied the hysteresis of $CuMn_{1\%}Ag_{0.5\%}$, $CuMn_{1\%}Al_x$ (x = 1 %, 2 %, 3 %), $CuMn_{1\%}Pt_x$ ($x = 47 \pm 3$ ppm, 100 ± 3 ppm, 300 ppm). Figures 6*a* and 6*b* represent the hysteresis results obtained at 1.45 K, for these as quenched samples.

We find that the properties just described above for $CuMn_{1\%}Au_x$ are also qualitatively found for these systems. In particular the distinction between unmodified properties and alloy dependent properties still holds. As evident from figures 6*a* and 6*b*, the value of the reversible magnetization slope and of the remanent magnetization is independent of Ag, Al or Pt in the range of concentration used. However

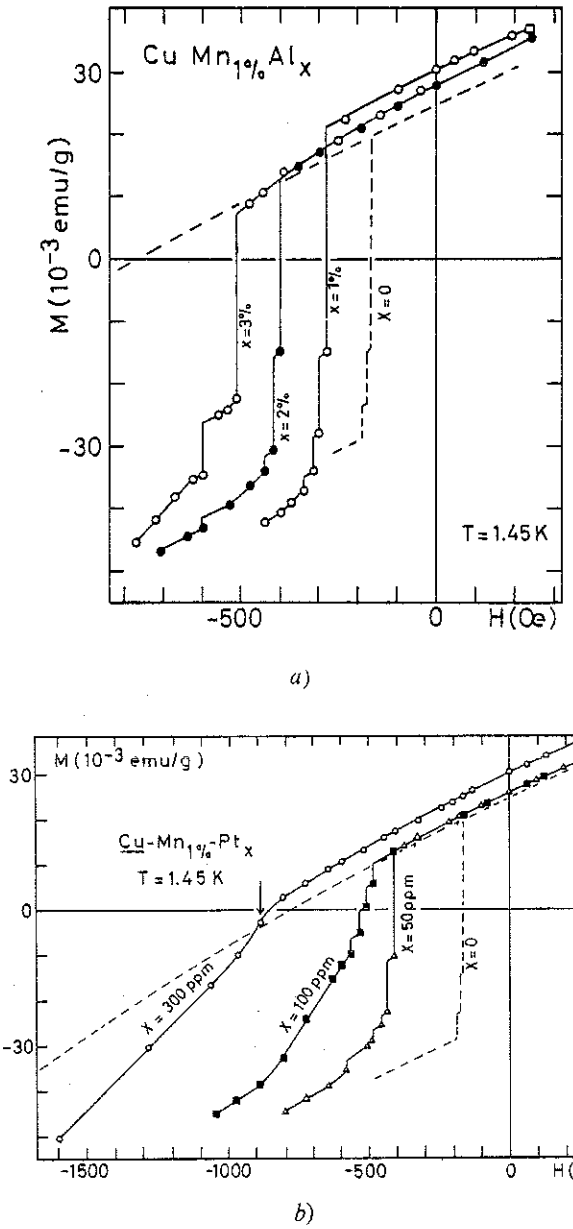

Fig. 6. — Hysteresis cycles in low field for as quenched $CuMn_{1\%}Al_x$ (Fig. 6*a*) and $CuMn_{1\%}Pt_x$ (Fig. 6*b*). The remanent magnetization is prepared in the same way as described in figure 2. The time constant associated with the reversal increases with the non magnetic impurity concentration as for figure 3. The dotted lines correspond to x = 0 % and 0.3 % Au for sake of comparison.

the increase of the reversal field H_r is observed to be very specific to the impurity present. In particular the effect on H_r of Ag impurities is, if it exists, very small and we only can infer a maximum value for the rate of increase of the reversal field by Ag (Table I).

The enhancement of H_r with increasing Al and Pt concentrations is represented on figures 5*a* and 5*b*. In figure 5*a* for comparison we indicate the extrapolated (dashed line) linear dependence of H_r on x for $CuMn_{1\%}Al_x$. In figure 5*b* the extrapolation from the $CuMn_{1\%}Au_x$ data is shown. The difference in the slope $\Delta H_r/\Delta x$ is more than 2 orders of magnitude

when comparing the effects of Al and Pt impurities. We shall discuss below the significance of such a difference.

2.5 OTHER SYSTEMS. — As we noticed, addition of Ag impurities in $\underline{Cu}Mn_{1\%}$ did not bring a sizeable effect on the value of the reversal field. The hysteresis cycle of a single cristal of $\underline{Ag}Mn_{1\%}$ (Fig. 7) at 1.6 K exhibits a behaviour similar to that of $\underline{Cu}Mn_{1\%}$. We can compare the remanent magnetization σ_r and the reversible susceptibility χ from the available data for $\underline{Cu}Mn_{1\%}$ at 1.45 K and $\underline{Ag}Mn_{1\%}$ at 1.6 K ; but we know [11] that σ_r and χ are functions of the reduced temperatures T/T_g (where T_g is the temperature of the maximum of the susceptibility), and as the values of T_g differ for these samples ($\sim$ 5 K for $\underline{Ag}Mn_{1\%}$, $\sim$ 10 K for $\underline{Cu}Mn_{1\%}$) the reduced temperatures T/T_g also differ ($\sim$ 0.14 for $CuMn_{1\%}$, $\sim$ 0.32 for $\underline{Ag}Mn_{1\%}$). We noticed before that H_r was temperature dependent but that the product $\sigma_r H_r$ was nearly independent on the temperature. So, rather than comparing the reversal fields for $\underline{Cu}Mn_{1\%}$ and $\underline{Ag}Mn_{1\%}$, it is more relevant to compare the product $\sigma_r H_r$ per mole :

$$\sigma_r H_r (\underline{Ag}Mn_{1\%}) = 590 \pm 50 \text{ erg/mole Ag}$$

$$\sigma_r H_r (\underline{Cu}Mn_{1\%}) = 280 \pm 30 \text{ erg/mole Cu} .$$

In a preliminary experiment, we measured a $\underline{Ag}Mn_{1\%}$ sample obtained by melting the constituents for a few hours in an alumina crucible in an electric furnace. We could not detect any reversal of magnetization. The $\underline{Cu}Mn$ alloys prepared in the same manner and studied by Tournier [8] also did not exhibit any reversal of magnetization. We know [3] that such a metallurgical preparation introduces in the samples some impurities, iron in particular. We believe that the presence of some ppm of these iron impurities are responsible of the disappearance of any detectable reversal of magnetization.

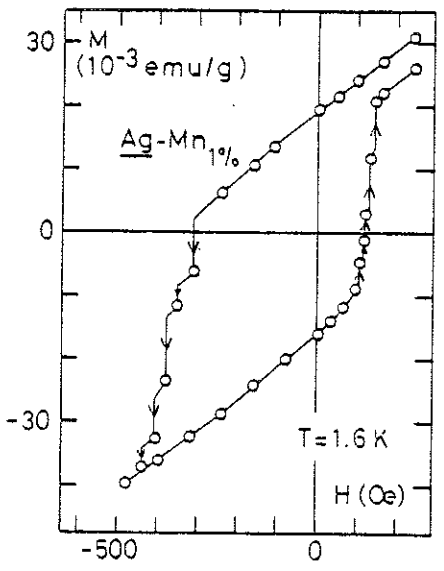

Fig. 7. — Hysteresis cycle in low fields of $\underline{Ag}Mn_{1\%}$ single crystal at 1.6 K. The remanent magnetization is prepared in the same way as described in figure 2. The time constant involved in the magnetization reversal is of the order of seconds.

3. **Discussion.** — In order to discuss our results in terms of an anisotropy field and anisotropy energy of the $\underline{Cu}Mn$ spin glass phase, we first briefly recall how these quantities are introduced at an elementary level in the discussion of the magnetostatic properties of a single, isolated magnetic particle. This is presented in far greater detail in the classical work of Stoner and Wolhfarth [12], Néel [13] and subsequently M. F. Brown [14] who used this analysis to interpret the hysteresis properties of hard magnetic materials. For a homogeneously magnetized spherical particle of moment M, possessing an uniaxial anisotropy energy K (of unspecified origin) in the presence of an external field H applied parallel to the anisotropy axis, the magnetic energy E is only a function of the magnetization angle θ with respect to the field (and anisotropy) axis :

$$E = K \sin^2 \theta - MH \cos \theta .$$

The stability condition $dE/d\theta = 0$ gives the equilibrium positions $\theta_{eq} = 0, \pi$. The metastability condition :

$$\left.\frac{d^2E}{d\theta^2}\right|_{\theta=\theta_{eq}} \geqslant 0$$

gives the range of field over which both equilibrium points are locally stable. Defining the anisotropy field H_A by $K = 1/2\, MH_A$ leads to :

$$- H_A < H < + H_A .$$

In this picture the hysteresis cycle is thus a *square* of height $2M$ and of width $\Delta H = 2 H_A$, centred at $H = 0$. We have shown in ref. [2] how this model can be applied for $\underline{Cu}Mn$ in the spin glass phase for describing the effect of a number of variables such as the magnetization amplitude, the field direction (in presence of a transverse field), the Mn concentration, the temperature and the sample preparation. The major conclusion was that whereas a hard ferromagnetic material can be considered as the juxtaposition of a wide distribution of such magnetic particles at a microscopic level (with generally poorly specified interactions) it appeared that the spin glass phase of $\underline{Cu}Mn$ had the properties of a single magnetic particle over a macroscopic sample. Furthermore, it was shown that the demagnetizing field was two orders of magnitude smaller than the anisotropy field, thus justifying the absence of domains or shape effects in our analysis. As we wish to extend this work to the present situation, a difficulty arises for the analysis of the hysteresis cycles shown in figure 3 for a concentration of Au above 0.1 % where the cycle can no longer be considered as a simple *square*. Indeed, as explained in the experimental section, only the

first instability can be well defined, but the associated magnetization reversal amplitude corresponds to a smaller and smaller fraction of the remanent magnetization as the Au concentration increases and the time constants involved become very long. Of course a natural way of defining the anisotropy energy would consist of taking it equal to 1/8 of the area of the hysteresis cycle, whatever its shape. We have not done this as this would take into account that part of the hysteresis cycle in large negative field where we think the magnetization proceeds with IRM type processes rather than by large scale remanent magnetization reversal. However there is at present no clear criterion to distinguish between these two mechanisms when their effect become comparable. Instead, we have retained as a single characteristic parameter the reversal field H_r at which the first instability occurs, i.e. assuming explicitly that all the magnetization should be reversed when waiting a long enough time at H_r. With this very important restriction we can proceed to evaluate the anisotropy energy for each Au concentration. Taking into account the observed fact that all cycles seem to close (when coming back towards positive value of field) near $H = 0$, we define K experimentally by

$$K = \tfrac{1}{4}\sigma_r H_r .$$

From the linear increase of H_r with Au concentration we can define the specific anisotropy energy per unit of Au concentration for $\underline{\text{Cu}}\text{Mn}_{1\%}$; we find :

$$\left(\frac{\Delta K_A}{\Delta x}\right)[\text{Au}] = (3.5 \pm 0.5).10^4 \text{ ergs/cm}^3 \text{ for } \underline{\text{Cu}}\text{Mn}_{1\%} .$$

The displacement field at the centre of the hysteresis loop being approximately $1/2\ H_r$ the corresponding *elastic* energy is found to be

$$\left(\frac{\Delta K_D}{\Delta x}\right)[\text{Au}] = (1.75 \pm 0.5).10^4 \text{ ergs/cm}^3 \text{ for } \underline{\text{Cu}}\text{Mn}_{1\%}$$

where the increased relative error allows for the fact that the centre of the cycle is often ill defined.

We remark as a conclusion of this analysis that in order to be able to define a specific anisotropy energy for an impurity as is done above we implicitly suppose that the anisotropy fields present in the $\underline{\text{Cu}}\text{Mn}_{1\%}$ are simply *additive* so that :

$$K(\text{alloy}) = K(\underline{\text{Cu}}\text{Mn}) + K(\text{Au})$$

with obvious notations. Such a simple relation will have to be present in any theoretical model dealing with this situation. The effect of other impurities (Al, Ag, Pt), although less documented than our Au measurements, again allows us to define an anisotropy field and an anisotropy energy using the same criterion as discussed for Au. The ensemble of our results appears in table II where we have calculated the anisotropy energy increment per % added impurity in $\text{CuMn}_{1\%}$ measured at 1.45 K, together with the hysteresis cycle width increment also per % added impurity in $\text{CuMn}_{1\%}$ at 1.45 K. The last line is the conduction electron spin flip scattering cross section measured from the spin resonance width increment studies of Cu containing these impurities. A special attention should be given in table II to the presence of Mn as an added impurity in $\underline{\text{Cu}}\text{-Mn}_{1\%}$. The reason is that we believe that the residual anisotropy measured in CuMn has its origin in the properties of the Mn ion itself. However as it was shown [2] that the scaling of the elastic energy K_D, and probably K_A as well, varies as the square of the Mn concentration, care should be exercized with the use of this number presented here for $\text{CuMn}_{1\%}$. This procedure enables one to compare the residual anisotropy in different Mn alloys. The results for $\underline{\text{Ag}}\text{Mn}_{1\%}$ and $\underline{\text{Pd}}\text{Mn}_{1.3\%}$ (measured by Guy *et al.* [5]) are presented on table III. It is striking to note that the order of magnitude of K_A is the same (within a factor of 2) for CuMn and AgMn.

The main conclusions to be drawn from table II concern the physical origin of the anisotropy in CuMn. As was shown as early as 1957 by Owen, Browne, Arp and Kip [15] from E.S.R. measurements

Table II.

	Mn (*)	Ag	Al	Au	Pt
$\Delta H_r/\Delta x$ Oe/% ([a])	170	< 60	117 ± 10	6 200 ± 400	34 000 ± 13 000
$\Delta K/\Delta x$ erg/%/mole Cu ([b])	70	< 44	60 ± 6	2 760 ± 400	15 300 ± 4 000
ΔZ ([c])	4	0	+ 2	0	− 1
$\Delta a/\Delta x$ (Å/%) ([d])	3.6×10^{-3}	5.6×10^{-3}	2.6×10^{-3}	5.6×10^{-3}	3.6×10^{-3}
σ_{sf} (cm²) ([e])	1.07×10^{-18}	$< 10^{-18}$	5.5×10^{-19}	$(1.2 \pm 0.3).10^{-17}$	$(4 \pm 1).10^{-17}$

([a]) Specific reversal field increment $\Delta H_r/\Delta x$ per % added impurity in $\underline{\text{Cu}}\text{Mn}_{1\%}$, measured at 1.45 K.
([b]) Specific anisotropy energy increment $\Delta K/\Delta x = \frac{1}{4}\sigma_r(\Delta H_r/\Delta x)$ per mole of alloy.
([c]) Impurity valence difference with Cu.
([d]) Lattice parameter increment $\Delta a/\Delta x$ (from Ref. [16]).
([e]) Conduction electron spin flip cross section σ_{sf} for these different impurities.
(*) Mn is presented assuming Mn in $\underline{\text{Cu}}\text{Mn}_{1\%}$ is involved through it's own spin orbit potential.

Table III. — *Comparison of the anisotropy energies per mole of alloys for* 3 *systems* : CuMn$_{1\%}$, AgMn$_{1\%}$ *(our work), and* PdMn (Ref. [5]).

	CuMn$_{1\%}$	AgMn$_{1\%}$	PdMn$_{1-3\%}$
$K = \frac{1}{2}\sigma_r H_r$ (erg/mole alloy)	70 ± 7	147 ± 13	< 50
Measurement temperature	1.45 K	1.6 K	4.2 K

of a single crystal of CuMn 5.6 at. % the anisotropy at 4.2 K is not linked to the crystal direction but only to the (field induced) remanent magnetization direction. This fact was enough to dismiss the single Mn ion anisotropy as a possible mechanism. In the same line of reasoning it is thus not surprising in our present experiment, to see that the impurity valence difference with Cu, which is + 2 for Al, − 1 for Pt and zero for Ag and Au do not play any significant role in the observed trends for the anisotropy increment as it might have done if the single ion crystalline field was at stake. The origin of anisotropy might also have been attributed to a size effect i.e. the deformation of the lattice, due to the different radii of the non magnetic atoms introduced in Cu [16]. This would also play a role in the presence of cold working. But we notice that the incremental change of the lattice parameter is identical for Au and Ag, and lower for Pt and Al (Table II). We thus can safely reject this mechanism for the origin of the anisotropy.

Quite differently we want to establish from the data presented in table II that the presence of a strong impurity induced anisotropy is governed by the square of the spin orbit potential of the impurity. This is best proven by the reasonable correlation shown on figure 8 between the specific anisotropy energy and

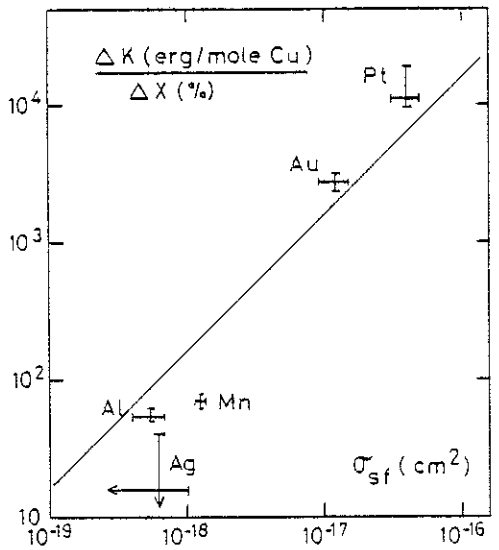

Fig. 8. — Incremental anisotropy energy *versus* conduction electron spin flip cross section for Ag, Al, Mn, Au and Pt. $\Delta K = \frac{1}{2}\sigma_r H_r$ (CuMn$_{1\%}$, I$_x$) − $\frac{1}{2}\sigma_r H_r$ (CuMn$_{1\%}$ pure). σ_{sf} is the conduction electron spin flip cross section for these different impurities in Cu [17, 18, 19]. Mn is presented assuming Mn in CuMn$_{1\%}$ is involved through it's own spin orbit potential.

the conduction electron spin flip cross section which varies as the square of the spin orbit splitting of the p (or d) level on the impurity. The cross sections have been measured from the increase in conduction electron spin resonance width with increasing impurity concentration, either following the method described by Asik *et al.* [17] or by Gossard *et al.* [18] on dilute magnetic alloys of CuMn in the paramagnetic regime. In ref. [19] a summary of these results is given. Although the data presented on figure 8 are admittedly scarce and imprecise because of our lack of precision in the evaluation of K through the product $\sigma_r H_r$ or because of the poor quality of the E.S.R. data yielding the spin flip cross section of some impurities (Pt, Al, Ag), we think that this gives enough evidence for the spin orbit mechanism as being the physical origin of the macroscopic anisotropy in CuMn and probably in other spin glasses. It accounts in a simple way for the variation over two orders of magnitude of the anisotropy induced by Al or Pt.

In a different context D. A. Smith and independently Levy and Fert [20] present a microscopic derivation of the impurity induced anisotropy of two Mn spins interacting *via* an isotropic Ruderman Kittel type exchange. He shows that the presence of a non magnetic impurity with a spin orbit potential gives rise to an anisotropy of the spin-spin interactions of the Dzyaloshinski Moriya [21, 22] type. Of course the link between this mechanism and the macroscopic anisotropy field associated with the remanent magnetization remains to be made. However we feel that this mechanism is intrinsically relevant to account for our observations. There exists some further experimental evidence of the impurity induced anisotropy mechanism *via* the spin orbit mechanism : the simplest one is the lack of observations (in ref. [3] on CuMn$_{2\%}$ and our measurement on AgMn$_{1\%}$) of any magnetization reversal. see section 2.5. Our interpretation is that the presence of Fe (in the 10 ppm range) in the alloy is such that the very large spin orbit scattering rate of Fe [23] becomes effective at broadening the hysteresis cycles beyond the field range where the magnetic instabilities are readily observed. However no quantitative measurement of the effect of Fe has been done at present. The second very important and much better documented evidence comes from the analysis of the spin resonance in the spin glass state of CuMn$_{2\%}$ at 4.2 K reported by Okuda and Date [24] when adding a number of impurities (Al, Zn, Ti, Ni, Fe, Co, Pd) in CuMn. These authors found that the spin resonance of CuMn$_{2\%}$ containing each of these impurities is shifted with respect to the bare alloy by an amount which varies linearly with the added impurity concentration. Furthermore the rate of increase of this shift per % impurity is specific to each impurity and varies from zero for Al to 6.6 × 10^3 G/% for Co in more or less the same way as does the spin flip cross section. This observation must be linked to the new inter-

pretation of this shift [25] as being due to the anisotropy field of the alloy rather than an antiferromagnetic resonance as originally proposed by Owen *et al.* [15]. The consequence of this is that the incremental shift of the spin resonance by an added impurity in the spin glass can serve as a direct measure of the anisotropy. The quantitative comparison between these two methods is at present lacking but the order of magnitude agreement is very favourable.

As a conclusion we think that we have demonstrated the role of spin orbit scattering in determining the magnitude of the macroscopic anisotropy field in the spin glass phase. This fact offers a satisfactory explanation to the otherwise not understood difference in hysteresis behaviour of CuMn and AuFe (see Fig. 1). A natural question is to what extend this elementary mechanism is also operative in concentrated magnetic materials. Concerning the physics of the spin glass phase, the possible role of the anisotropy in determining the appearance of the susceptibility cusp remains to be established. Finally it should be emphasized that the independence of the remanent magnetization on added impurity concentration strongly suggests that this magnetization is an intrinsic property of the spin glass phase.

Acknowledgments. — We thank Mr. Rosso for his very carefull preparation and handling of CuMn and ternary alloys.

We thank M. Goddard and Dr Chapelle for growing AgMn single crystals.

We wish to acknowledge many fruitfull discussions with Dr J. Souletie, J. L. Tholence, R. Tournier, A. Fert and P. M. Levy, as well as with Mrs M. Lambert, who suggested we check the size effect.

We thank Dr S. J. Williamson for a critical reading of the manuscript.

References

[1] KOUVEL, J. S., *J. Phys. Chem. Solids* **21** (1961) 57.

[2] MONOD, P., PREJEAN, J. J., TISSIER, B., *Magnetism and Magnetic Materials* (New York) 1979 ; *J. Appl. Phys.* **50** (1979) 7324. See also
MONOD, P., PRÉJEAN, J. J., LT 15, *J. Physique Colloq.* **39** (1978) C6-910.

[3] TOURNIER, R., Thesis, Grenoble (1965), unpublished.

[4] ISHIKAWA, Y., TOURNIER, R., PHILIPPI, J., *J. Phys. Chem. Solids* **26** (1965) 1727.

[5] GUY, C., STRON OLSON, J., *J. Phys. C.* **11** (1978) 1645.
GUY, C., HOWARTH, W., *Amorphous Magnetism* II, Levy R. A., Hasagawa, R., editors (Plenum Press New York and London) 1977, p. 169.

[6] FERRÉ, J., POMMIER, J., RENARD, J. P., KNORR, K., *J. Phys. C* (1979), to be published.

[7] JACOBS, I. S. and SCHMITT, R. W., *Phys. Rev.* **113** (1959) 459.

[8] BETHOUX, O., CORNUT, B., FERRARI, M., *Revue Phys. Appl.* **5** (1970) 865 ;
BETHOUX, O. *et al.*, to be published.

[9] As mentioned in [2], cold working a $CuMn_{0.5\%}$ (from a diameter of 7 mm to a square 5 × 5 mm) don't change either the remanent magnetization or the reversible susceptibility within a few per-cents but broaden significantly the reversal field i.e. the field where occurs the first partial magnetization reversal.

[10] As it is well known [3, 7, 11], the value of the remanent magnetization is a function of the magnetic and thermal history : it depends for example on the speed which at the field is removed. Our experimental technique introduces some other causes of uncertainties : heating of the sample and of the helium bath by eddy currents (in the sample and in the metallic parts of the cryostat) induced when removing the high field necessary to obtain a saturated thermoremanent magnetization, heating of the bath by the support of the sample when it is lowered in the measuring section of the apparatus down to 30 cm below the superconducting coil used to create high fields. The high sensitivity of the value of the remanent magnetization to thermal history is an essential cause of the dispersion of our experimental results. In order to avoid these uncertainties it is necessary to use an experimental technique [11] where all these inconvenients are the best minimized. We used such a technique to compare with much more care $CuMn_{1\%}$ and $CuMn_{1\%}Au_{1\%}$ as it is described further in the text.

[11] PREJEAN, J. J., Thèse, Univ. Grenoble (1980).

[12] STONER, E. C., WOLHFARTH, E. P., *Philos. Trans. R. Soc., London* A **240** (1948) 599.

[13] NÉEL, L., *C.R. Hebd. Sean. Acad. Sci.* **246** (1958) 2313.

[14] BROWN, W. F., *J. Physique Colloq.* **32** (1971) C1-1037 and *Magnetostatic principles in ferromagnetism* (North Holland Ed., Amsterdam) 1962.

[15] OWEN, J., BROWN, M. E., ARP, V., KIP, A. F., *J. Phys. Chem. Solids* **2** (1957) 85.

[16] PEARSON, W. B., *A. Handbook of lattice spacings and structures of metals and alloys* (Pergamon Press) 1968.

[17] ASIK, J. R., BALL, M. A., SLICHTER, C. P., *Phys. Rev.* **181** (1969) 645.

[18] GOSSARD, A. C., HEEGER, A. J., WERNICK, J. H., *J. Appl. Phys.* **38** (1967) 1251.

[19] MONOD, P., SCHULTZ, S., to be published (*J. Phys. F*).

[20] SMITH, D. A., *J. Magn. Magn. Mat.* **1** (1976) 214 ; FERT, A. and LEVY, P. M., to be published.

[21] DZYALOSHINSKY, I., *J. Phys. Chem. Solids* **4** (1958) 241.

[22] MORIYA, T., *Phys. Rev. Lett.* **4** (1960) 5.
MORIYA, T., *Phys. Rev.* **120** 1 (1960) 91.

[23] RITTER, A. L., SILSBEE, R. H., *Phys. Rev.* **17** (1978) 2833.

[24] OKUDA, K., DATE, M., *J. Phys. Soc. Japan.* **27** (1969) 639.

[25] MONOD, P., BERTHIER, Y., *Int. Conf. of Magn.*, Munich (1979) *J. Magn. Magn. Mat.* (1980), to be published.

CHAPITRE VII

IMPURETES MAGNETIQUES INTERAGISSANTES DANS L'ETAT NORMAL D'UN SUPRACONDUCTEUR - CORRELATION ENTRE LEUR AIMANTATION ET LES VARIATIONS DE H_{c_2}

1 - L'effet des impuretés magnétiques diluées dans une matrice supraconductrice sur la valeur de la température critique T_c a été l'objet de nombreuses études théoriques et expérimentales.

Très tôt, deux cas considérés comme simples ont suscité l'intérêt :

- Abrikosov et Gorkov[1] (1960) ont traité le problème d'impuretés magnétiques supposées sans interaction. Le résultat bien connu (une décroissance monotone de T_c quand on augmente la concentration c d'impuretés) a été vérifié expérimentalement dans de nombreux systèmes.

- Quand les impuretés présentent un caractère Kondo, Muller-Hartmann et Zittartz[2] (1971) ont prédit un effet réentrant dans la dépendance en c de T_c. Ce comportement a été observé dans $LaAl_2Ce$. Nous avons également étudié cet aspect à l'aide d'un modèle de spin effectif dépendant de la température[3].

2 - La valeur du champ critique H_c est également affectée par la présence d'impuretés magnétiques. Crow, Guertin et Parks (1967) ont été les premiers à observer, dans la dépendance de $H_{c_2}(T)$ du système La_3InGd, l'effet réentrant prédit par De Gennes et Sarma (1966). Divers auteurs ont essayé de construire des modèles corrélant la décroissance du champ critique avec l'aimantation M des impuretés. Bennemann (1969) notamment a donné une expression simple de cette corrélation :

$$H_{c_2}(T,c=0) - H_{c_2}(T,c) \sim M[H_{c_2}(T,c),T]$$

et déduit des résultats expérimentaux de Crow et al un ordre magnétique hélicoïdal des impuretés de gadolinium diluées dans La_3In.

Cependant, aucun test expérimental direct de mesure d'aimantation n'avait été effectué. C'est pourquoi nous avons repris l'étude du système $\underline{La_3In}$ Gd pour diverses concentrations c de gadolinium en mesurant à la fois la variation du champ critique $H_{c_2}(T,c)$ et l'aimantation M des impuretés dans l'état normal.

Nous démontrons que cette aimantation obéit aux lois d'échelles $\frac{M}{c} = f(\frac{H}{c},\frac{T}{c})$ significatives du caractère verre de spins du système (en contradiction avec les déductions de Bennemann).

Nous vérifions le résultat essentiel de Bennemann en exprimant nos valeurs expérimentales dans une loi de décroissance du champ critique :

$$\frac{H_c(T,c=0) - H_c(T,c)}{c} = \alpha + f(\frac{M[H_c(T),T,c]}{c})$$

Nous exposons ces résultats dans la publication suivante ("Interactions of impurities in the normal state of a superconductor and the correlation of their magnetization with the variation of H_{c_2}") présentée au Congrès de Magnétisme de Moscou (1973).

Référence

(1) Abrikosov, A.A., Gorkov, L.P., JETP 39 (1960) 1781, in English Sov. Phys. JETP 12 (1961) 1243.

(2) Muller-Hartmann, E., Zittartz, J., Phys. Rev. Lett. 26 (1971) 428.

(3) Préjean, J.J., Souletie, J., Teixeira, J., J. Phys. F 5 (1975) L6.

INTERACTIONS OF IMPURITIES IN THE NORMAL STATE OF A SUPERCONDUCTOR, AND THE CORRELATION OF THEIR MAGNETIZATION WITH THE VARIATIONS OF H_{c2}

J.J. Préjean and J. Souletie

Centre de Recherches sur les Très Basses Températures, Grenoble, FRANCE.

Introduction - Crow et al. (1) were the first to observe in La_{3-x} In Gd_x the non monotic variations of the second critical field $H_{c2}(T)$, vs. temperature, that De Gennes and Sarma (2) had previously predicted. Much in the same line several authors (3) (4) correlated the decrease of the critical field with the magnetization $M(H_{c2}(T), T)$ of the impurities at the corresponding field and temperature. For example Bennemann gave an expression : $H_{c2}(c,T,M = 0) = H_{c2}(c,T, M) + Jg^{-1}\mu_B^{-2}M$, $M = M(H_{c2},T)$, which contains only one parameter : the magnetization.

In the following, we first give some details about the preparation of samples of La_{3-x} In Gd_x and describe the experimental method of measurement of their magnetization. The results, shown in the second part, obey scaling laws typical of a magnetic glass of impurities interacting through the RKKY (Rudermann-Kittel-Kasuya-Yoshida) interactions ($1/r^3$). In the third part, we show that the decrease of the critical field may indeed be correlated with the magnetization of the impurities and we develop a very crude model able to account for the main features of the observed effect.

I - Experimental details

The samples of La_{3-x} In Gd_x, for different concentrations (0, 1, 1.5, 2, 2.5 at %), were prepared by melting the constituants under vacuum in a h.f. furnace, that ensures an energetic mixing, and hence a good homogeneity (5). The ingots were poured from the melt into a water cooled copper mould and stocked in liquid nitrogen to avoid their oxydation and to minimize the segregation. The starting materials and the ingots were cut in kerosene by the arc erosion technique, to avoid any pollution in the alloys.

The magnetization, at temperatures from 0.5K to 50K, in fields from 0 to 50KOe, was measured by the extraction method (6).

II - Magnetization results

Impurity magnetization - The magnetization curves of the matrix (fig. 1) between its critical field $H_{c20}(T)$ and 50KOe, for temperatures from 3.5K to 30K can all be superimposed in a diagram $M=f\left(\frac{H}{T+5.2K}\right)$. We suppose that this phenomenological law is also able to describe the matrix contribution to the magnetization in alloys containing Gd, where the critical field $H_{c2}(T)$ is lower than $H_{c20}(T)$.

In the following, the contribution of the impurities will be taken to be $M_{imp.} = M_{alloy} - M_{matrix}$.

On fig. 2, we represent M_{imp}/c vs.H/c for different Gd concentration (1, 1.5, 2, 2.5 at %). Such reduced diagrams are caracteristic of magnetic glasses where the interactions between impurities are oscillating and decreasing like r^{-3} (RKKY). This result noticiably differs from the expectation of Bennemann who concluded from magnetization curves (which he deduced from the $H_{c2}(T)$ variations and his theory) to the presence of helicoïdal ordering.

We notice a systematic shift in the reduced diagrams toward higher values of the magnetization for increasing concentrations. We know (7) that giant moments exist for c>3 at %. Such shifts can easily be accounted by some enhancement of the matrix magnetization. The effective moment deduced from susceptibility measurements is a little bit higher than the one given by the magnetization saturation. The latter corresponds to the theoretical value of $7\mu_B$.

Critical field - The critical field $H_{c2}(T)$ is well defined by the point where there is a discontinuity in slope of the isothermal magnetization curve, both in increasing and in decreasing fields. This discontinuity is more easily recognized with the help of the reduced diagrams (fig. 2) which give an idea of the curvature of the normal state magnetization at $H_{c2}(T)$. We observe the general effects already described by Crow et al. (non monotonous temperature dependance of the critical field). However our $H_{c2}(T)$ values are larger for equivalent concentration. This must be traced to the fact that Crow et al. defined $H_{c2}(T)$ as the value of the externally applied field for which the sample resistance R was $\frac{1}{2}$ the normal state resistance Rn ; they indicate that the breadth of the transition (defined as $\Delta H = H_{(R/Rn = 0.9)} - H_{(R/Rn = 0.1)}$) was approximately 5 to 10 % of the applied field.

III - Dependance of the $H_c(T)$ value on the magnetization of the impurities

We have represented (fig.4) the difference between the matrix upper critical field $H_{c20}(T)$ and the alloy critical field $H_{c2}(T)$ as a function of the magnetization $M(H_{c2}(T), T)$, in a diagram $\frac{H_{c20}(T)-H_{c2}(T)}{c} = f(M/c)$. We verify an essential result of Benneman : the variations of the critical field depend only on the magnetization. When the value of the magnetization is not too near the saturation value, we have approximately $\frac{\Delta H_{c2}(T)}{c} = A + B \frac{M}{c} (H_c)$.

Microscopic model:by a very crude model we are able to account for the main features of this result. Impurities break pairs : one electron of each pair is used to screen the impurity, the other electron goes to the conduction band. The latter is free to combine to form other pair if the impurity spins are random (paramagnetic or antiferromagnetic glass). On the other hand, if the impurity spins are aligned in the external field, all unpaired electrons are similarly polarized and they cannot combine with one another. Then we have two pair breaking coefficients : $\alpha_{\perp}$ and $\alpha_{//}$, the second being more efficient than the former. We understand that, for a certain range of concentrations, the low temperature state, where the spins are aligned in a high critical field, may be less favourable to superconductivity than a higher temperature state, where the impurities are in a paramagnetic state. This would explain the $H_{c2}(T)$ maximum. At higher Gd concentrations, the critical field is much lower and so the internal random magnetic field dominates. Then the low temperature state again favours superconductivity, and the maximum vanishes.

From the above, we would write :

$H_{c2}(T) = H_{c20}(T) - \alpha_{//} \; c(M/M_{sat}) - \alpha_{\perp} c(1 - M/M_{sat})$

This would account for the straight line (fig.) with :

$\alpha_{//} = 57.4$KOe/ % $\alpha_{\perp} = 22.4$KOe/ %

The ratio $\alpha_{//}/\alpha_{\perp}$ is appoximately 2 which is what we could expect from the above model : either c or 2c electrons are respectively abstracted from the superconducting state.

Conclusion - We have shown experimentaly that the upper critical field decrease, due to magnetic impurities, was a function of the impurity magnetization. A very simple model can account for the superconductivity destruction phenomena. The kind of magnetic order which is observed in the normal state of those alloys belongs to the type known as "magnetic glass", with a parasitic effect, probably due to a slight enhancement of the matrix.

L I T E R A T U R E

1. J. E. Crow, R. P. Guertin, R. D. Parks, Phys. Rev. Letters 19, 77, 1967.
2. P. G. De Gennes, G. Sarma, Solid State Commun., 4, 449, 1966.
3. K. H. Bennemann, J. W. Garland, F. M. Mueller, Phys. Rev. Letters, 23, 169, 1969.
4. R. Benda, Thesis, Frankfurt, 1968.
5. O. Bethoux, B. Cornut, M. Ferrari, Rev. de Phys. Appl., 5, 865, 1970.
6. J. A. Careaga, A. Lacaze, R. Tournier, L. Weil, 10th Intern. Conf. on Low Temp. Physics, LT10, Moscou, 1966.
7. R. P. Guertin, J. E. Crow, R. D. Parks, Phys. Rev. Letters, 16, 1095, 1966.

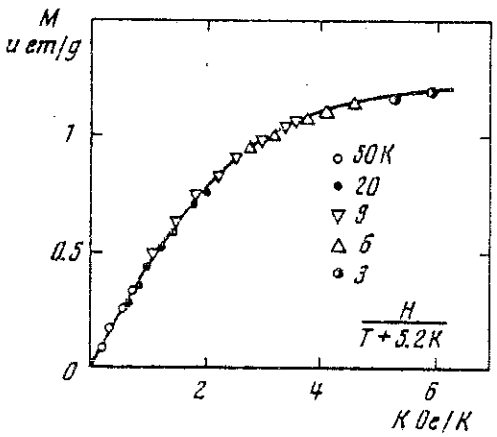

Fig. 1 The magnetization of the matrix : $M = f\left[\frac{H}{T + 5.2\ K}\right]$

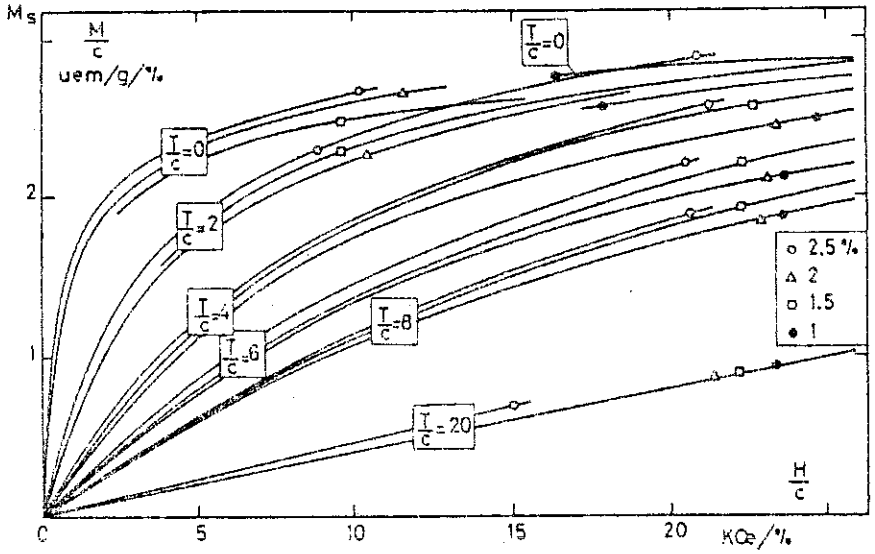

Fig. 2 The impurity magnetization $M = M_{alloy} - M_{matrix}$ in a reduced diagram : $\frac{M}{C} = f\left[\frac{M}{C}, \frac{T}{C}\right]$

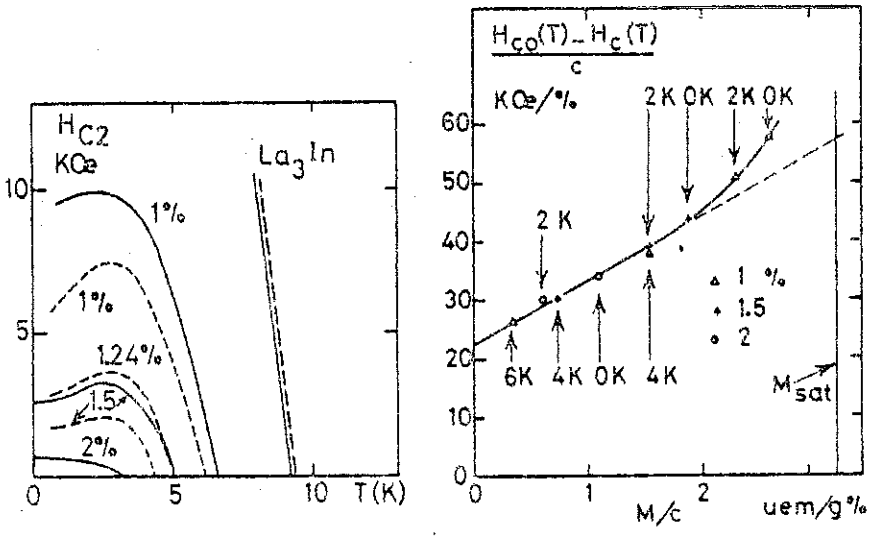

Fig. 3 The variations of the second critical field vs. T; full line = our data, dashed line = the data of Crow et al.

Fig. 4 The variations of $H_{c2}(T)$ vs. the impurity magnetization.

C O N C L U S I O N

Nous pouvons conclure, à partir des résultats expérimentaux que nous avons présentés, quelques points fondamentaux caractérisant les verres de spins métalliques :

La relaxation des aimantation et énergies associées, à $T < T_g$, révèle la présence de larges distributions des temps de relaxation et des niveaux d'énergie du système. On peut traduire ces propriétés en terme de barrières de potentiel largement distribuées séparant des niveaux différents en énergie.

La corrélation temps-température de ces relaxations indiquent que le franchissement de ces barrières de potentiel est gouverné par des processus d'activation thermiques. Dans une large gamme de température $T < T_g$ et de champs, il est possible d'exprimer les résultats expérimentaux en fonction d'une variable unique $T \mathrm{Ln} \frac{t}{\tau_o}$, où τ_o semble constant dans la limite de précision de la détermination expérimentale ($\sim 10^{-11}$ s dans CuMn, $\sim 10^{-13}$ s dans AuFe).

Nous avons pu déterminer des lois d'échelle générales en tenant compte du libre parcours moyen électronique dans la dépendance en concentration des températures caractéristiques et d'une éventuelle tendance au ferromagnétisme à haute concentration pour les entités magnétiques entrant en jeu dans la construction des aimantations.

Nous avons pu lever l'ambiguité concernant la question des cycles d'hystérésis dépendant du système et en déduire le rôle dominant de l'interaction RKKY dans le processus de construction et de relaxation de l'aimantation.

Il reste à résoudre encore un certain nombre de problèmes toujours obscurs aujourd'hui :

1 - Nous n'avons pas montré s'il existait ou non une transition de phase à T_c. Nous avons simplement émis une hypothèse pouvant réconcilier les résultats contradictoires obtenus d'une part en temps longs (en $TLn \frac{t}{\tau_o}$) et d'autre part en temps courts (T_g ne dépendant pas ou peu de la fréquence).

2 - * Nous n'avons rien dit sur l'origine de τ_o et seulement évalué sa valeur dans une gamme étendue en température et champ.

* Par ailleurs, des mesures préliminaires de relaxation de l'aimantation thermorémanente obtenue à partir de faibles champs (50 Oe) semblent montrer que la valeur de τ_o à $T_g/4$ est supérieure de plusieurs ordres de grandeur à celle déterminée précédemment ($\sim 10^{-6}$ s au lieu de 10^{-11} s). La connaissance précise des lois de relaxation dans ce cas peut apporter des renseignements intéressants sur une éventuelle distribution de τ_o. Les problèmes expérimentaux sont alors très complexes : définition rigoureuse de l'histoire thermique et magnétique, précision dans la mesure de relaxation d'aimantation (l'aimantation est très faible et la relaxation très lente à bas champs), écrantage de tout champ parasite etc.

* La dépendance en concentration de τ_o ne peut être déterminée qu'en réalisant des mesures sur de larges gammes de concentration, l'estimation de la valeur de τ_o étant pratiquement impossible à mieux qu'un facteur 10 près.

3 - Des mesures soigneuses en haut champ peuvent permettre de préciser l'effet du champ sur les entités magnétiques (modification et destruction éventuelle des corrélations).

Nous nous sommes attachés également à déterminer (par une méthode de susceptibilité alternative à $T \sim 50$ mK en présence d'un champ statique ou par l'étude de petits cycles de Rayleigh en haut champ) la contribution additionnelle $M_o(H)$ ($\simeq \chi_o H$ en bas champ). La connaissance de cette contribution est intéressante pour nous renseigner sur les formes des distributions $P(W)$ et $P(\varepsilon)$ que l'on pourrait extraire des courbes $M(H) - M_o(H)$.

Malheureusement, nous n'avons pu obtenir des précisions suffisantes pour conclure valablement sur la dépendance en champ de $M_o(H)$.

4 - Les mesures de relaxation d'énergie associée à la présence d'une aimantation rémanente, les mesures de dégagement d'énergie dans les sauts d'aimantation (cycle d'hystérésis du CuMn par exemple), sont essentielles pour la compréhension des phénomènes thermiques : avalanche d'origine thermique ou non dans les sauts d'aimantation, question du contrôle de la stabilité de température dans l'ensemble de l'échantillon lors de la relaxation d'aimantation, apport dans la détermination de $P(w)$ et $P(\varepsilon)$. C'est à ce travail que s'est particulièrement attaché J. Odin qui possède une instrumentation à la fois très souple et d'une précision remarquable.

A P P E N D I C E

APPAREIL DE MESURES D'AIMANTATIONS MAGNETIQUES DANS DES CHAMPS DE 0 A 80 kOe ET A DES TEMPERATURES DE 50 mK A 150 K

Les mesures de relaxation d'aimantation dans les verres de spin nécessitent l'utilisation d'un appareil à la fois susceptible de détecter de très faibles variations d'aimantation et dans lequel la stabilité thermique de l'échantillon soit suffisante pour ne pas introduire d'incertitude dans l'étude de l'évolution temporelle de l'aimantation à température constante.

Nous nous sommes largement inspiré de l'appareil de mesures d'aimantations de B. Tissier et dont la conception a été largement détaillée dans sa thèse. Aussi, nous nous contenterons d'un bref rappel du principe des mesures.

Notre apport essentiel a été la modification du calorimètre employé usuellement au laboratoire dans ce type de technique afin d'optimiser la stabilité thermique de l'échantillon.

I - PRINCIPE DE LA MESURE

Le porte-échantillon, le sel paramagnétique (dont la désaimantation est utilisée pour obtenir les très basses températures), les fils de chauffage, les thermomètres sont placés dans une cellule scellée plongée dans le bain d'hélium. Cette cellule se déplace le long de l'axe du champ magnétique produit par une bobine supraconductrice constituée de 22000 spires en Nb-Ti et pouvant créer un champ de 80 kOe homogène à 10^{-3} près sur une longueur de 6 cm.

Le déplacement de l'échantillon dans un champ constant, entre deux enroulements bobinés en sens inverse et connectés en série, crée une variation de flux $\frac{d\Phi}{dt}$ dans ces enroulements. La tension recueillie aux bornes est amplifiée par un amplificateur galvanométrique (gain 10^4) et intégrée par un voltmètre numérique intégrateur. Le signal intégré au cours d'une extraction de l'échantillon du centre de l'un des enroulements au centre du second est alors directement proportionnel à l'aimantation de l'échantillon. L'étalonnage se fait par mesure du signal produit par l'aimantation d'un système bien connu (nous avons choisi le platine et l'or). Nous pouvons détecter des variations d'aimantation de l'ordre de 8.10^{-5} uem.

II - CALORIMETRE ET PORTE-ECHANTILLON

Les températures comprises entre 1.4 K et 4.2 K sont obtenues par pompage sur le bain d'hélium. La thermalisation de l'échantillon s'effectue en introduisant une faible pression d'hélium gazeux dans la cellule de mesure.

Les températures inférieures à 1.4 K et supérieures à supérieures à 4.2 K sont obtenues respectivement par désaimantation adiabatique d'un sel paramagnétique et par chauffage de l'échantillon, la cellule étant sous vide de 10^{-6} Torr.

Le sel paramagnétique ($FeNH_4(SO_4)_2$, $12H_2O$) est cristallisé sur un support constitué d'une grille de cuivre constituée de fils de 0,4 mm de diamètre dont une extrêmité est soudée sur une pièce de cuivre taraudée sur laquelle vient se visser le porte-échantillon. Le sel se présente sous la forme d'un cylindre de 20 mm de diamètre et de 100 mm de long.

Ce sel est scellé dans un container en araldite, ce qui permet un pompage à chaud du calorimètre sans danger de dégradation du sel.

Le porte-échantillon est constitué de 50 fils de cuivre de 0,4 mm de diamètre (fig. 1). Ces fils sont usinés pour avoir une forme semi-cylindrique, ils sont assemblés et collés au moyen d'une résine époxy, pour former un tube dont les diamètres intérieur et extérieur sont de 7 mm et 8,4 mm. Ce tube est fendu suivant une génératrice, et les fils de cuivre sont soudés à une extrêmité sur une vis de cuivre qui permet de fixer le porte-échantillon sur la source froide et qui assure le contact thermique (voir figure 1).

L'échantillon est placé dans ce tube porte-échantillon. Sa surface cylindrique est en contact thermique avec les fils de cuivre, et un tube de nylon placé autour du tube porte-échantillon assure un bon contact thermique entre les fils de cuivre et l'échantillon, par différence de contraction à basse température.

Un tube en kapton graphite suspend l'ensemble sel et porte-échantillon à l'intérieur de la cellule et assure ainsi leur isolement thermique par rapport au bain d'hélium (en l'absence de gaz d'échange).

Les apports parasites de chaleur sont essentiellement dus :
- aux radiations provenant du haut du tube de pompage du calorimètre et qui se trouve à la température ambiante,
- à la conduction thermique des fils de mesure des résistances nécessaires à la mesure des températures,
- à la qualité de l'isolation thermique du support de l'ensemble sel-porte-échantillon.

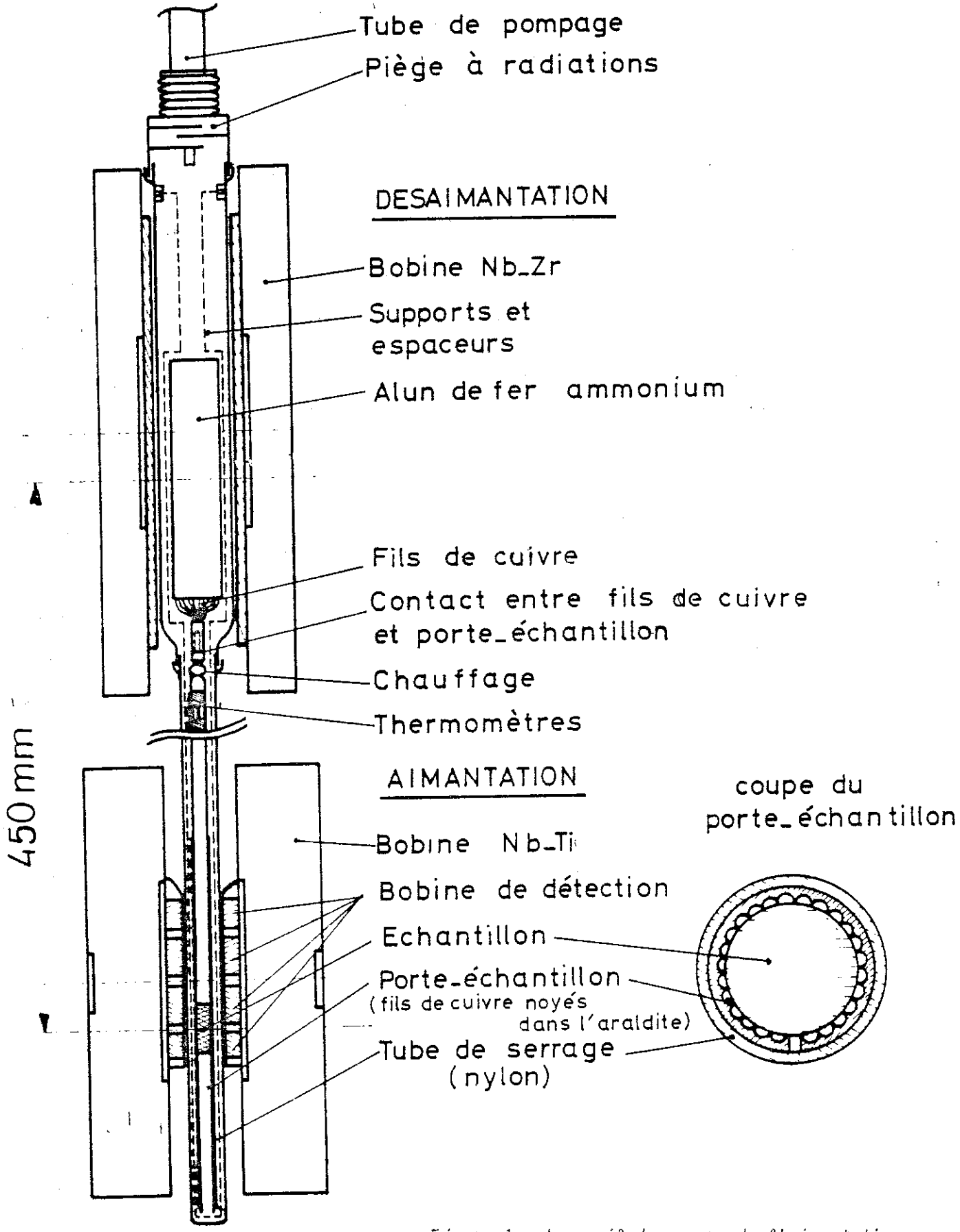

Figure 1 : *Appareil de mesure de l'aimantation.*

Pour pallier à ces difficultés, nous avons, en profitant de diverses expériences au laboratoire, conçu un nouveau type de cellule de mesure donnant entière satisfaction et comportant :

(i) Un piège à radiation (figure 2) dont les principales caractéristiques sont :

a) d'une seule pièce, il est plongé dans le bain d'hélium et les fils de mesure y sont collés sur une grande longueur : on a à ce niveau une thermalisation parfaite avec le bain d'hélium (contrairement à l'ancien système ou le piège n'était que vissé à l'enceinte) ;

b) le piège est revêtu à l'intérieur d'une peinture au graphite et a une disposition permettant une absorption maximale des radiations (ancien système : pas de peinture, larges fentes et chemin très court pour les radiations).

(ii) Une suspension du sel paramagnétique depuis le piège, réalisé avec un tube de 0,5 mm d'épaisseur en Kapton graphité bien moins conducteur que l'ancien système avec tube de nylon.

(iii) Enfin, fermeture de l'enceinte avec un joint silastène (plastique durcissant à l'air) : nous n'avons jamais eu de fuite. D'un maniement très facile, cette technique évite de chauffer comme dans la technique de soudure au métal de wood avec les risques que cela comporte (cassage des fils, etc ...).

Compte tenu des pertes en hélium et de la capacité limitée du vase en hélium, nous maintenons la température en dessous de 50 mK pendant 2^h15, en dessous de 100 mK pendant 3^h15.

Ce dispositif a aussi l'avantage de permettre, pendant 2 heures après l'établissement d'une température $T > 4.2$ K, une parfaite stabilité en température (même en l'absence de régulation) compte tenu du remarquable isolement thermique de la cellule et de la grande capacité calorifique de l'ensemble sel-porte échantillon.

Cette stabilité est d'autant plus recherchée que nos mesures de variations en temps des aimantations rémanentes sont très sensibles à des variations de température de l'ordre du % sur 2 heures.

Piège à radiations

échelle : 1cm = 5mm

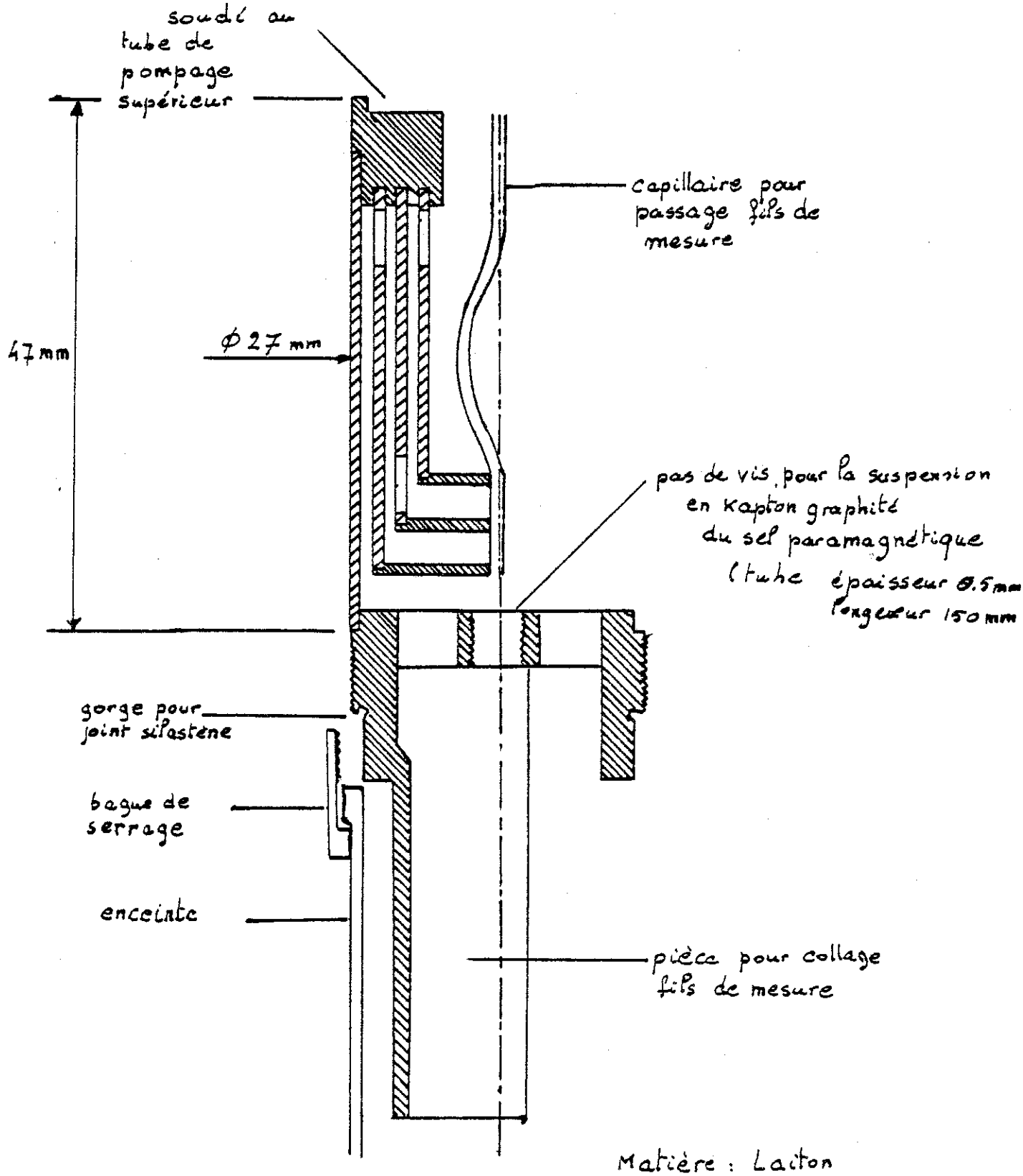

Fig. 2

Matière : Laiton

Soudure : à l'argent

Peinture au graphite sur toutes les parois.

Les températures sont mesurées au moyen de résistances de carbone placées à 30 cm de l'échantillon. Ces résistances sont collées au moyen d'une résine époxy (Stycast) dans un cylindre de cuivre pur qui est maintenu en contact thermique avec les fils de cuivre de la même manière que l'échantillon.

Les températures inférieures à 1.6 K sont mesurées à l'aide d'une résistance carbone 220 Ω (Speer) amincie (épaisseur 1 mm) et placée dans une protection en cuivre. La diffusivité thermique est ainsi augmentée, les contacts thermiques améliorés.

La mesure de la pression de vapeur saturante de l'hélium à l'aide de manomètres à mercure ou à huile permet d'indiquer la température entre 1.6 K et 4.2 K lorsque l'ensemble sel-échantillon est mis en contact thermique avec le bain au moyen de gaz d'échange.

Les températures supérieures à 4.2 K sont obtenues par chauffage de l'ensemble sel-échantillon. Ces températures sont régulées à l'aide d'une résistance de 220 Ω, 1/2 W (Speer) et mesurées avec une diode AsGa préalablement étalonnée.

Référence

B. TISSIER, Thèse - Grenoble (1977).

dernière page de la thèse

AUTORISATION DE SOUTENANCE

VU les dispositions de l'article 5 de l'arrêté du I6 Avril 1974,

VU les rapports de M. ~~ossieu~~ BLANDIN.....

M. ~~ossieu~~ PHILLIPS.....

M. ~~ossieu~~ SOULETIE.....

M. ~~ossieu~~ PRÉAN Jean Jacques..... est autorisé à présenter une thèse en soutenance pour l'obtention du grade de DOCTEUR D'ETAT ES SCIENCES.

Fait à GRENOBLE, le 9 janvier 1980

Le Président de l'U.S.M.G.

Dr G. CALA

UNIVERSITÉ SCIENTIFIQUE ET MÉDICALE DE GRENOBLE

Le Président de l'I.N.P.G.

Ph. TRAYNARD
Président
de l'Institut National Polytechnique